ECF-200PO1-09-2352
Revision 1

# 200-PO-1 Remedial Investigation Report - Central Plateau Groundwater Fate and Transport Modeling

Prepared for the U.S. Department of Energy
Assistant Secretary for Environmental Management

Contractor for the U.S. Department of Energy
under Contract DE-AC06-08RL14788

CH2MHILL
Plateau Remediation Company

**P.O. Box 1600**
**Richland, Washington 99352**

Approved for Public Release:
Further Dissemination Unlimited

ECF-200PO1-09-2352
Revision 1

# 200-PO-1 Remedial Investigation Report - Central Plateau Groundwater Fate and Transport Modeling

Document Type: RPT Program/Project: EP&SP

T. M. Clemo
INTERA, Inc.

Date Published
September 2011

Prepared for the U.S. Department of Energy
Assistant Secretary for Environmental Management

Contractor for the U.S. Department of Energy
under Contract DE-AC06-08RL14788

CH2MHILL
Plateau Remediation Company

**P.O. Box 1600**
**Richland, Washington**

Release Approval 9/15/2011 Date

Approved for Public Release:
Further Dissemination Unlimited

**TRADEMARK DISCLAIMER**

Reference herein to any specific commercial product, process, or service by trade name, trademark, manufacturer, or otherwise, does not necessarily constitute or imply its endorsement, recommendation, or favoring by the United States Government or any agency thereof or its contractors or subcontractors.

This report has been reproduced from the best available copy. Available in paper copy.

Printed in the United States of America

CH2MHILL
Plateau Remediation Company

# Environmental Calculation Cover Page

**Part 1: Completed by the Responsible Manager**

**Project: 200-PO-1 Remedial Investigation** **Date: 1 Sep 2011**

**Calculation Title & Description:** 200-PO-1 Remedial Investigation Report - Central Plateau Groundwater Fate & Transport Modeling
**This calculation describes the purpose, approach, computational tools, inputs, and results of simulations to estimate the future fate of contaminants found in groundwater within the 200-PO-1 Groundwater Operable Unit.**

| | |
|---|---|
| **Preparer:** TJ Clemo | **Basis of Qualification:** Experience and education |
| **Checker:** S Mehta | **Basis of Qualification:** Experience and education |
| **Senior Reviewer:** WE Nichols | **Basis of Qualification:** Experience and education |

**Part 2: Completed by Preparer**

**Calculation No.:** ECF-200PO1-09-2352 **Revision No.:** 1

**Revision History:**

| Revision No. | Description | Date | Affected Pages |
|---|---|---|---|
| 0 | Original issue | 25 Feb 2010 | All |
| 1 | Revised to clarify model domain extent and distinguish from near and far field analysis regions | 1 Sep 2011 | All |

**Part 3: Document Review & Approval:**

**Preparer:**
TJ Clemo / Senior Modeler
NAME/POSITION
Tom Clemo
SIGNATURE
9/7/2011
DATE

**Checker:**
S Mehta / Senior Modeler
NAME/POSITION
SIGNATURE
09/07/2011
DATE

**Senior Reviewer:**
WE Nichols / Modeling Team Leader
NAME/POSITION
SIGNATURE
7 Sep 2011
DATE

**Responsible Manager:**
AH Aly / Risk & Modeling Integration Manager
NAME/POSITION
SIGNATURE
9/7/2011
DATE

# Contents


1 **Purpose** ..... **5**

2 **Methodology** ..... **6**

3 **Assumptions and Inputs** ..... **9**

3.1 Model Domain ..... 9

3.2 Simulation Periods ..... 13

3.3 Processes Simulated and Limitations ..... 13

3.4 Boundary Conditions ..... 14

3.5 Initial Hydraulic Head Distribution ..... 15

3.6 Contaminant Initial Conditions ..... 15

3.7 Transport Properties ..... 19

4 **Software Applications** ..... **22**

4.1 Approved Software ..... 22

4.1.1 Description ..... 22

4.1.2 Software Installation and Checkout ..... 23

4.1.3 Statement of Valid Software Application ..... 24

5 **Calculation** ..... **25**

5.1 Overview of the Flow Solution ..... 25

5.2 Contaminant Concentration Distributions ..... 32

5.2.1 Tritium ..... 33

5.2.2 Nitrate ..... 39

5.2.3 Iodine-129 ..... 45

5.2.4 Trichloroethene ..... 51

5.2.5 Technetium-99 ..... 55

5.2.6 Uranium 61

5.2.7 Strontium-90 ..... 67

5.2.8 Tetrachloroethene ..... 71

5.2.9 Carbon Tetrachloride ..... 71

6 **Results/Conclusions** ..... **74**

6.1 Uncertainty in Simulated Future Conditions ..... 74

6.1.1 Uncertainty in Initial Contaminant Distribution ..... 74

6.1.2 Uncertainty from Neglecting Future Contribution from Vadose Contaminant Sources to Groundwater ..... 77

6.1.3 Conceptual Model Uncertainty ..... 77

6.1.4 Hydraulic Parameter Value Uncertainty ..... 78

6.1.5 Uncertainty in Transport Parameters ..... 79

6.1.6 Summary of Uncertainty in Fate and Transport Simulations ..... 80
**7 References ..... 81**

## Appendices

A. **Software Checkout and Installation Forms** ..... 83

## Figures

Figure 2-1. Central Plateau Model Domain ..... 7
Figure 2-2. Stream Tube Locations Outside Central Plateau Model Domain for the 200-PO-1 OU ..... 8
Figure 3-1. Hydrostratigraphic Units of Layer 1 ..... 10
Figure 3-2. Hydrostratigraphic Units of Layer 2 ..... 11
Figure 3-3. Hydrostratigraphic Units of Layer 3 ..... 11
Figure 3-4. Hydrostratigraphic Units of Layer 4 ..... 12
Figure 3-5. Hydrostratigraphic Units of Layer 5 ..... 12
Figure 3-6. Flow Model Boundary Conditions ..... 15
Figure 5-1. Initial Hydraulic Head Distribution ..... 27
Figure 5-2. 1-Year Hydraulic Head Distribution ..... 28
Figure 5-3. 25-Year Hydraulic Head Distribution ..... 29
Figure 5-4. 75-Year Hydraulic Head Distribution ..... 30
Figure 5-5. 125-Year Hydraulic Head Distribution ..... 31
Figure 5-6. Simulated Monitoring Locations ..... 33
Figure 5-7. Initial Distribution of Tritium (2008) ..... 34
Figure 5-8. Tritium Distribution after 1 Year (2009) ..... 35
Figure 5-9. Tritium Distribution after 25 years (2034) ..... 35
Figure 5-10. Largest Tritium Concentrations at Monitor Locations ..... 37
Figure 5-11. Initial Concentrations for Nitrate (2008) ..... 40
Figure 5-12. Nitrate Concentrations after One year of Transport (2009) ..... 41
Figure 5-13. Nitrate Concentrations after 25 years of Transport (2034) ..... 41
Figure 5-14. Nitrate Concentrations after 75 years of Transport (2084) ..... 42
Figure 5-15. Nitrate Concentrations after 125 years of Transport (2134) ..... 42
Figure 5-16. Largest Nitrate Concentrations at Monitor Locations ..... 43
Figure 5-17. Initial Iodine-129 Concentrations (2008) ..... 46
Figure 5-18. Iodine-129 Concentrations after One Year of Transport (2009) ..... 46
Figure 5-19. Iodine-129 Concentrations after 25 Years of Transport (2034) ..... 47
Figure 5-20. Iodine-129 Concentrations after 75 Years of Transport (2084) ..... 47
Figure 5-21. Iodine-129 Concentrations after 125 Years of Transport (2134) ..... 48

Figure 5-22. Largest Iodine-129 Concentrations at Monitor Locations ..... 50
Figure 5-23. Initial Trichloroethene Distribution (2008) ..... 51
Figure 5-24. Trichloroethene after One Year of Transport (2009) ..... 52
Figure 5-25. Trichloroethene after 25 Year of Transport (2034) ..... 52
Figure 5-26. Initial Technetium 99 Distribution (2008) ..... 55
Figure 5-27. Technetium 99 Distribution after One Year of Transport (2009) ..... 56
Figure 5-28. Technetium 99 Distribution after 25 Years of Transport (2034) ..... 56
Figure 5-29. Technetium 99 Distribution after 75 Years of Transport (2084) ..... 57
Figure 5-30. Technetium-99 Concentrations at Monitor Locations ..... 60
Figure 5-31. Initial Uranium Distribution (2008) ..... 62
Figure 5-32. Uranium Distribution after One Year of Transport (2009) ..... 62
Figure 5-33. Uranium Distribution after 25 Years of Transport (2034) ..... 63
Figure 5-34. Uranium Distribution after 75 Years of Transport (2084) ..... 63
Figure 5-35. Uranium Distribution after 125 Years of Transport (2134) ..... 64
Figure 5-36. Uranium Concentrations at Monitor Locations ..... 65
Figure 5-37. Initial Strontium-90 Distribution (2008) ..... 67
Figure 5-38. Initial Carbon Tetrachloride Distribution (2008) ..... 71
Figure 5-39. Carbon Tetrachloride Distribution after 25 Years of Transport (2034) ..... 72
Figure 5-40. Carbon Tetrachloride Distribution after 75 Years of Transport (2084) ..... 72
Figure 5-41. Carbon Tetrachloride Distribution after 125 Years of Transport (2134) ..... 73
Figure 5-42. Carbon Tetrachloride Distribution after 175 Years of Transport (2184) ..... 73

## Tables

Table 3-1. Hydrostratigraphic Units and Flow Parameters ..... 9
Table 3-2. Temporal Discretization of the 200-PO-1 RI Simulations ..... 13
Table 3-3. Aquifer Dependent Transport Parameter Values for the Central Plateau Model ..... 20
Table 3-4. Constituent Dependent Transport Parameter Values for the Central Plateau Model ..... 21
Table 5-1. Maximum Concentration of Tritium (pCi/L) for Monitoring Locations at Selected Time Steps ..... 38
Table 5-2. Maximum Concentration of Nitrate (μg/L) for Monitoring Locations at Selected Time Steps ..... 44
Table 5-3 Maximum Concentration of Iodine-129 (pCi/L) for Monitoring Locations at Selected Time Steps ..... 49
Table 5-6. Maximum Concentration of Uranium (μg/L) for Monitoring Locations at Selected Time Steps ..... 65
Table 5-7. Maximum Concentration of Strontium-90 (pCi/L) for Monitoring Locations at Selected Time Steps ..... 69

# Terms

| | |
|---|---|
| COPC | contaminant of potential concern |
| DOE | U.S. Department of Energy |
| FS | Feasibility Study |
| GHB | general head boundary |
| HEIS | Hanford Environmental Information System |
| HSU | hydrostratigraphic unit |
| MCL | maximum contaminant level |
| MODFLOW | MODular three-dimensional finite-difference groundwater FLOW model (software package) |
| MT3DMS | modular three-dimensional multi-species transport model for simulation of advection, dispersion, and chemical reactions of contaminants in groundwater systems (software package) |
| NRDWL | Non-radioactive Defense Waste Landfill |
| OU | Operable Unit |
| PUREX | plutonium-uranium extraction |
| RI | Remedial Investigation |
| ROD | Record of Decision |
| SALDS | State Approved Liquid Disposal Site |
| TCE | trichloroethene |
| TEDF | Treated Effluent Disposal Facility |

# 1 Purpose

The purpose of this calculation is the simulation of the fate and transport of contaminants in groundwater within the portion of the affected aquifer associated with the 200-PO-1 Operable Unit (OU) at the US Department of Energy's (DOE's) Hanford Site. The modeling results will be used for the following purpose:

- Estimating future groundwater concentrations of contaminants of concern to support risk screening within the OU.

The scope of this modeling effort is confined to estimating the future down gradient concentrations of selected contaminants of potential concern (COPCs) within the unconfined aquifer underlying the 200-PO-1 OU. The COPCs that were simulated using this model for the 200-PO-1 Remedial Investigation (RI) are: carbon tetrachloride, trichloroethene, tetrachloroethene, tritium, strontium-90, iodine-129, technetium-99, nitrate, and uranium. Selection of the COPCs is described in Chapter 6 of DOE/RL-2009-85 RI report for the 200-PO-1 Groundwater OU.

The objectives of the modeling effort is to provide a basis for making an informed remedial action decision based on description of current and expected future groundwater contaminant concentrations at decision points within the OU boundaries.

# 2 Methodology

The approach to the groundwater fate and transport modeling utilizes a mathematical hydrogeological construct to represent the physical conditions within the aquifer of the OU. This construct was developed using modified versions of the acquired computer software called MODFLOW and MT3DMS. MODFLOW provided the calculation of water flow within the Central Plateau unconfined aquifer. The flows calculated by MODFLOW were then used by the MT3DMS program to simulate the movement of each contaminant. To expedite the development of a simulation capability for the 200-PO-1 RI, the MODFLOW model originally developed to perform contaminant fate and transport simulations in support of the 200-ZP-1 OU Final Record of Decision (ROD) was adopted and modified. Modifications to this model, to upgrade it for use over the entire Central Plateau region, and subsequent calibration are described in the ECF-200PO1-10-0259 Rev. 0, *MODFLOW Model for the Central Plateau.*

Figure 2-1 depicts the domain of model simulation. To the north, south, and west, the domain is constricted by basalt sub-crops above the water table of the aquifer. These sub-crops are assumed to be impermeable boundaries to flow. There are two gaps in the basalt sub-crops along the northern boundary. In these two regions, the water table is above the basalt surface. The westernmost region is referred to as the western gap and the eastern region is referred to as the Gable Gap. Along the eastern boundary and the westernmost part of the southern boundary the water table is also above the basalt surface. Cold Creek (located in the slot along the western boundary) and Dry Creek (the gap in the basalt sub-crops in the southwest corner of the domain) are sources of inflow to the Central Plateau. Surface boundary conditions include aquifer recharge from precipitation and the surface disposal of water from site operations. Source and sink terms are included to account for planned pumping in the 200-ZP-1 OU and elsewhere.

This environmental calculation file describes simulations of transport in the portion of the OU that lies within the model domain shown in Figure 2-1. Contaminant fate and transport estimates downstream of the model were performed using stream tube based analytical approach along three transport pathways (Figure 2-2) as described in ECF-200PO1-09-2007, Rev. 2, *200-PO-1 Operable Unit Remedial Investigation Report –Contaminant Fate and Transport Modeling in the Distal Portion of OU .*

The basic methodology for the development and application of the Central Plateau model for the 200-PO-1 Groundwater OU is as follows:

1. Construct a representative model of the Central Plateau within the MODFLOW framework using site-specific descriptions of the local physical and hydrogeologic conditions. See ECF-200PO1-10-0259, *MODFLOW Model for the Central Plateau.*

2. Verify the representativeness of the model by comparing the construct to available geologic descriptions, well logs, cross sections, and other appropriate sources of information. See ECF-200PO1-10-0259, *MODFLOW Model for the Central Plateau.*

3. Define appropriate boundary conditions to the defined model domain. See ECF-200PO1-10-0259, *MODFLOW Model for the Central Plateau*, and in Section 3.4.

4. Calibrate the hydraulic performance of the model by comparing the simulated groundwater head at selected locations to actual measurements (position and screen interval) at nearby wells; and comparing the simulated resultant groundwater gradient to the observed gradient in nearby wells (history matching). This calibration is implemented for over the time period from 1944-2008. Transport calculations are not part of the historic calibration. See ECF-200PO1-10-0259, *MODFLOW Model for the Central Plateau.*

5. Define the physical characteristics of the COPCs (e.g., distribution coefficient [$K_d$], soil grain density, etc.) that will be used as site and/or contaminant-specific variables.

6. Define the initial contamination conditions using current groundwater monitoring results to prepare initial contaminant distribution surface(s) within the model domain.

7. Run the model to calculate resultant concentrations at selected down gradient locations.

8. Fluid and contaminant mass fluxes at the entrance locations of the three stream tubes (called Pipe Pathways) are recorded and subsequently used as upstream boundary conditions for the transport calculations in the distal portion of the OU. See ECF-200PO1-09-2007, Rev. 2 for details.

9. Post-process and reduce the simulation results to produce usable graphic presentations of the simulation in meaningful units.

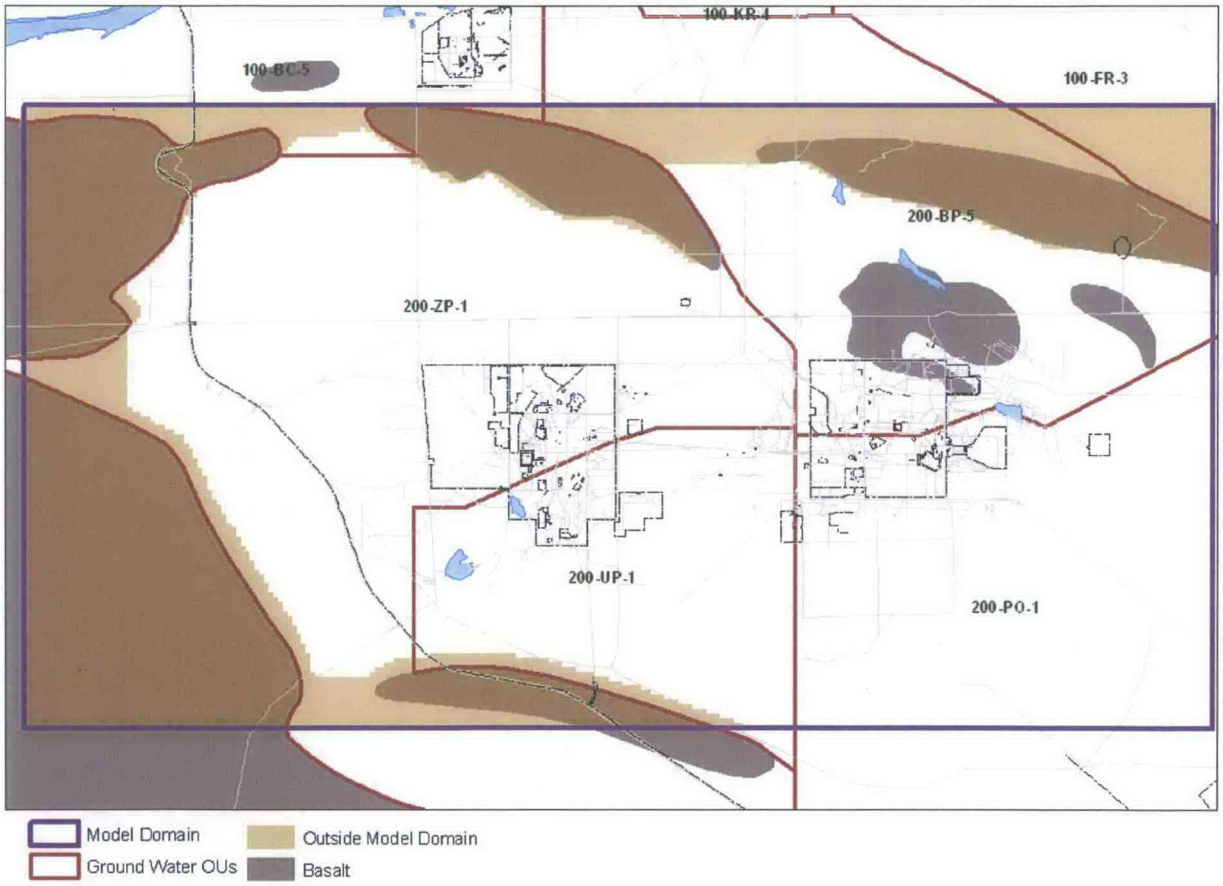


**Figure 2-1. Central Plateau Model Domain**

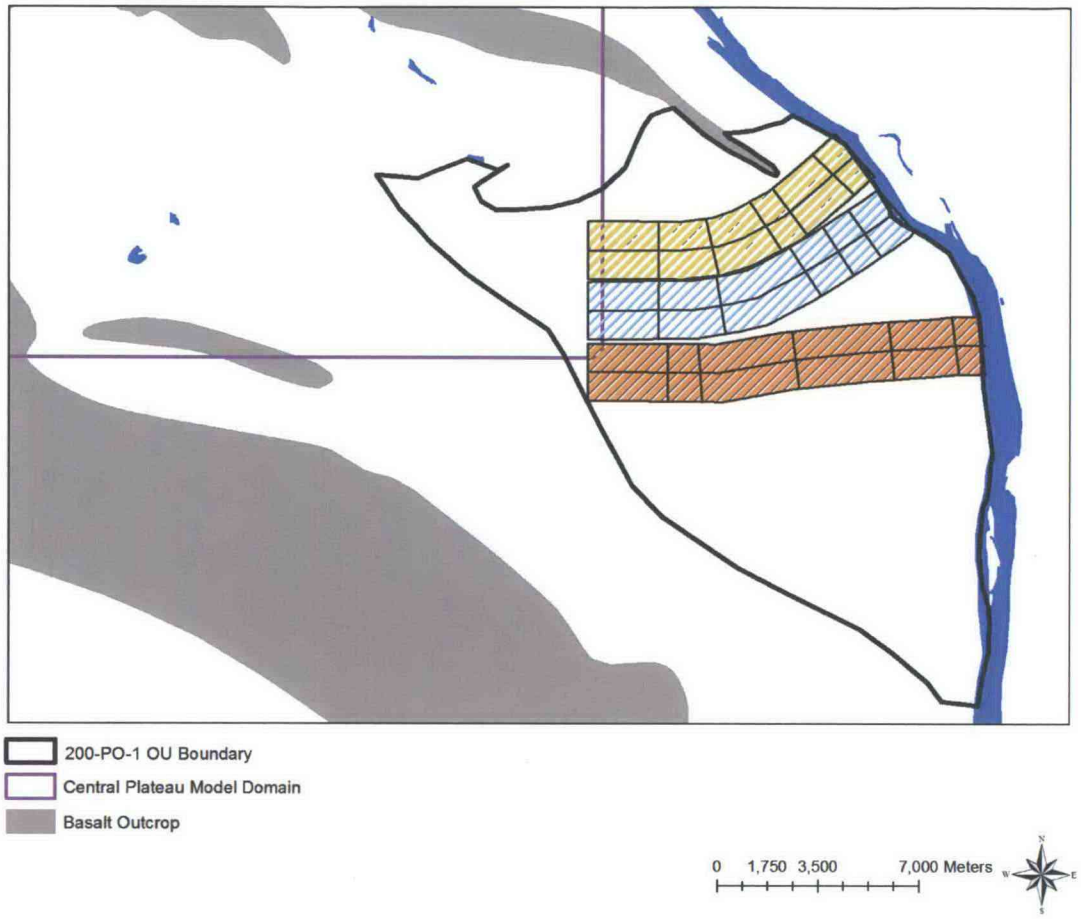


**Figure 2-2. Stream Tube Locations Outside Central Plateau Model Domain for the 200-PO-1 OU**

# 3 Assumptions and Inputs

Assumptions and input parameter development are detailed in this section.

## 3.1 Model Domain

The three-dimensional rectangular grid extent of the Central Plateau model has the following characteristics:

- 13.4 km north-south extent
- 25.6 km east-west extent
- Thickness of the domain varies to incorporate the entire saturated thickness of the aquifer above the basalt bedrock.
- Lower left corner: Easting 555650 m, Northing 129850 m Washington State Coordinate System: NAD_1983_StatePlane_Washington_South_FIPS_4602

The model domain is represented by a finite difference grid composed of 100 m square cells in map view and five layers vertically. The layers vary with thickness of the hydrostratigraphic units (HSUs) they represent. To reiterate, the layers are not of constant thickness.

The HSUs and flow parameters are listed in Table 3-1. Refer to ECF-200PO1-10-0259, *Central Plateau MODFLOW Model-Version 2*, for more detail.

**Table 3-1. Hydrostratigraphic Units and Flow Parameters**

| HSU | Hydraulic Conductivity (m/day) | Porosity | Bulk Density ($g/cm^3$) | Color in Figures 3-1 through 3-5 |
|---|---|---|---|---|
| Hanford formation | 8500 (horizontal) [a]<br>850 (vertical) [b] | 0.15 [c] | 1.93 [d] | Blue |
| Eastern portion of the Cold Creek unit [e] | 100 (horizontal) [a]<br>10 (vertical) [b] | 0.15 [c] | 1.93 [d] | Pink |
| Coarse grained upper Ringold Unit E | 5 (horizontal) [a]<br>0.5 (vertical) [b] | 0.15 [c] | 1.90 [d] | Orange |
| Ringold lower mud unit (Ringold B & C) | 0.3 (horizontal) [a]<br>0.03 (vertical) [b] | 0.15 [c] | 1.90 [d] | Brown |
| Coarse grained Ringold Unit A | 3.5 (horizontal) [a]<br>0.35 (vertical) [b] | 0.15 [c] | 1.90 [d] | Green |

a. Value from model calibration

b. Assumed equal to 1/10 of horizontal conductivity

c. PNNL-18564 Table 6.2

d. DOE/RL-2007-28

e. This portion has also been called the Pre-Missoula gravel.

Figure 3-1 through Figure 3-5 display the representation of the five HSUs in the five layers. The color scheme is given above. The inactive portion of the model domain is shown in black. Roads of the Central Plateau are shown in yellow to help orient the reader.

Layer 1 represents the HSUs at the water table during maximum water table conditions of the operational period of the Hanford Reservation. Current and predicted future water table elevations are lower, resulting in some of the upper layers being unsaturated. In much of the 200-BP-5 OU the water table has dropped below the upper surface of the basalt.

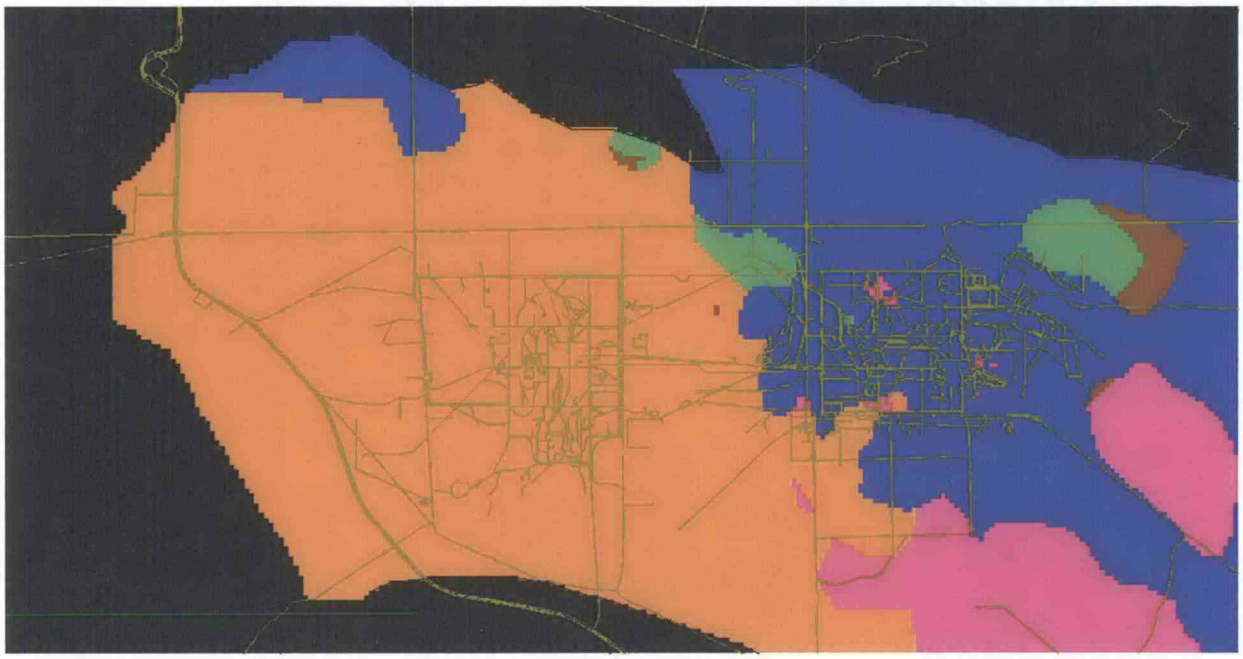

Central Plateau Model Version 2 - Layer 1

**Figure 3-1. Hydrostratigraphic Units of Layer 1**

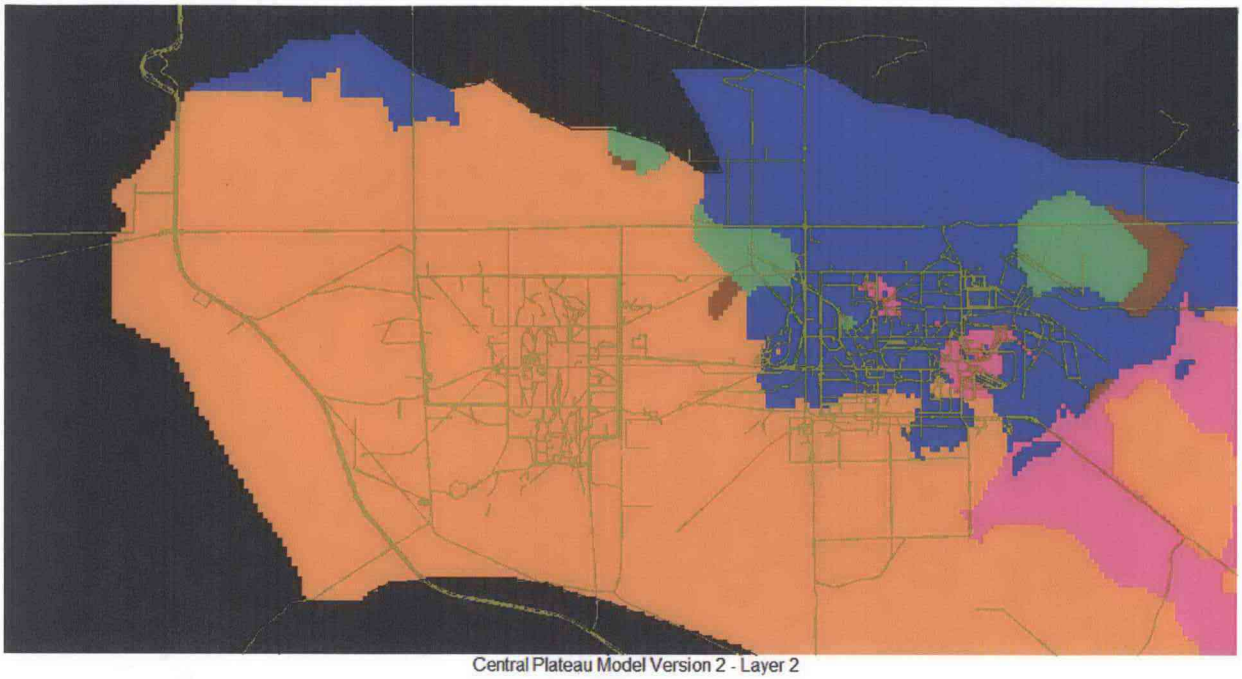

Central Plateau Model Version 2 - Layer 2

**Figure 3-2. Hydrostratigraphic Units of Layer 2**

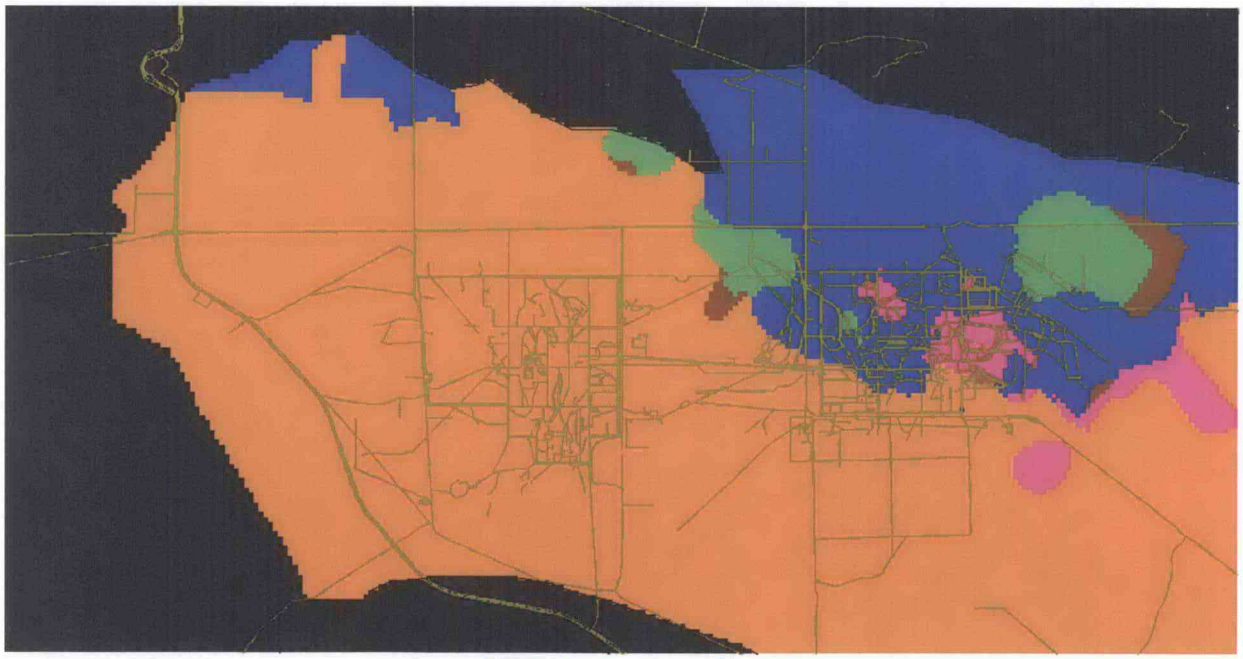

Central Plateau Model Version 2 - Layer 3

**Figure 3-3. Hydrostratigraphic Units of Layer 3**

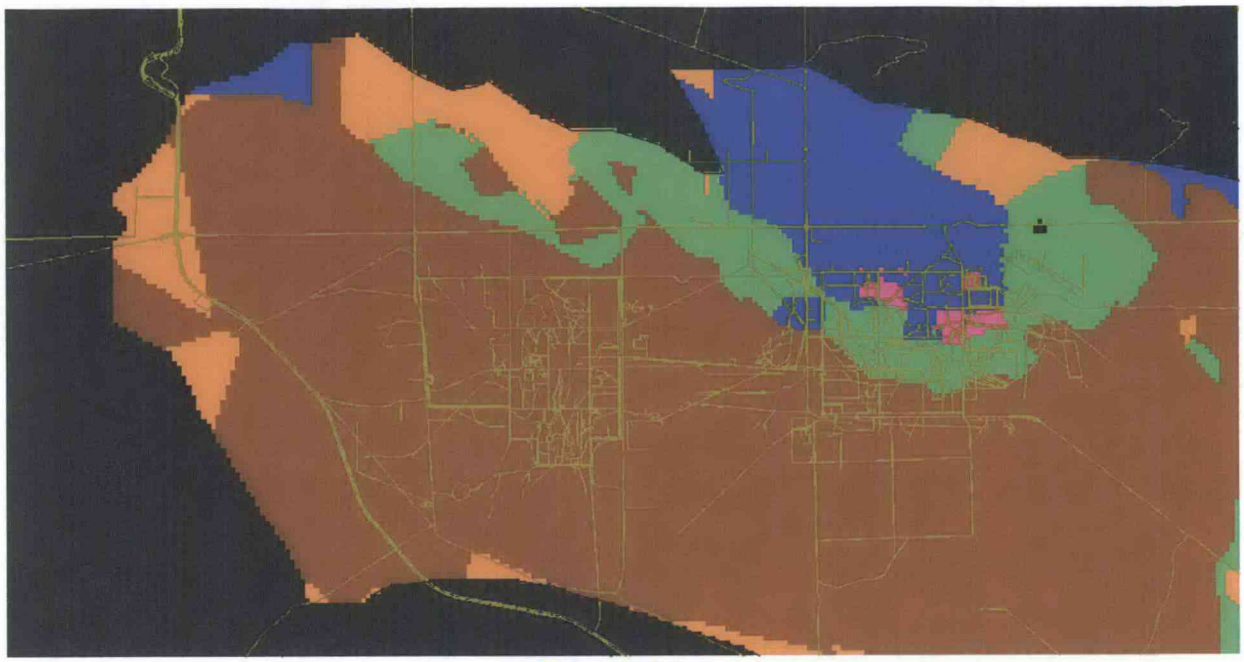

Central Plateau Model Version 2 - Layer 4

**Figure 3-4. Hydrostratigraphic Units of Layer 4**

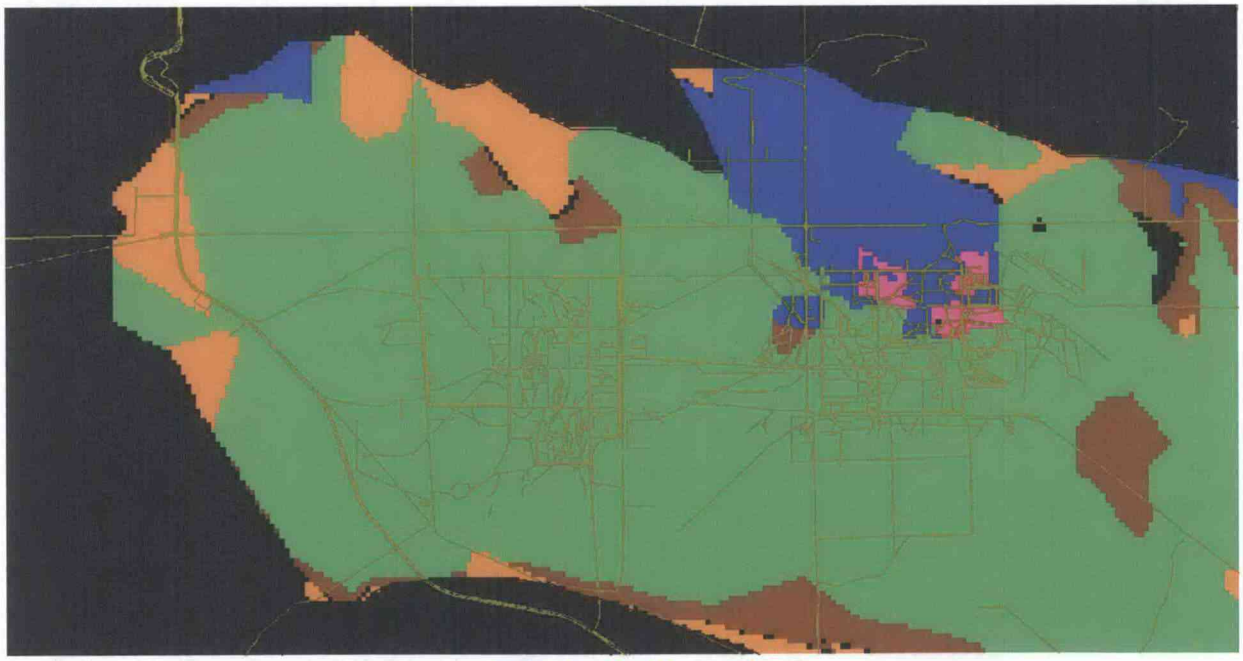

Central Plateau Model Version 2 - Layer 5

**Figure 3-5. Hydrostratigraphic Units of Layer 5**

## 3.2 Simulation Periods

Predictive simulation periods are summarized in Table 3-2. The predictive simulations are divided into four segments. Dates given are an approximate reference. The exact time period would depend on the actual start first phase of the ZP-1 pump-and-treat system.

An initial three year segment from 2008 to 2011 simulates "current" conditions. Pumping rates simulate the "phase 0" period of the ZP-1 pump-and-treat system. The second segment is also three years in duration, from 2011 to 2014. This simulates phase 1 (1000 gpm) period of the ZP-1 pump-and-treat system. The third segment is 22 years in duration, from 2014 to 2026. This simulates phase 2 (2000 gpm) period of the ZP-1 pump-and-treat system. The fourth and final segment simulates 975 years of post-ZP-1 pump-and-treat system implementation, when it is assumed no pumping will occur.

**Table 3-2. Temporal Discretization of the 200-PO-1 RI Simulations**

| Model | Stress Period | Duration | Description |
|---|---|---|---|
| 200-PO-1 RI | 1 | 3 years | Current 200-ZP-1 interim remedial measure, operating at approximately 350 gpm total extraction/injection rate. |
| 200-PO-1 RI | 2 | 3 years | First phase of final 200-ZP-1 pump-and-treat remedy operating at 1,000 gpm. |
| 200-PO-1 RI | 3 | 22 years | Second phase of final 200-ZP-1 pump-and-treat remedy operating at 2,000 gpm. |
| 200-PO-1 RI | 4 | 975 years | Post-ZP-1 pump and treat system implementation, when it is assumed no pumping will occur |

gpm = gallons per minute

## 3.3 Processes Simulated and Limitations

The Central Plateau flow model is limited to saturated flow in the unconsolidated aquifer above the basalt basement with the following limitations:

- Fluid flow and transport in the vadose zone above the aquifer are not simulated
    - Transport of contaminants from the vadose zone, or other sources, to the saturated aquifer is not simulated as a future process
- Fluid flow through the basalt bedrock is assumed to be zero
- Recharge from flow along the basalt surface into the aquifer is simulated as recharge to the aquifer.

The Central Plateau transport model simulates advection, dispersion, diffusion, and sorption of contaminants, and simulates decay for radionuclide and chemical reaction as a decay process for some contaminants with the following limitations:

- The transport model assumes linear sorption and non-interacting (i.e., independent) species.
- Fluid density variations due to fluid chemistry, contaminant concentrations, or temperature variations are assumed to be negligible.

Continuing sources to the groundwater from the overlaying unsaturated zone are not simulated, therefore transport results are not predictions of future contaminant concentrations. The model results are, instead, predictions of the contribution of present contamination in the groundwater to future contaminant concentrations. Inclusion of continuing sources is planned for the later Feasibility Study (FS) of the 200-East Area.

## 3.4 Boundary Conditions

The basalt top elevation defines the bottom and most side boundaries. These are depicted as the grey regions in Figure 3-6.

Two gaps where the water table is above the top of Gable Ridge/Mountain are treated as specified head. These are shown as blue lines in Figure 3-1 Hydraulic head is held constant at the 2008 level for predictive calculations, based upon data used for the model calibration period (1944-2008). The western gap water level assigned from well 699-63-90 acquired from the Hanford Environmental Information System (HEIS). The Gable Gap was assigned from water level data for well 699-60-60 acquired from HEIS.

Eastern boundary below Gable Mountain treated as a mixed boundary condition (MODFLOW general head boundary, or GHB); this boundary is depicted with a vertical green in Figure 3-1. The GHB conductance was determined through model calibration as described in ECF-200PO1-10-0259 MODFLOW Model for the Central Plateau.

The southeastern boundary is shown with a horizontal green line in Figure 3-6. The part of the southeastern boundary directly north of the rattlesnake ridge sub-crop was determined through model calibration to act as a no flow boundary. East of this portion of the southeastern boundary, a mixed boundary condition was used.

With regard to the recharge flux boundary applied at the top of the model domain:

- For the predictive simulations the primary source of recharge to groundwater is aerial precipitation, together with recharge from the ephemeral Cold Creek and Dry Creek stream beds, and injection/discharge at the Treated Effluent Disposal Facility (TEDF) and State Approved Liquid Disposal Site (SALDS) facilities.
- Rates determined for 2009 were held constant during the simulation.

With regard to pumping well operations (sink terms), current and planned operation of the ZP-1 pump-and-treat system were used to set future pumping rates for the predictive simulation:

- Locations and rates from DOE/RL-2008-78, 200 West Area 200-ZP-1 Pump and Treat Remedial Design Remedial Action Work Plan, Draft A.
- Phase 1 of the ZP-1 pump and treat system was assumed to start in year three of the simulation. Current operational conditions of the system were assumed to continue for the first three years.
- A program called AllocateQwell was used to apportion the total pumping rate of the wells between layers based on the open screen intervals of the wells, hydraulic conductivity of the layers, and the saturated thickness of the layers. The flow is apportioned to be consistent with the transmissivity of each layer.
- The ZP-1 pump and treat system was assumed to be shut down after three years of phase 1 and 22 years of phase 2 operation.

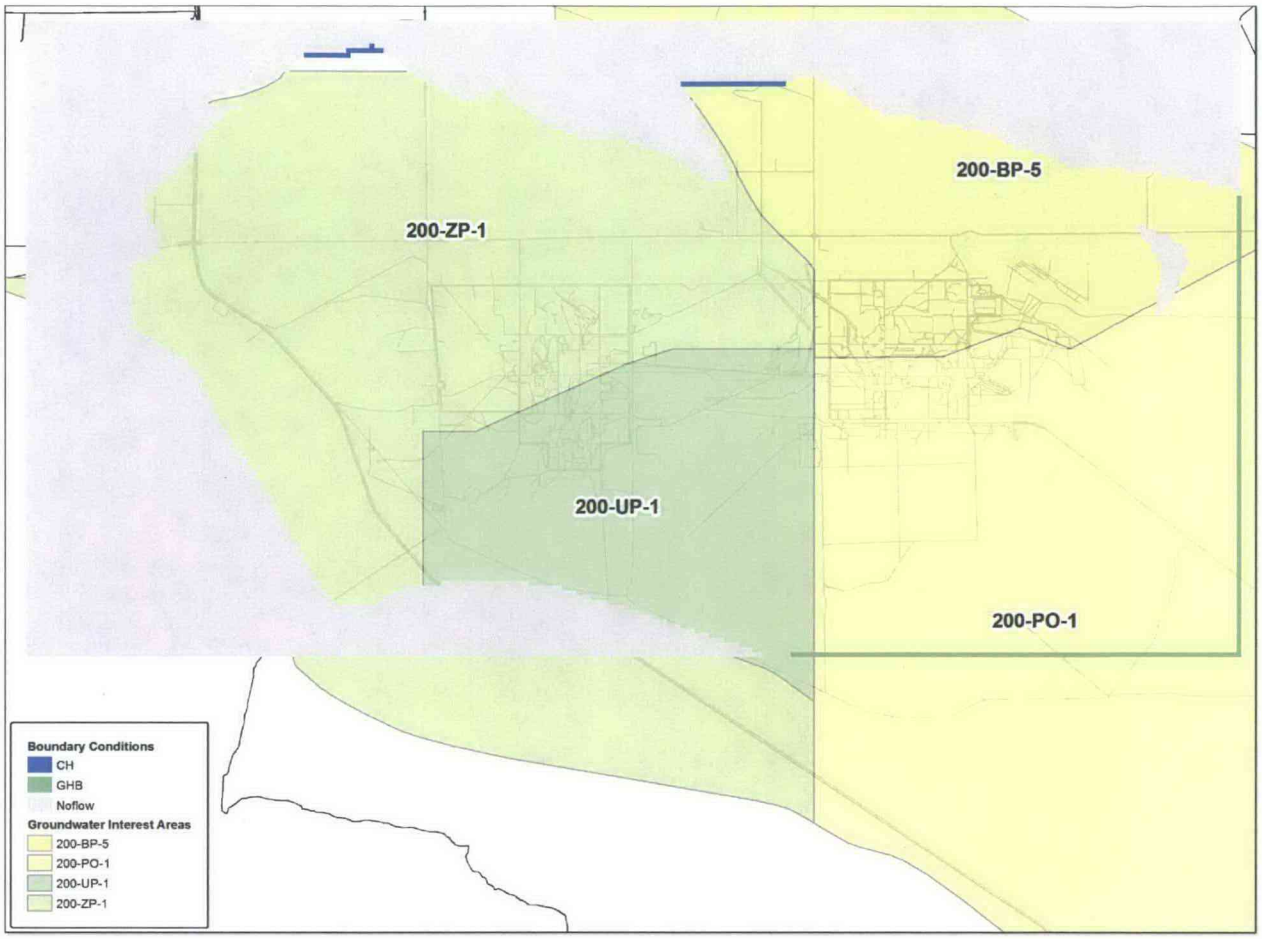


**Figure 3-6. Flow Model Boundary Conditions**

## 3.5 Initial Hydraulic Head Distribution

The unconfined aquifer of Central Plateau is not presently in a steady state condition. It is still recovering from the disposal of large quantities of water during the operational period of the Hanford Reservation. The hydraulic head calculated for the last year of the historic flow model was used as the initial hydraulic head distribution for the predictive simulations. (See ECF-200PO1-10-0259 MODFLOW Model for the Central Plateau) This distribution was extracted from the head solution file *ZP_H_V6.hds* of the historic simulation using the utility program *starthead_d.exe.*

## 3.6 Contaminant Initial Conditions

Contaminant transport simulations performed for the following constituents: carbon tetrachloride, trichloroethene, tetrachloroethene, tritium, strontium-90, iodine-129, technetium-99, nitrate, and uranium. Selection of the COPCs is described in Chapter 6 of DOE/RL-2009-85.

HEIS qualified data for measured contaminant concentrations measured in 2008 was primarily used to estimate the spatial distribution of contaminants of concern in 2008, the nominal starting point for future transport predictions. The measured contaminant concentration was acquired in four ways then combined into a master database (AllWellData_4:.accdb):

1. The measured contaminants samples from screened wells data set was organized as four separate queries of HEIS that were segregated by OU domain:

    a. 200PO1_Filtered_LimitedCons.mdb

    b. 200UP1 Supporting Tables2003.mdb

    c. 200ZP1_05_Data.mdb

    d. 200BP5_05_Data.accdb

    These are combined into Table RA_combined in the master database.

2. For measured contaminant samples from discrete sample surveys, separate queries of HEIS were conducted to gather all of the discrete sample survey data for the entire model domain. These were later combined into a separate table (August_26_depth_samples) of the master database.

3. The combined data set from the ZP-1 RI/FS (DOE/RL-2007-28) (this is Table AditionalZP-1 of the master database):

    a. The initial data compilation was a collective effort by personnel from Pacific Northwest National Laboratory (PNNL); S.S. Papadopoulos and Associates, Inc. (SSP&A); Fluor Hanford, Inc.; and Vista Engineering Technologies, LLC. This is described further in *Spatial Analysis of Contaminants in 200 West Area Groundwater in Support of the 200-ZP-1 Operable Unit Pre-Conceptual Remedy Design* (PNNL-18100).

    b. That database includes well sample data, well construction information, water table elevations, fields describing the sources of the concentration data, and data quality flags, for wells with sample data throughout the 200-West area. Those data were drawn from several sources that can be traced back to standard Hanford data sources, including:

        i. The Hanford Environmental Information System (HEIS) database and the Hanford Well Information System (HWIS) database:

        ii. The 200-ZP-1 OU RI data set (DOE/RL-2006-24, Remedial Investigation Report for the 200-ZP-1 Groundwater Operable Unit)

        iii. The 200-ZP-1 FS data set (DOE/RL-2007-28)

    In addition to the three-dimensional, depth-discrete concentration data, this database was supplemented by two-dimensional data sets used to map contaminants in *Hanford Site Groundwater Monitoring for Fiscal Year 2007* (DOE/RL-2008-01).

    There is duplication of data in the combined data set from the ZP-1 RI/FS and other data sources. Duplications are identified and eliminated by the kriging program QuantVar.

4. Data from US Ecology acquired from an e-mail data transmission Robert Haight to John McDonald, August, 11, 2009. These data are supplemental to HEIS and provide information in a region not covered in the HEIS database.

    a. USENONRADGW08.xls

    b. USEGWTRITto CH2M.xls

    c. USEGW07to CH2M.xls

d. USEGURANto CH2M.xls

e. USEG08to CH2M.xls

Well location and well screen data was added to the database.

The combined data sets were processed using Microsoft Access©[1]. The following steps were used in the processing:

1. Data is rejected if the samples were filtered or they are identified with a Z or Y (suspect) flag in the LAB_QUALIFIER.
2. Data was rejected as non-representative if it was acquired prior to 2005.
3. In many cases, contaminant concentrations were less than the detection limit, which is noted in the "laboratory qualifier" field in the database. These concentrations were flagged as "non-detect." Non-detect concentrations were replaced by half of their stated detection value, which is a common practice in environmental analysis (*Statistical Methods for Environmental Pollution Monitoring* [Gilbert 1987]). Nitrate samples with a non-detect qualifier were set at the non-detect value rather than ½ of the non-detect value. The values listed Iodine-129, tritium, and strontium-90 with non-detect qualifiers were also used at the reported value unless they were less than zero, in which case zero was used.
4. For each screened well, data was gathered into cohorts by year and an average value for that year was calculated.
5. If the data set for a screened well contained data in year 2008 then the average for the year 2008 was used as the measured value for that well. The year 2008 was used in preference to 2009 because the 2008 data set was more complete that 2009 and was stable in 2009 when this processing was being done.
6. If there were no 2008 data available for a well then the averaged data for the most recent year in the period 2009-2005 was used.

Well location and well screen data was used in combination with the model elevations to identify which model layers the measured concentrations for a well applied to. If the well screen overlapped a model layer then the data was assumed to apply to that layer. If discrete samples were within a layer they were applied to that layer. Multiple discrete samples within a layer were averaged. The data for screened wells and discrete samples were processed separately and then merged. If the combined data sets resulted in two samples at the same location the largest sample was used.

The computer program well-layers was used to find the layers that were overlapped by well screens. Inputs to well-layers are the .dis file used to define the Central Plateau model and the starting head file which defined initial water table elevations for the predictive model transport. These water elevations form a good and convenient estimate of the water table when the measurements were made. The program also requires well location and screen top and bottom elevations along with reference coordinates for the Central Plateau model.

On a contaminant by contaminant basis, the master database was programmed to provide separate lists of well coordinates, representative sample value for the well and the well name for each layer. Data for screened measurements and depth discrete samples were processed separately. These lists are collected in

1 Microsoft and Access are registered trademarks of Microsoft Corporation in the United States and other countries.

separate file folders using the file name convention datatype_contaminant_layer (e.g., Screened_Tech-99_L1 contains the list for representative technetium-99 concentration values from wells with screens that overlap layer 1 of the model). The files were condensed to form combined data screen and depth discrete values for each layer and then combined again to form the data input for layers 1 through 3. Input instructions for the program QuantVar were added to the top of these lists to form input files for QuantVar. As described in the next paragraph, the data was processed differently in 200-West and 200-East Areas. Therefore, two input files were formed from the same layer 1 through layer 3 data.

The original concept of segregating contaminant measurements by layer was to provide the most rigorous method for defining variations of contamination with depth. With more appreciation of the variability of model layers with depth and the scarcity of well-defined depth profiles of contamination the approach was rejected for all contaminants except carbon tetrachloride. For carbon tetrachloride the data sets for each of the top three layers was processed using the program QuantVar separately. For all other contaminants the data for the top three layers was combined into a single data set. As with the combining of discrete and screened data, if two data samples existed for a well with differing values the largest value was used.

The program QuantVar was used to interpolate the measured concentrations for a contaminant onto the Central Plateau model grid. QuantVar was used for the analysis of plume extents for the ZP-1 RI/FS as described in DOE/RL-2008-56. The use of QuantVar in the 200-PO-1 RI analysis differs from the use for the ZP-1 RI/FS as follows:

The Central Plateau model domain was divided into two sections. The two sections represent the 200-West area where the predominant flow direction is to the northeast and the 200-East Area where the predominant flow direction is to the southeast. The input to QuantVar in the west specified an orientation of the kriging variogram as 45 degrees east of north. The input to QuatVar in the west specified an orientation of the kriging variogram as 135 degrees east of north. Variogram anisotropy was usually set with a major axis of 1400 m and a minor axis of 700 m. This was varied for some contaminants to reflect the smaller or larger scale of the plumes. The exact variogram specification for each contaminant is preserved in the input files for QuatVar.

The influence of a single data point on kriging is laterally symmetric. Since contaminant plumes tend to be much smaller upstream of the source area, control points were used to limit the extent of the plumes in upstream directions. The plume contours presented in Hanford Site Groundwater Monitoring for Fiscal Year 2008 were downloaded from HEIS. These contours were visualized along with generated contaminant concentrations from QuantVar to appraise the generated contaminant distributions. The contours were primarily used to define region of continuous contaminant plumes. Control points were added to provide concurrence in the continuity of generated plumes and the plume contours.

In a few instances control points were added near representative sample values to increase grid concentrations. This was done when the localized contaminant above the maximum contaminant level (MCL) was at a smaller scale than a single cell of the model. The control points were added to bring the contaminant value of the cell above MCL. These cases are:

- Technitium-99 near well 299-E25-93
- Strontium-90 near well 299-E17-14

Contaminant distributions for the entire model domain were created by merging the 200-West and 200-East distributions. At this stage in the process the contaminant distributions were truncated at concentration levels below ½ MCL. In the case of nitrate, the truncation level was set to 35 mg/L (78% of

MCL). The reason for truncation is that the interpolated concentrations become increasingly unreliable far away from sample locations. Small concentration estimates are biased toward the mean of the representative sample values which are themselves biased by the need to sample where contamination occurs. Truncation was introduced to reduce the influence of this bias.

The contaminant distribution maps were post-processed to ensure that the initial concentrations at model cell locations for wells in and near the Non-radioactive dangerous waste landfill (NRDWL) were the same as the representative contaminant values at the wells. The program NRDWL_conc replaces the kriged values from QuantVar with the measured values at specified well locations. The input files for NRDWL_conc are named contaminant_NRDWL.dat where contaminant is replaced with the name of the estimated contaminant. Estimated contaminant distributions modified by NRDWL_conc are labeled contaminant_layer+NRDWL.asc.

QuantVar creates an ARC/INFO ASCII formatted output file of contaminant distributions. After removing the first five header lines of the file it can be directly read into as input data for MT3DMS. The same data file was used to define the initial contaminant concentration for first three layers of the Central Plateau model, except for carbon tetrachloride for which separate concentrations were interpolated for each layer. In some locations the initial water table was below the bottom of layer three. For these locations the estimated contaminant distribution was applied to layers four and five.

In retrospect, some significant improvements to the determination of initial contaminant concentration could be made. The approach used for the ZP-1 RI/FS of defining contaminant distributions by depth-below-water-table rather than by model layer would have been better. For the majority of contaminants where discrimination by depth is not possible, an algorithm that uses HSU information to translate the interpolated concentrations into model cells would improve the resolution of the initial contaminant distributions.

Plots of the initial plume distributions are presented in Section 5 (these are reported in that section to aid in comparisons to plots of the transport results).

## 3.7 Transport Properties

Table 3-3 contains transport properties that are aquifer properties that may are may not vary with HSU. Table 3-4 contains the constituent specific transport parameters used in the predictive modeling for 200-PO-1 RI.

**Table 3-3. Aquifer Dependent Transport Parameter Values for the Central Plateau Model**

| Property | Value and Units | Comments |
|---|---|---|
| Porosity | 0.15 | Approximate central value; Table D-2 DOE/RL-2007-28 |
| Longitudinal Dispersivity | 50 m | DOE/RL-2008-56 |
| Transverse Dispersivity | m | DOE/RL-2008-56 |
| Vertical al Dispersivity | 0 m | DOE/RL-2008-56 |
| Molecular Diffusion Constant | $m^2$/day | Negligible Term |
| Bulk Density-Hanford | 1.93 g/$cm^3$ | PNNL-18564 Table 6.2 |
| Bulk Density-Cold Creek | 1.93 g/$cm^3$ | PNNL-18564 Table 6.2 |
| Bulk Density-Ringold E | 1.90 g/$cm^3$ | PNNL-18564 Table 6.2 |
| Bulk Density-Ringold Mud | 1.90 g/$cm^3$ | PNNL-18564 Table 6.2 |
| Bulk Density-Ringold A | 1.90 g/$cm^3$ | PNNL-18564 Table 6.2 |

**Table 3-4. Constituent Dependent Transport Parameter Values for the Central Plateau Model**

| Final COPCs | $K_d$ (ml/g) | Half-Life (yr) | Half-Life (day) | Degradation Rate (1/day) | Reference for $K_d$ | Reference for Degradation Rate | Specific Activity (pCi/g) |
|---|---|---|---|---|---|---|---|
| Nitrate | 0.00E+00 | | | No Decay | PNNL-18564, Table 6.9, Sandy Gravel sediment type | | |
| Strontium | 1.20E+01 | 2.88E+01 | 1.05E+04 | 6.601E-05 | PNNL-18564, Table 6.9, Sandy Gravel sediment type | | 1.379E+14 |
| Uranium | 4.00E-01 | 4.47E+09 | 1.63E+12 | 4.25E-13 | PNNL-18564, Table 6.9, Sandy Gravel sediment type | | 3.360E+05 |
| Iodine-129 | 1.00E-01 | 1.57E+07 | 5.73E+09 | 1.21E-10 | PNNL-18564, Table 6.9, Sandy Gravel sediment type | | 1.765E+08 |
| Technetium-99 | 0.00E+00 | 2.11E+05 | 7.71E+07 | 8.99E-09 | PNNL-18564, Table 6.9, Sandy Gravel sediment type | | 1.711E+10 |
| Tritium | 0.00E+00 | 1.23E+01 | 4.50E+03 | 1.54E-04 | PNNL-18564, Table 6.9, Sandy Gravel sediment type | | 9.664E+15 |
| Carbon Tetrachloride | 3.00E-03 | 4.13E+01 | 1.51E+04 | 4.60E-05 | PNNL-16100 (Rev 1), 200-UP-1 sediments, Phase 2 (Table 5.5) | PNNL-13560, Table 18, Most Probable Value | |
| Tetrachloro-ethene (PCE) | 7.49E-02 | | | No Decay | See Empirical Calc sheet | No Hanford relevant reference | |
| Trichloro-ethene (TCE) | 2.50E-02 | | | No Decay | See Empirical Calc sheet | No Hanford relevant reference | |

# 4 Software Applications

In accordance with PRC-PRO-IRM-309, *Controlled Software Management*, software applications fit one of two categories, spreadsheets, or utility calculation. Software used in this calculation is approved software.

## 4.1 Approved Software

The following software was used to perform calculations and were approved and compliant with PRC-PRO-IRM-309 (PRC-PRO-IRM-309, *Controlled Software Management)*. These software are managed under the following documents consistent with PRC-PRO-IRM-309: CHPRC-00257 Rev 0, *MODFLOW and Related Codes Functional Requirements Document*, CHPRC-00258 Rev 0, *MODFLOW and Related Codes Software Management Plan*, CHPRC-00259 Rev 0, *MODFLOW and Related Codes Software Test Plan*, CHPRC-00260 Rev 0, *MODFLOW and Related Codes Acceptance Test Report*, and CHPRC-00261 Rev 0, *MODFLOW and Related Codes Requirements Traceability Matrix*. CHPRC-00259 Rev 0 distinguishes between safety software and support software based on whether the software managed calculates reportable results or provides run support, visualization, or other similar functions. Brief descriptions of the software used are provided below.

### 4.1.1 Description

Descriptions for the software packages used in the calculation follow.

#### *4.1.1.1 MODFLOW-2000*

- Software Title: MODFLOW-2000 (Open File Report 00-92, MODFLOW-2000, the U.S. Geological Survey modular ground-water model -- User guide to modularization concepts and the Ground-Water Flow). Used for flow modeling; solves the transient groundwater flow equations using the finite difference discretization technique.
- Software Version: Version 2.1.18 modified for minimum thickness (Build: mf2k_1_18_mst_Dec10_2009_dble)
- HISI Identification Number: HISI #2517 (Classified as Safety Software, Graded Level C).
- Workstation type and property number: See Software Installation and Checkout Forms (attachments)

#### *4.1.1.2 MT3DMS-2000*

- Software Title: MT3DMS-2000 (SERDP-99-1, *MT3DMS: A modular three-dimensional multispecies transport model for simulation of advection, dispersion, and chemical reactions of contaminants in groundwater systems; Documentation and user's guide*). Used for transport modeling: solves the transient advection/dispersion transport equations using the finite difference discretization technique.
- Software Version: Version 5.2 (Build: mt3d_reaction_dble)
- HISI Identification Number: HISI #2518 (Classified as Safety Software, Graded Level C).
- Workstation type and property number: See Software Installation and Checkout Forms (attachments)

#### *4.1.1.3 Support Software*

Support software used that will be added to next revision of the MODFLOW and Related Codes Software Management Plan:

- **allocateQ**: constructs a MODFLOW well package ("WEL") file. Identifies water table elevations at proposed remedy well locations, and processes the hydraulic conductivity and saturated thickness data so that, so that flow for fully-penetrating wells that penetrate multiple model layers can be properly apportioned according to layer transmissivity.

- **Read-lst-budget**: creates a file "prefix"-budget.out that will be bought into a spreadsheet to tabulate and plot (a) the volumetric budget terms (IN and OUT), and (b) the mass balance error of the MODFLOW simulation, as reported by MODFLOW at the end of each interval specific in the output control (OC) file.

- **Read-MT3D-Out-Budget**: This is an error checking routine that compiled the mass balance reports of MT3D into a single readable file, in a manner similar to READ-LST-BUDGET for MODFLOW.

    - **Starthead**: created the initial hydraulic head conditions for the predictive flow calculations by plucking the last time step head result from historic run heads output.

    - **MakeRecharge**: created the RCH input files for both the historic and predictive model simulations, specifying recharge values from natural, artificial, and overland flow data sets.

    - **Well-layers:** determined the layers in the model that a well screen of a particular well overlaps.

    - **NRDWL_conc:** replaced the contaminant concentrations from QuantVar program with specified concentrations at specific cell locations.

    - **Groundwater Vistas:** collated model information into MODFLOW input files, provided graphical tools used for model quality assurance.

#### *4.1.1.4 Single-Purpose Software*

Single purpose software is software whose calculation products are approved through quality assurance and technical review of this environmental calculation file:

- **Quantvar**: used to create estimated plume initial conditions. The routine undertakes a uniform-score ("quantile") transform of the variable using a rank-and-percentile table constructed using the input variable, performs ordinary kriging (GSLIB routine KT3 ; Deutsch and Journel, 1992, *GSLIB Geostatistical Software Library and User's Guide*) on the transformed variable, and back-transforms the kriging estimates using the same rank-and-percentile table.

### 4.1.2 Software Installation and Checkout

Safety Software (MODFLOW, MT3DMS) were checked out in accordance with procedures specified in CHPRC-00258 Rev 0. Executables were obtained from the Software Owner who maintains the configuration managed copies in MKS Integrity, installation tests identified in CHPRC-00259 Rev 0 performed and successful installation confirmed, and Software Installation and Checkout Forms were completed and approved for installations used to perform model runs reported in this environmental calculation file. Copies of the Software Installation and Checkout Forms for approved users and installations are provided in Appendix 1. Approved Users are registered in HISI for safety software.

The actual programs used were modified from the original CHPRC Build 0001 (single precision compilation) to overcome numerical problems associated with the transport calculations. The version used has not yet been placed under CHPRC-00259 Rev 0 control.

### 4.1.3 Statement of Valid Software Application

The software packages identified above was used consistent with their respective intended uses for CHPRC as identified in CHPRC-00257 Rev 0 and are valid uses of these software packages for the problems addressed in this application. These software packages were used within their limitations.

The actual programs used were modified from the original CHPRC Build 0001 (single precision compilation) to overcome numerical problems associated with the transport calculations. The version used has not yet been placed under CHPRC-00259 Rev 0 control.

# 5 Calculation

Details of the calculation and resulting simulation predictions are provided in this section.

## 5.1 Overview of the Flow Solution

An overview of the flow solution is presented in this section. Figure 5-1 displays the initial hydraulic head distribution used as the initial condition in the model. The initial hydraulic head was obtained from last stress period of the historic flow model used to calibrate the Central Plateau model as explained in Section 3.5.

The plots of hydraulic head and contaminant transport are all on the same scale to make comparisons of transport distances and concentration changes more readily apparent than would be the case if the scales were chosen to maximize the resolution of each plot. The background images of all the plots are the same. The outline of the model domain is shown with a dark band. The grey areas just inside the boundary are regions that are not actively used in the model. These are mostly regions where basalt subcrops above the water table but also includes small regions in the northern part of the model that are between the domain boundary and the fixed hydraulic head boundaries of the model.

The model interior is shown in white, black, and grey. White indicates regions where at least one layer in the model is partially saturated. Black is used for regions of the model domain where all the layers are unsaturated in the predictive model run. These regions had saturated layers during the peak water table elevations during the historic period used for model calibration. Grey is used to depict small regions where the water table never rises above the basalt even in the calibration period. Roads of the Central Plateau are also shown in grey. Within the model domain blue lines indicate boundaries of the active model that are open to flow. As discussed in Section 3.4 these boundaries are variously constant flux, fixed head or of mixed type.

Prominent features of the head distribution are the relatively flat gradients in most of the 200-PO-1 OU especially under the 200-East area. In the northeast portion of 200-PO-1 the gradients dip steeply to the northeast. These steep gradients indicate flow blockage caused by the Ringold mud unit in this region. The extensive black regions in the northern portion of the model reveal that the connection of the 200-East region to the Gable gap has been almost completely severed by basalt above the water table. Thus flow from the northern edge of western portion of the model domain is simulated to move southeast rather than north as was true in the past.

In the 200-West area and west of there the gradient is mostly due east. The steep gradient is caused by the much lower hydraulic conductivity of the Ringold A and E units compared to the Hanford formation and the Cold Creek HSU.

Near the western gap the influence of a small patch of saturated Hanford formation is causing the flat gradient next to the gap. Divergence of fluxes from the cold creek stream and the much smaller dry creek are clearly evident along the western boundary of the domain.

The hydraulic head one year into the simulation is displayed in Figure 5-2. The head distribution has changed very little except under 200-West where the impact of the current ZP-1 pump and treat system is evident. During the ZP-1 pump-and-treat operation, twenty-five years into the simulation (Figure 5-3), the pumping and extraction wells form prominent features in the hydraulic head distribution. After another fifty years (Figure 5-4) the flow pattern has the same basic shape as the initial conditions but the gradients in the western portion of the domain are much less steep. The hydraulic head under 200-West has dropped by approximately five meters, whereas the head under 200-East has dropped by less than a meter. This

indicates that simulated flow velocities are predicted to be much slower at this time compared to the beginning of the simulation period. Figure 5-5 shows that the simulated water table in 200-West has dropped another meter in the fifty years from year 75 to year 125 of the simulation. At year 125, the Central Plateau aquifer simulation has almost entirely recovered from the water table buildup of the operational period.

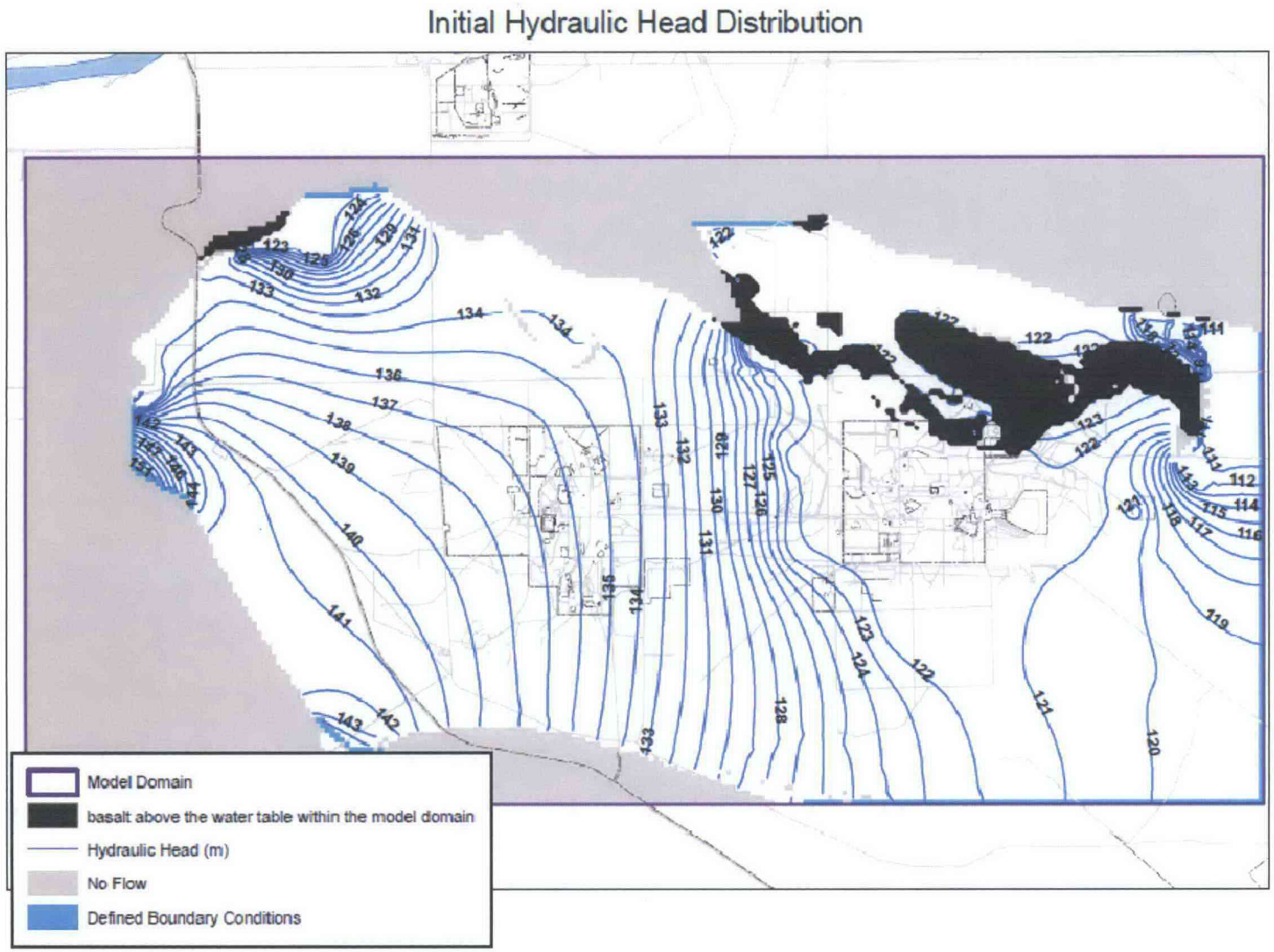


**Figure 5-1. Initial Hydraulic Head Distribution**

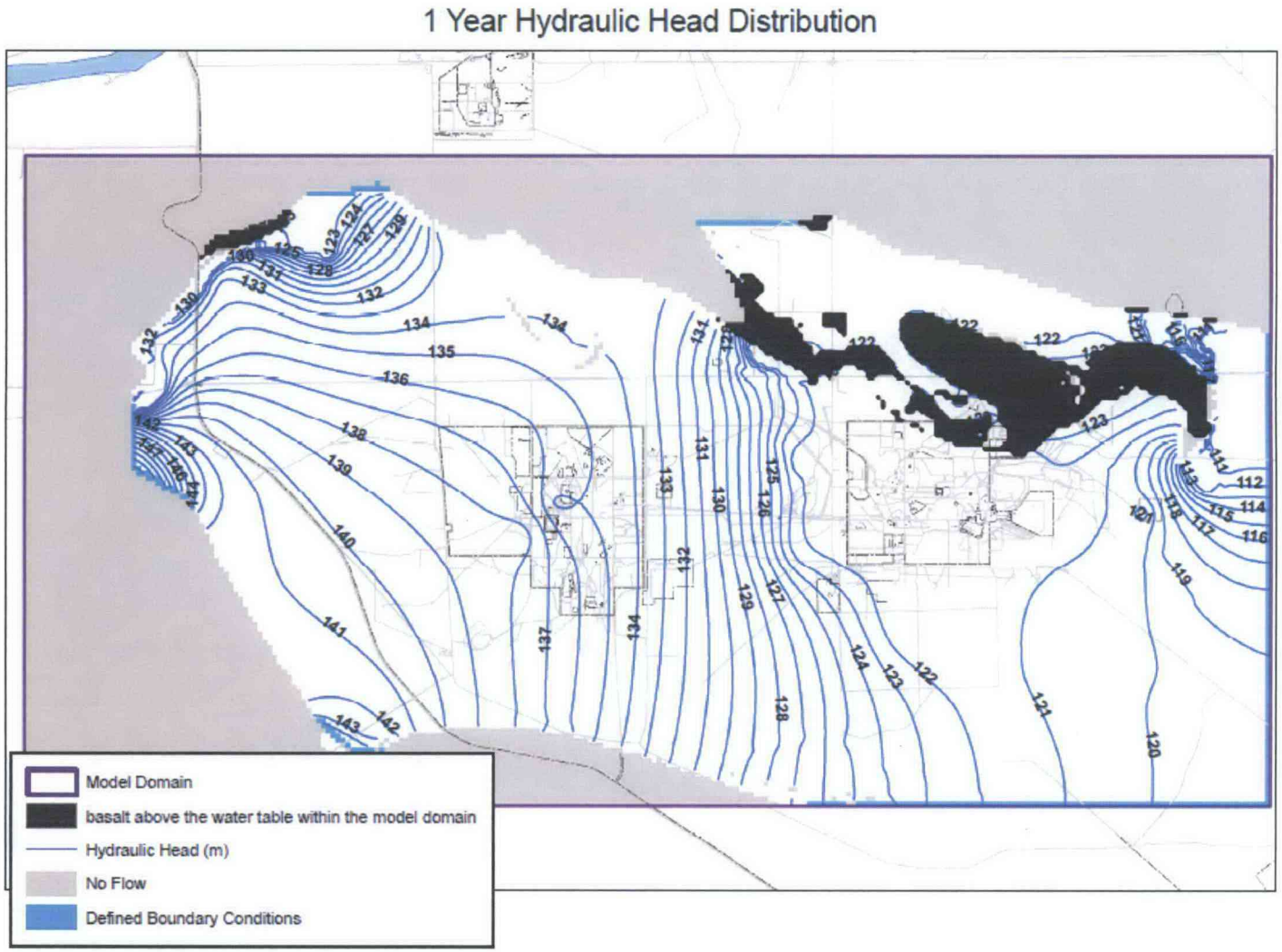


**Figure 5-2. 1-Year Hydraulic Head Distribution**

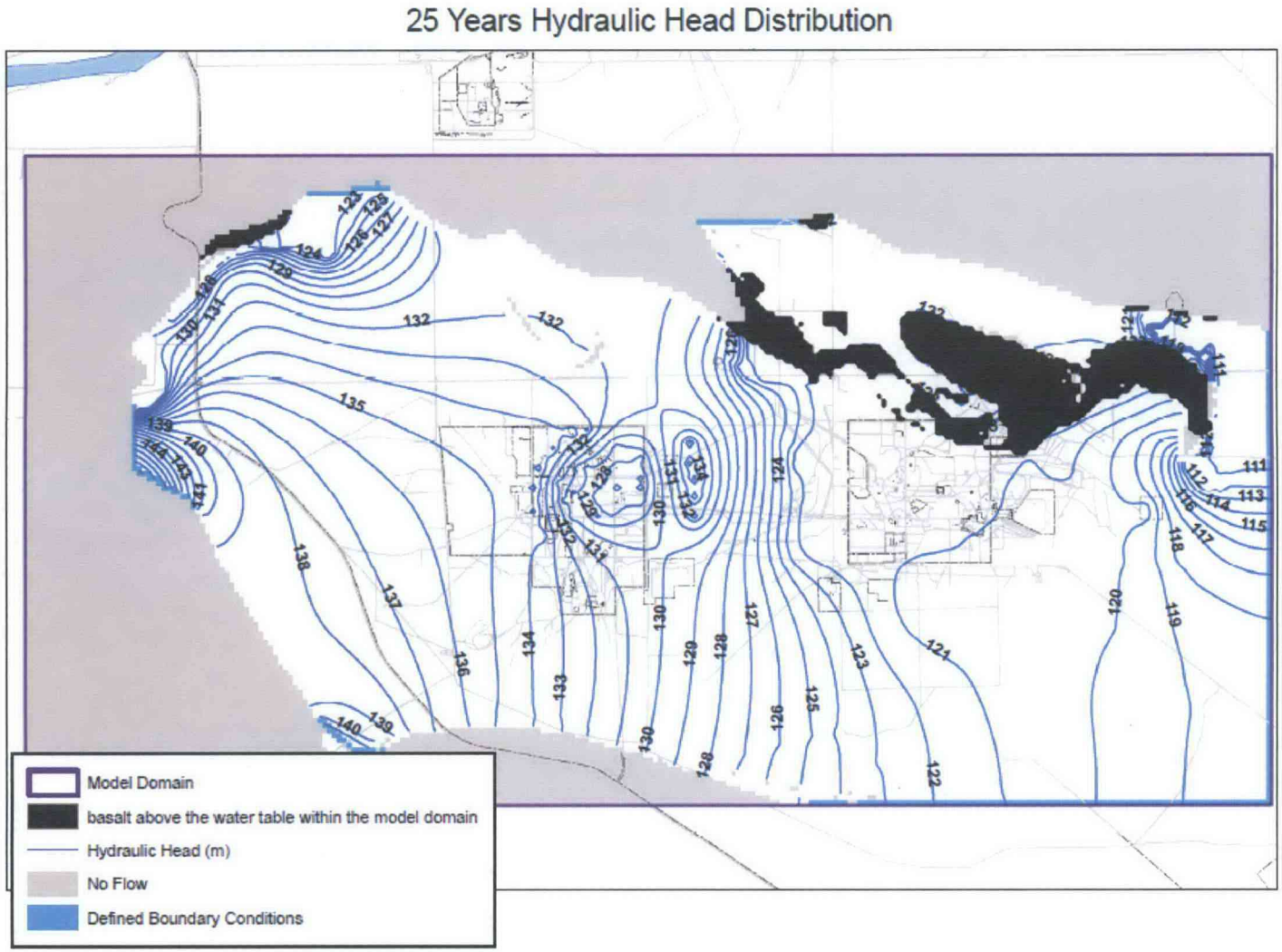


**Figure 5-3. 25-Year Hydraulic Head Distribution**

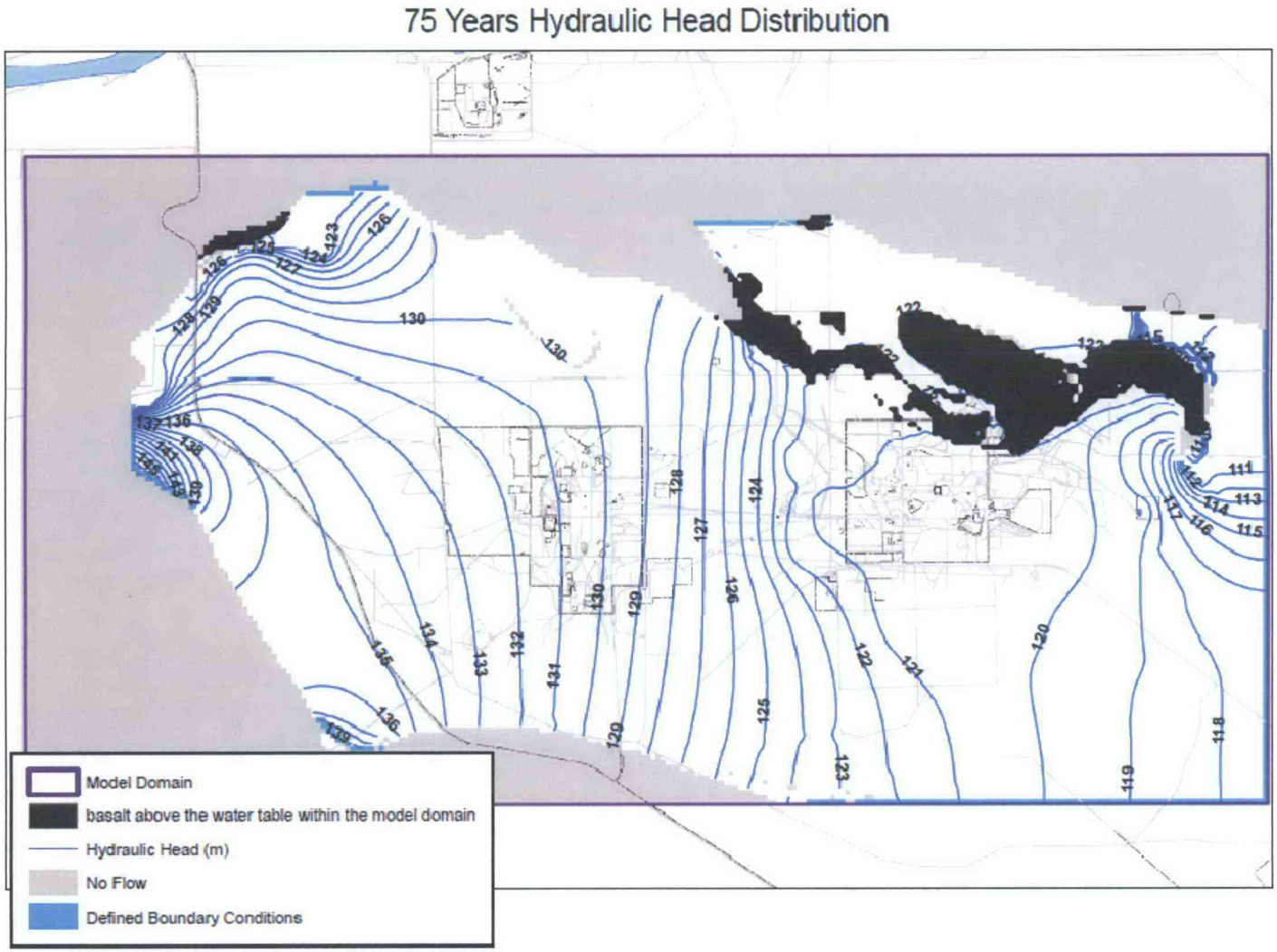


**Figure 5-4. 75-Year Hydraulic Head Distribution**

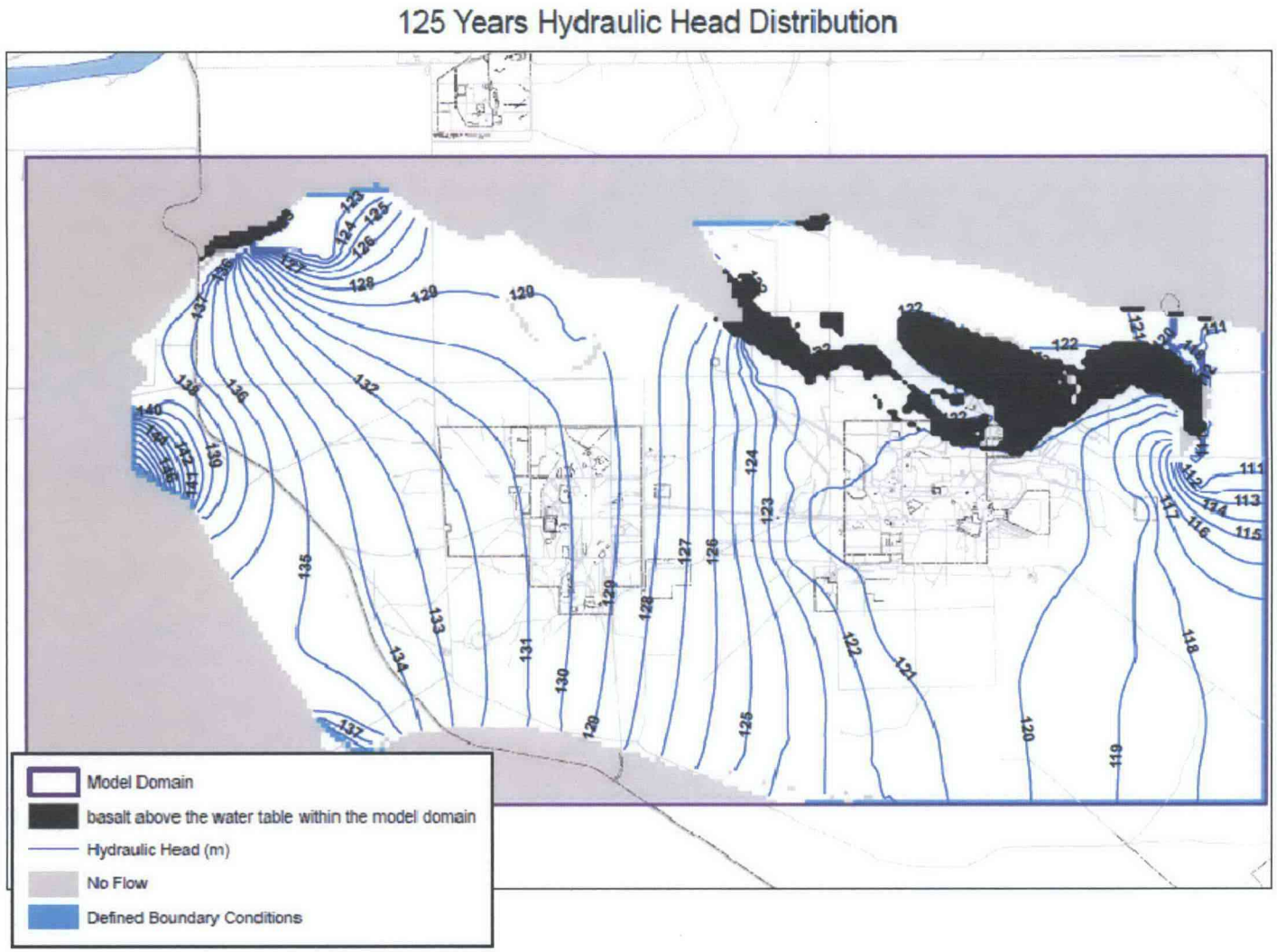


**Figure 5-5. 125-Year Hydraulic Head Distribution**

## 5.2 Contaminant Concentration Distributions

Contaminant concentration distributions were recorded at five time points; The initial distribution, one year into the simulation, after 25 years of simulation, after 75 years of simulation, and after 125 years of simulation. These contaminant distributions are presented in Figure 5-7 through 5.10.4. The greatest concentration that was calculated throughout the five layers at any position is plotted as the concentration for that position.

The contamination distributions are presented in terms of their respective MCL. Contamination below ½ MCL is not shown. One-half MCL was chosen as the cut-off because the initial plume distributions were truncated at ½ MCL to avoid unwanted bias in the total mass of contaminants introduced by the estimation procedure (See Section 3.6). The initial distributions are plotted using a color scale from ½ MCL to peak concentration. Concentrations ranging from ½ MCL to MCL are depicted in green. Concentration ranging from MCL to 10×MCL are depicted in light pink. Concentration ranging from 10×MCL to 100×MCL are depicted in dark pink. There were no initial or simulated concentrations above 100×MCL. The plots show peak concentration in any model layer at that position.

In addition, the estimated COPC concentrations in groundwater as a function of time are presented for selected locations in the model. A total of twenty three monitoring locations are selected based on the plume configuration and its spatial extent for the purpose of presenting the results. The monitoring locations are shown in **Error! Reference source not found.**. Locations that coincide with the existing monitoring wells are identified by the well name. Others are identified using Central Plateau for control point. The concentrations observed in groundwater for these COPCs at the initial conditions were all sufficiently high as to form a basis for remedial action based on the COPC selection and exposure point concentration analysis presented in Chapter 6 of this report. The time varying concentration results for each COPC at all of the selected locations is presented in a tabular manner. Note that the model has five layers and thus concentration data for a given spatial location are available from each model layer. To make the comparisons more meaningful, only the highest concentration among the five layers is reported at the given time for each monitoring location. For the purpose of presentation, the number of time points have been reduced from the number of model reported time steps, but care is taken to retain enough time points to capture the trend in concentration variation. The simulated time period is 1000 years.

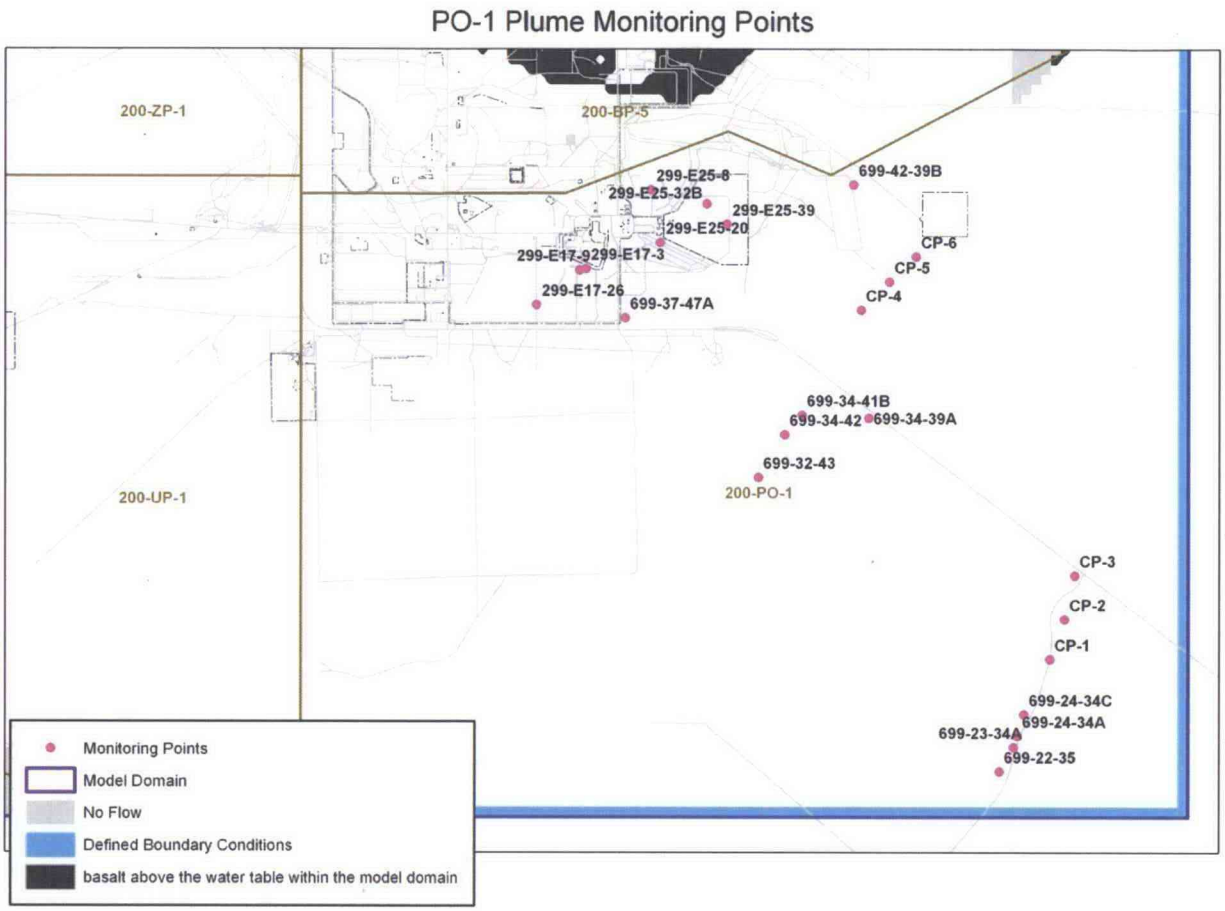


**Figure 5-6. Simulated Monitoring Locations**

### 5.2.1 Tritium

The estimated distribution of current tritium contamination is presented in Figure 5-7. Tritium above the MCL exists in the 200-PO-1 OU below B-Pond and in the highly transmissive channel between the 200-East Area and the southeast corner of the model domain (see Figure 5-7). The reader should not infer that the complexity displayed in the initial concentration shapes indicates knowledge of contaminant distributions at the scale of the complexities. The uncertainty range in the spatial distribution varies with the density of monitoring locations. Monitoring locations are sparse in most of the channel region. Hence, the complexity evident in this area is consistent with the contaminant data but has a large uncertainty associated with it.

There is a very large plume of tritium above MCL in the 200-UP-1 OU. The initial distribution of this plume partly resides in the Ringold E unit. The contamination of the Ringold E is an assumption (Section 3.6). In the high conductivity channel, data to support or refute this assumption is lacking (See Section 6.1.1). The transmissive channel of the Hanford unit coincides with the southeastern extent of this plume.

Figure 5-2 presents the simulated transport results after one year. The southward movement of the ½ MCL boundary of the plume is caused by transport through the Hanford formation unit in 200-East southwestward into the highly transmissive channel. This is a good place to remind the reader that replenishment of the plume by continuing sources is not simulated. The simulation indicates an extension

of the UP-1 plume into the channel region. Once in the channel it gets diluted by flux coming in from the north.

Figure 5-9 shows the simulated tritium distribution after 25 years of transport and radioactive decay. Radioactive decay has reduced tritium concentrations to approximately ¼ of the original levels. The residual concentrations above MCL are associated with the > 10×MCL region of the initial concentration distribution. The residual high concentrations are in the Ringold E (layer three) HSU. Ringold E has a hydraulic conductivity of 5 m/day in the model compared to 8500 m/day and 100 m/day respectively for overlaying Hanford and Cold Creek HSUs. Correspondingly transport velocities within Ringold E are much less in this region. Within the UP-1 OU the size of the tritium plume has reduced by radioactive decay.

Tritium concentrations after 50 years of simulated transport are all below ½ MCL. Therefore, no tritium plots are presented for either the 50 year or 125 year time frames.

Table 5-1 presents the time varying concentration results for the monitoring locations. Temporal plots of concentration at monitor locations are presented in Figure 5-6. Only locations that have concentrations above 0.1×MCL at some time are displayed.

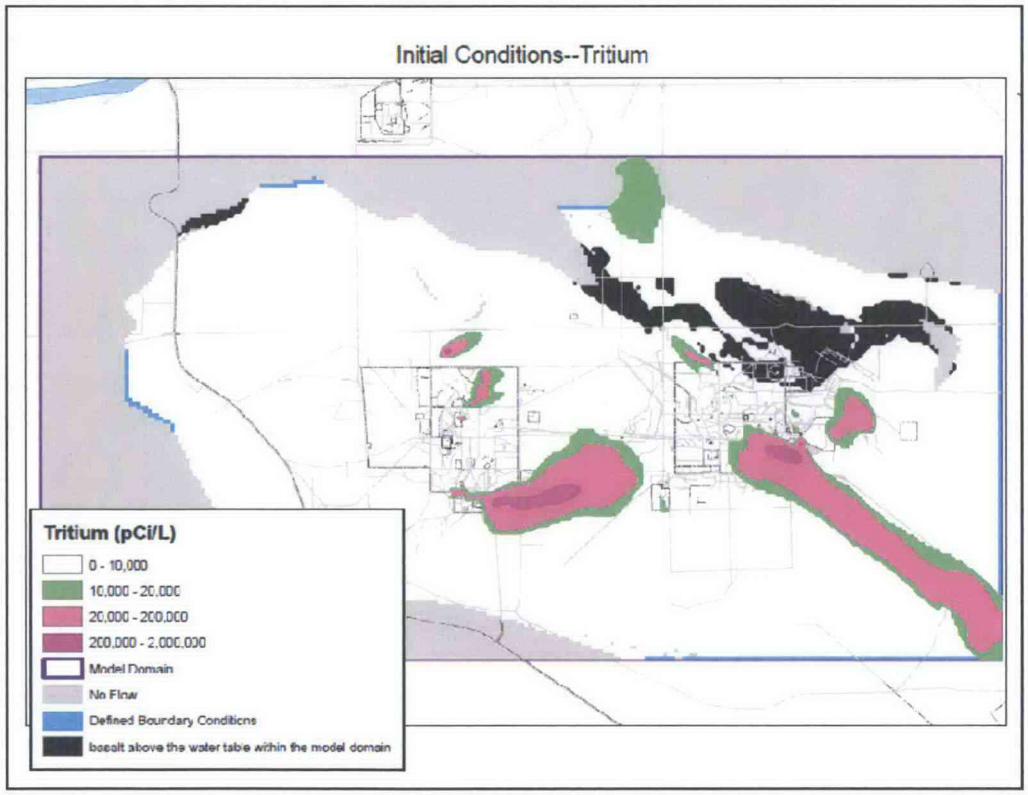


**Figure 5-7. Initial Distribution of Tritium (2008)**

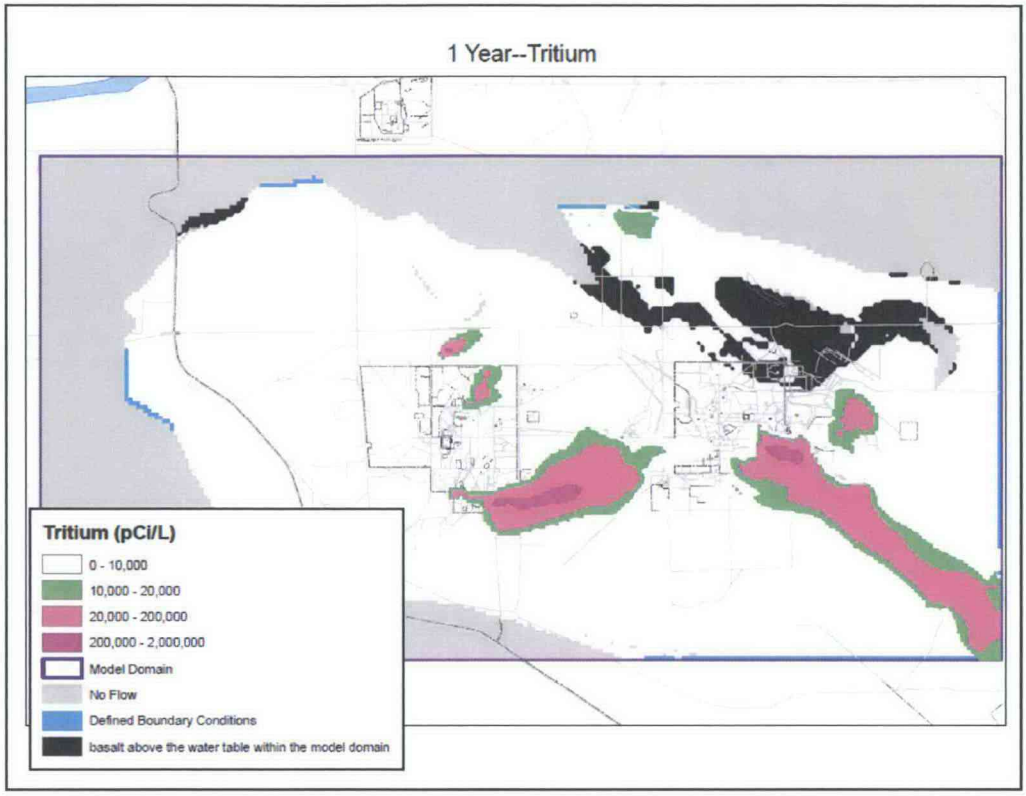


**Figure 5-8. Tritium Distribution after 1 Year (2009)**

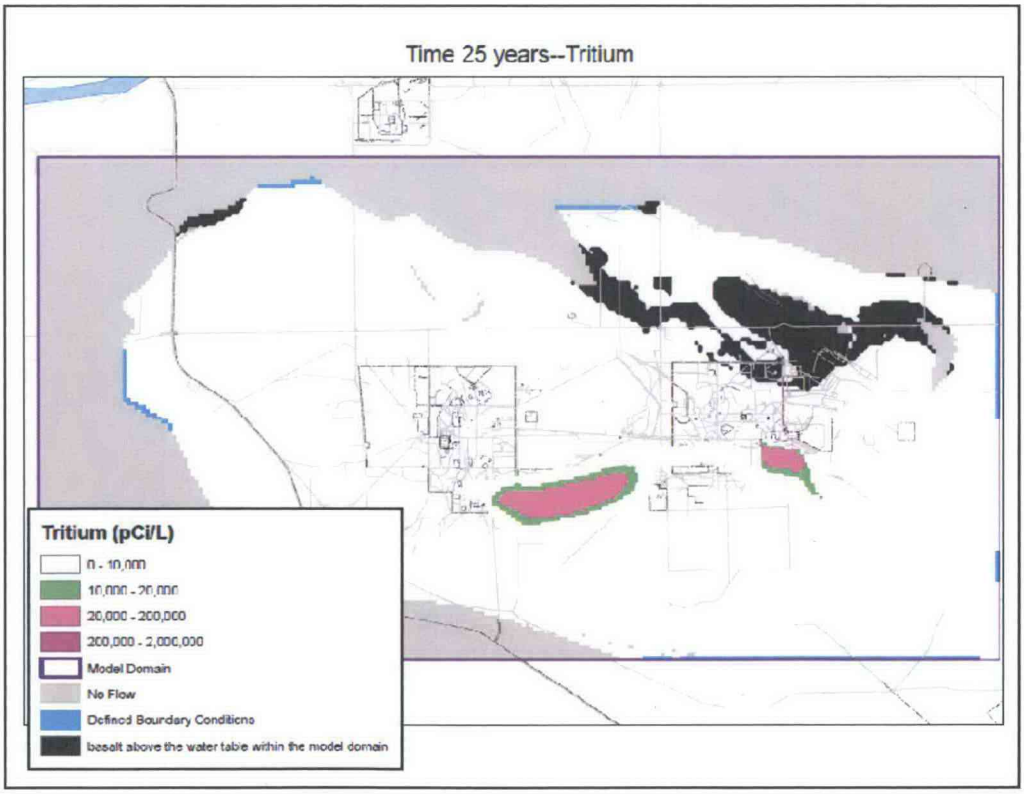


**Figure 5-9. Tritium Distribution after 25 years (2034)**

This page intentionally left blank.

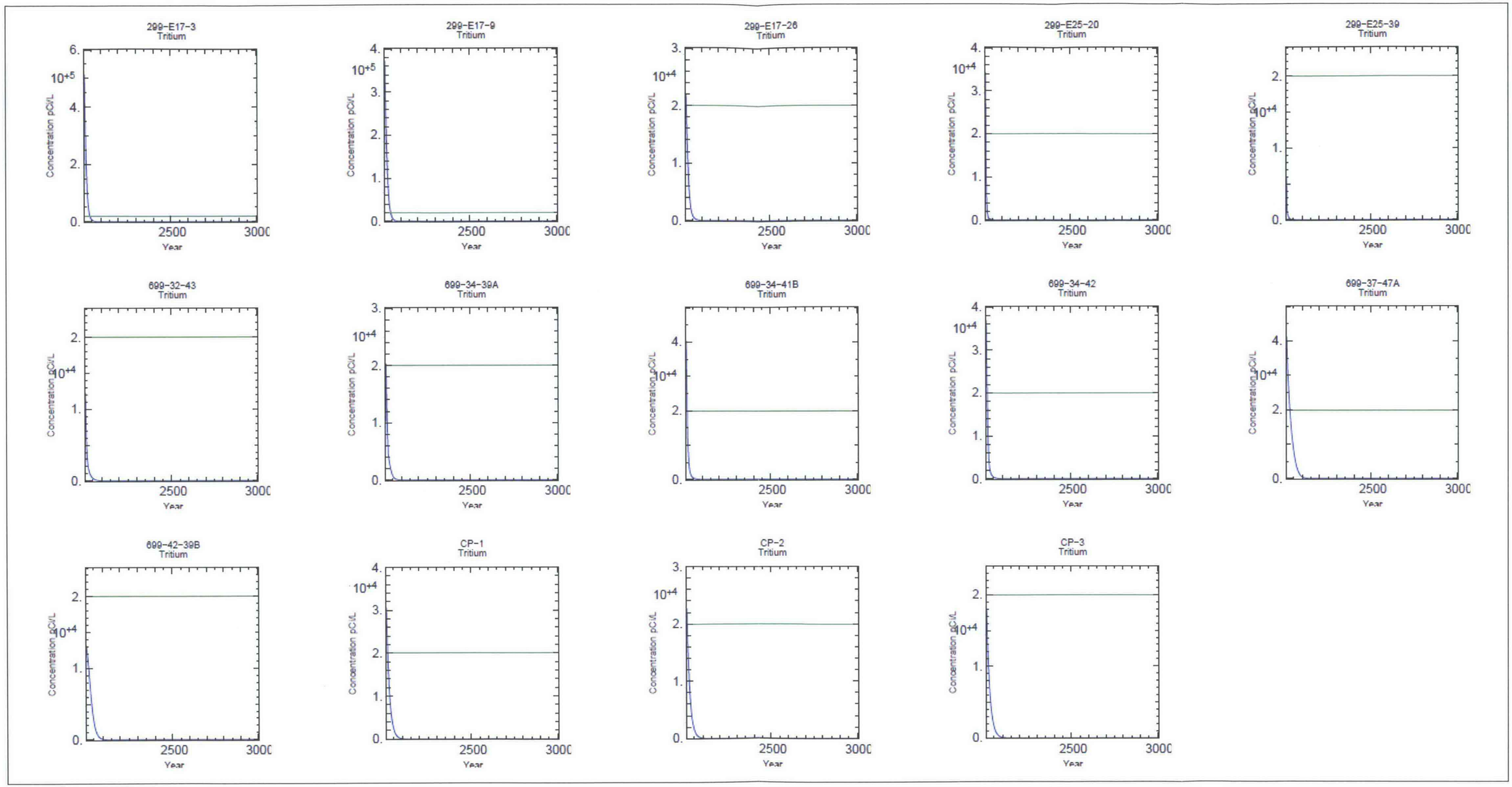


**Figure 5-10. Largest Tritium Concentrations at Monitor Locations**

**Table 5-1. Maximum Concentration of Tritium (pCi/L) for Monitoring Locations at Selected Time Steps**

| Time (Years) | 299-E17-26 | 299-E17-3 | 299-E17-9 | 299-E25-20 | 299-E25-32B | 299-E25-39 | 299-E25-8 | 699-22-35 | 699-23-34A | 699-24-34A | 699-24-34C | 699-32-43 | 699-34-39A | 699-34-41B | 699-34-42 | 699-37-47A | 699-42-39B | CP-1 | CP-2 | CP-3 | CP-4 | CP-5 | CP-6 |
|---|---|---|---|---|---|---|---|---|---|---|---|---|---|---|---|---|---|---|---|---|---|---|---|
| 1 | 2.19E+04 | 5.13E+05 | 3.72E+05 | 3.42E+04 | 2.55E+02 | 5.87E+03 | 4.46E+02 | 8.58E-10 | 1.79E-06 | 1.79E-08 | 3.25E+02 | 1.23E+04 | 1.04E+04 | 4.03E+04 | 3.68E+04 | 4.12E+04 | 1.31E+04 | 3.06E+04 | 2.27E+04 | 1.79E+04 | 1.57E-03 | 1.70E-10 | 5.27E-12 |
| 5 | 1.79E+04 | 3.37E+05 | 2.68E+05 | 7.27E+03 | 8.15E+02 | 1.21E+03 | 7.87E+02 | 1.00E-05 | 6.30E-04 | 1.76E-01 | 8.76E+02 | 6.54E+03 | 1.71E+04 | 2.39E+04 | 2.51E+04 | 3.49E+04 | 1.21E+04 | 2.35E+04 | 1.77E+04 | 1.40E+04 | 1.57E+01 | 2.53E-03 | 7.00E-05 |
| 10 | 1.23E+04 | 1.92E+05 | 1.73E+05 | 1.83E+03 | 6.26E+02 | 6.73E+02 | 2.83E+02 | 8.00E-05 | 1.05E-01 | 7.80E-01 | 6.02E+02 | 3.23E+03 | 8.84E+03 | 1.02E+04 | 1.04E+04 | 2.89E+04 | 1.10E+04 | 1.71E+04 | 1.28E+04 | 1.06E+04 | 5.12E-01 | 2.16E-01 | 3.97E-02 |
| 50 | 3.98E+02 | 2.76E+03 | 3.84E+03 | 3.88E+01 | 2.95E+01 | 3.46E+01 | 2.24E+01 | 8.40E-04 | 2.67E-01 | 1.05E+00 | 4.76E+01 | 2.63E+02 | 3.69E+02 | 2.53E+02 | 2.77E+02 | 5.72E+03 | 1.65E+03 | 1.42E+03 | 9.77E+02 | 1.10E+03 | 2.74E+00 | 2.73E+00 | 1.80E+00 |
| 100 | 2.14E+01 | 6.13E+01 | 5.32E+01 | 2.11E+00 | 9.86E-02 | 3.30E-01 | 5.64E-01 | 1.80E-04 | 4.43E-02 | 1.42E-01 | 2.86E+00 | 1.49E+01 | 1.20E+01 | 1.19E+01 | 1.39E+01 | 2.99E+02 | 6.82E+01 | 5.98E+01 | 4.40E+01 | 5.48E+01 | 8.55E-01 | 1.03E+00 | 3.74E-01 |
| 200 | 6.56E-02 | 4.25E-02 | 5.17E-02 | 4.84E-03 | 9.70E-04 | 6.80E-04 | 8.80E-04 | 1.52E-06 | 2.30E-04 | 5.80E-04 | 7.69E-03 | 4.27E-02 | 2.31E-02 | 2.54E-02 | 3.26E-02 | 2.30E-01 | 7.07E-02 | 9.38E-02 | 9.74E-02 | 1.21E-01 | 5.18E-03 | 8.84E-03 | 6.41E-03 |
| 300 | 1.90E-04 | 4.00E-05 | 7.00E-05 | 1.00E-05 | 3.94E-06 | 1.74E-06 | 1.61E-06 | 4.95E-09 | 6.35E-07 | 1.50E-06 | 2.00E-05 | 1.00E-04 | 4.00E-05 | 5.00E-05 | 7.00E-05 | 6.80E-04 | 6.00E-05 | 1.80E-04 | 3.10E-04 | 3.70E-04 | 1.00E-05 | 2.00E-05 | 1.00E-05 |
| 400 | 5.71E-07 | 6.30E-08 | 1.17E-07 | 1.97E-08 | 1.15E-08 | 5.35E-09 | 3.51E-09 | 1.26E-11 | 1.45E-09 | 3.39E-09 | 3.87E-08 | 2.12E-07 | 9.49E-08 | 1.08E-07 | 1.45E-07 | 1.96E-06 | 8.21E-08 | 5.21E-07 | 8.63E-07 | 9.72E-07 | 2.90E-08 | 2.70E-08 | 2.45E-08 |
| 500 | 1.55E-09 | 1.12E-10 | 2.36E-10 | 4.47E-11 | 3.04E-11 | 1.91E-11 | 8.94E-12 | 2.78E-14 | 3.02E-12 | 7.01E-12 | 8.32E-11 | 4.69E-10 | 2.09E-10 | 2.36E-10 | 3.28E-10 | 6.92E-09 | 1.24E-10 | 1.43E-09 | 2.25E-09 | 2.57E-09 | 8.61E-11 | 5.70E-11 | 5.05E-11 |
| 600 | 3.94E-12 | 2.67E-13 | 5.09E-13 | 1.18E-13 | 7.88E-14 | 7.37E-14 | 8.09E-14 | 5.89E-17 | 6.58E-15 | 1.55E-14 | 1.91E-13 | 1.08E-12 | 7.11E-13 | 1.11E-12 | 1.24E-12 | 2.31E-11 | 1.96E-13 | 3.85E-12 | 5.75E-12 | 6.61E-12 | 2.44E-13 | 1.53E-13 | 1.07E-13 |
| 700 | 9.57E-15 | 1.46E-15 | 1.32E-15 | 1.29E-15 | 9.00E-16 | 7.97E-16 | 1.19E-15 | 1.78E-19 | 1.51E-17 | 3.56E-17 | 4.14E-16 | 2.32E-15 | 2.57E-15 | 6.99E-15 | 7.61E-15 | 7.47E-14 | 3.20E-16 | 1.04E-14 | 1.49E-14 | 1.66E-14 | 6.82E-16 | 4.37E-16 | 2.47E-16 |
| 800 | 2.17E-17 | 1.91E-17 | 1.24E-17 | 1.99E-17 | 1.32E-17 | 1.14E-17 | 1.83E-17 | 5.85E-22 | 4.53E-20 | 8.44E-20 | 7.38E-19 | 9.76E-18 | 9.33E-18 | 3.82E-17 | 4.26E-17 | 2.37E-16 | 7.65E-19 | 2.83E-17 | 3.86E-17 | 4.18E-17 | 2.06E-18 | 1.33E-18 | 6.61E-19 |
| 900 | 3.06E-20 | 3.12E-19 | 1.84E-19 | 3.30E-19 | 2.06E-19 | 1.76E-19 | 3.01E-19 | 1.87E-24 | 1.34E-22 | 2.59E-22 | 2.64E-21 | 4.66E-20 | 5.31E-20 | 1.74E-19 | 2.03E-19 | 7.45E-19 | 8.87E-21 | 7.71E-20 | 9.81E-20 | 1.04E-19 | 1.27E-20 | 1.15E-20 | 2.53E-21 |
| 1000 | 0.00E+00 | 4.72E-21 | 2.83E-21 | 5.03E-21 | 3.28E-21 | 2.80E-21 | 4.62E-21 | 5.84E-27 | 3.75E-25 | 7.61E-25 | 9.05E-24 | 2.08E-22 | 6.87E-22 | 7.89E-22 | 8.39E-22 | 2.35E-21 | 1.35E-22 | 2.04E-22 | 2.12E-22 | 2.31E-22 | 1.81E-22 | 1.72E-22 | 3.10E-23 |

### 5.2.2 Nitrate

Nitrate (as the $NO_3^-$ ion) is present in the model domain in a plume extending from the southeast side of the Plutonium-Uranium Extraction (PUREX) plant and associated with the PUREX cribs. The 200-PO-1 Groundwater OU nitrate plume is not readily distinguishable from nitrate associated with sources in 200-BP-5 Groundwater OU. The nitrate plume is mostly collocated with other plumes in 200-PO-1 Groundwater OU [e.g., tritium, iodine-129, trichloroethene (TCE), and uranium]. An important exception where only nitrate has been found above ½ MCL is a plume to the east of the 200-East area. This plume is in the low conductivity Ringold A and Ringold mud units. Figure 5-11 presents the nitrate initial concentrations. These initial concentrations are truncated at 78% of MCL rather than 50% of MCL to remove low concentration artifacts. There are concentrations above MCL in the 200-East area and just to the east of it. At the southeastern tip of the plume (in 200-East), the Ringold E HSU exists in Layer 3 of the model. Just to the west of this tip the Ringold E unit has been thoroughly removed. The plume east of 200-East resides in both the Ringold E unit and the Ringold Lower Mud unit. There is a very large nitrate plume in the 200-UP-1 OU as well as a number of smaller plumes in the southern part of 200-West.

Figure 5-12 presents the nitrate concentrations after one year of transport. For the last time, the reader is reminded that continuing release of nitrate to the groundwater is not simulated. The figure reveals transport from the 200-BP-5 OU into the 200-PO-1 OU reducing concentrations in 200-BP-5 significantly. The remaining large plume above MCL in the 200-BP-5 portion of 200-East is in a patch of the Cold Creek unit that is surrounded by the more permeable Hanford formation. Flow to the south-southeast is bypassing the patch of Cold Creek to some extent. In the 200-PO-1 OU, where the initial plume resided completely in the Hanford unit, the concentrations have been reduced to below ½ MCL. Where the initial plume distribution was also in Ringold E, the concentrations are still above MCL in that unit. Note that the edge of the ½ MCL plume has moved southeast in the transmissive channel approximately one kilometer. Movement of the plume in the low conductivity units east of 200-East is not discernable. In the UP-1 OU very little transport is evident after one year, except at the western edge of the plume where the plume is entering the channel region.

Twenty-five years into the simulation (Figure 5-13), the 200-East has almost been completely reduced to below ½ MCL except for the small area where the plume started in the Ringold E unit. The size of the plume east of 200-East has been reduced by roughly half. The half that has been reduced was initially in Ringold E unit in layer three. The half that remains is in the Ringold lower mud of layer 4 and 5 because the upper three layers are unsaturated at the start of the simulation. The nitrate plume in 200-UP-1 has changed dramatically. This shows the strong influence of the ZP-1 pump-and-treat system on the nitrate plumes in the 200-UP-1 OU which stopped operation at this time. The southern plumes have been pulled north and largely dispersed to below MCL. The eastern injection wells of the pump-and-treat system have pushed much of the plume into the extraction wells, but have also pushed the northern portion of western edge of the plume into the channel where it has been diluted below ½ MCL. Note the tongue above ½ MCL entering the channel region at the western edge.

At 75 years (Figure 5-14), the plume in the Ringold E portion of 200-East has almost been reduced to below ½ MCL while the plume in the lower mud unit remains above MCL though significantly smaller. In 200-UP-1, the ZP-1 system has been off-line for 50 years. There a residual above ½ MCL near 200-West and still a large plume west of 200-West that is above MCL.

At 125 years (Figure 5-15) only the plume trapped in the mud remains above ½ MCL in the PO-1 OU. This simulated plume has changed only slightly in the last 50 years. In the 200-UP-1 OU the plume has continued to move eastward toward the channel. The concentrations displayed in Figure 5-15 above MCL are in the Ringold mud unit.

Table 5-2 presents the time varying concentration results for the monitoring locations. Temporal plots of concentration at monitor locations are presented in Figure 5-16. Only locations that have concentrations above 0.1×MCL at some time are displayed.

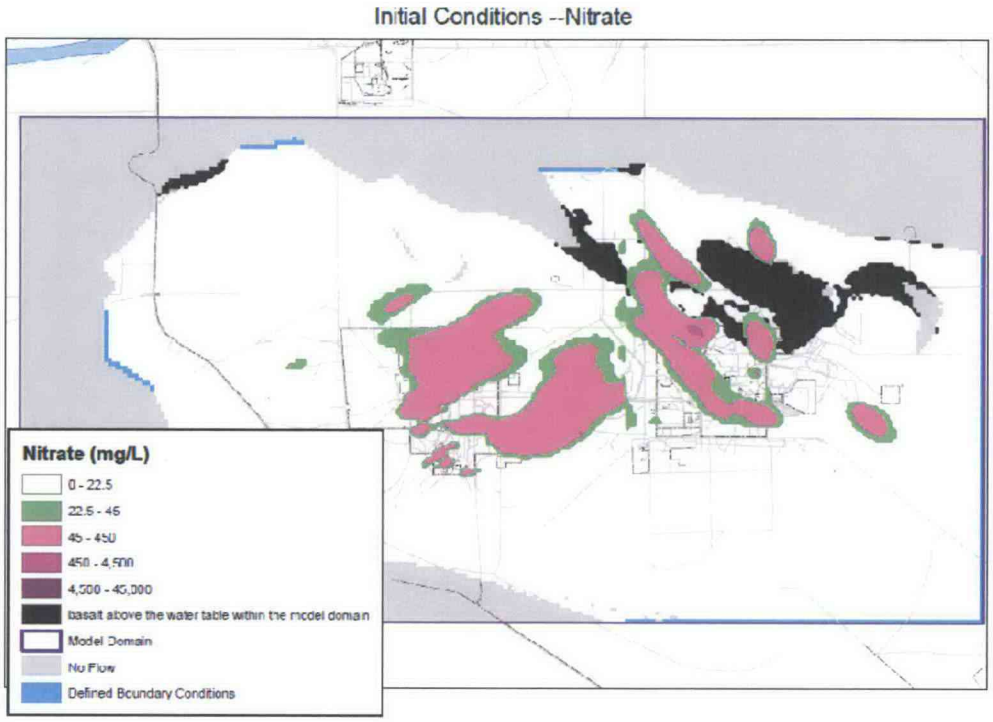


**Figure 5-11. Initial Concentrations for Nitrate (2008)**

1 Year --Nitrate

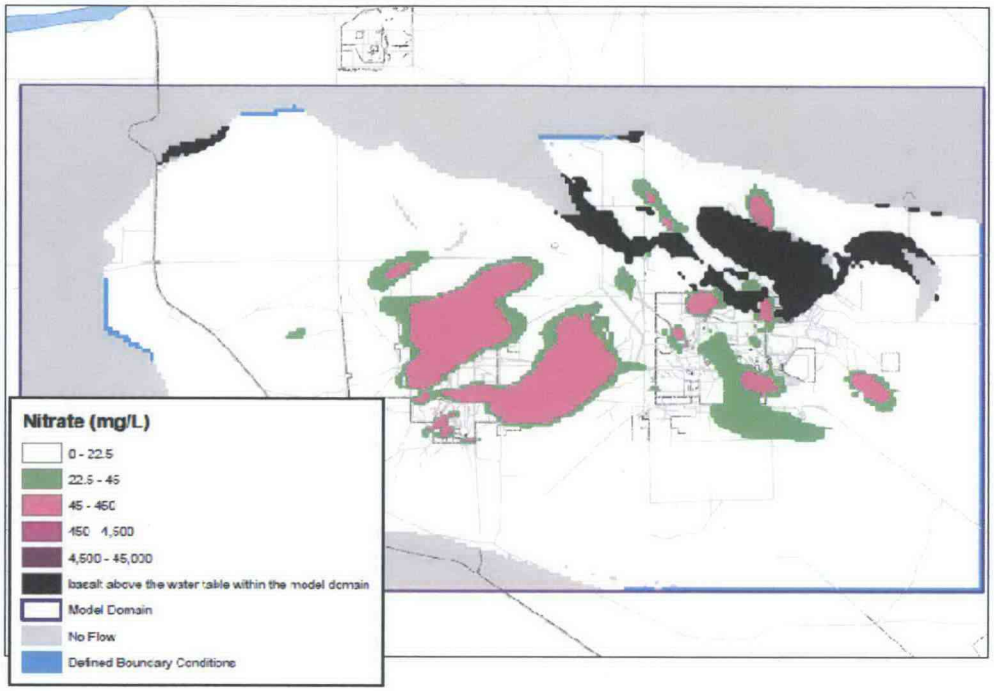


**Figure 5-12. Nitrate Concentrations after One year of Transport (2009)**

Time 25 years --Nitrate

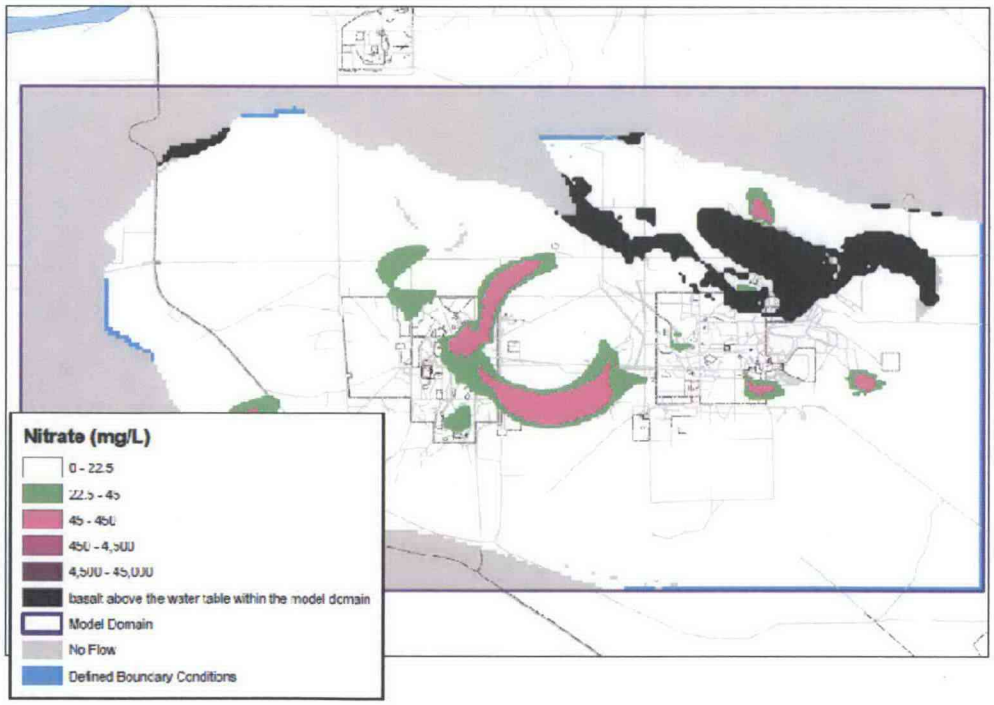


**Figure 5-13. Nitrate Concentrations after 25 years of Transport (2034)**

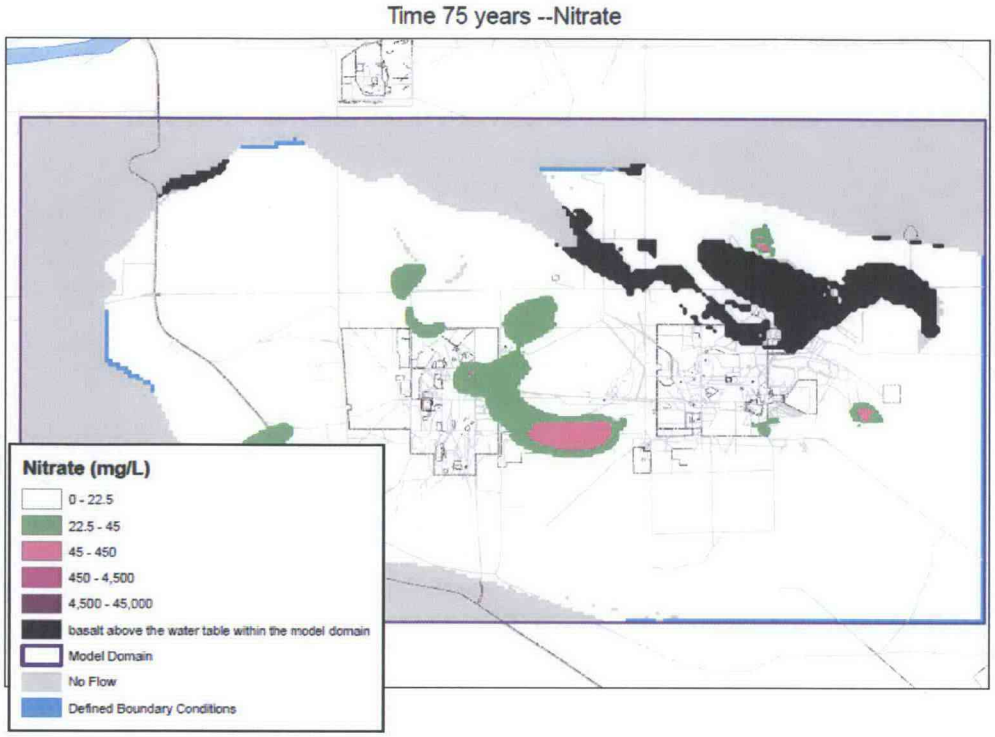


**Figure 5-14. Nitrate Concentrations after 75 years of Transport (2084)**

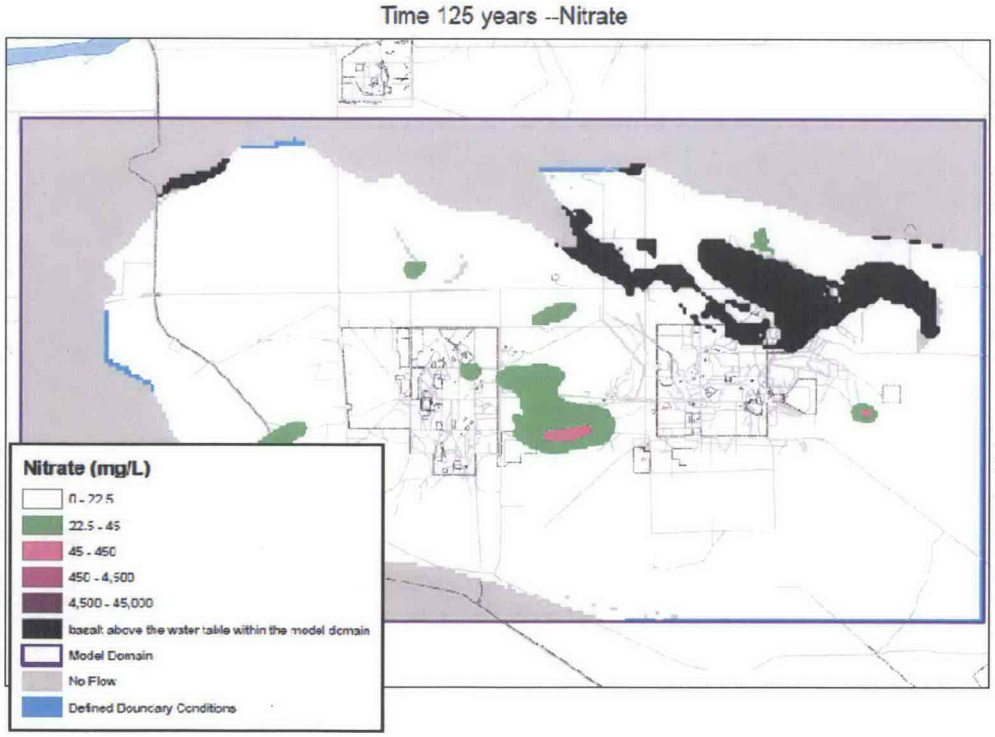


**Figure 5-15. Nitrate Concentrations after 125 years of Transport (2134)**

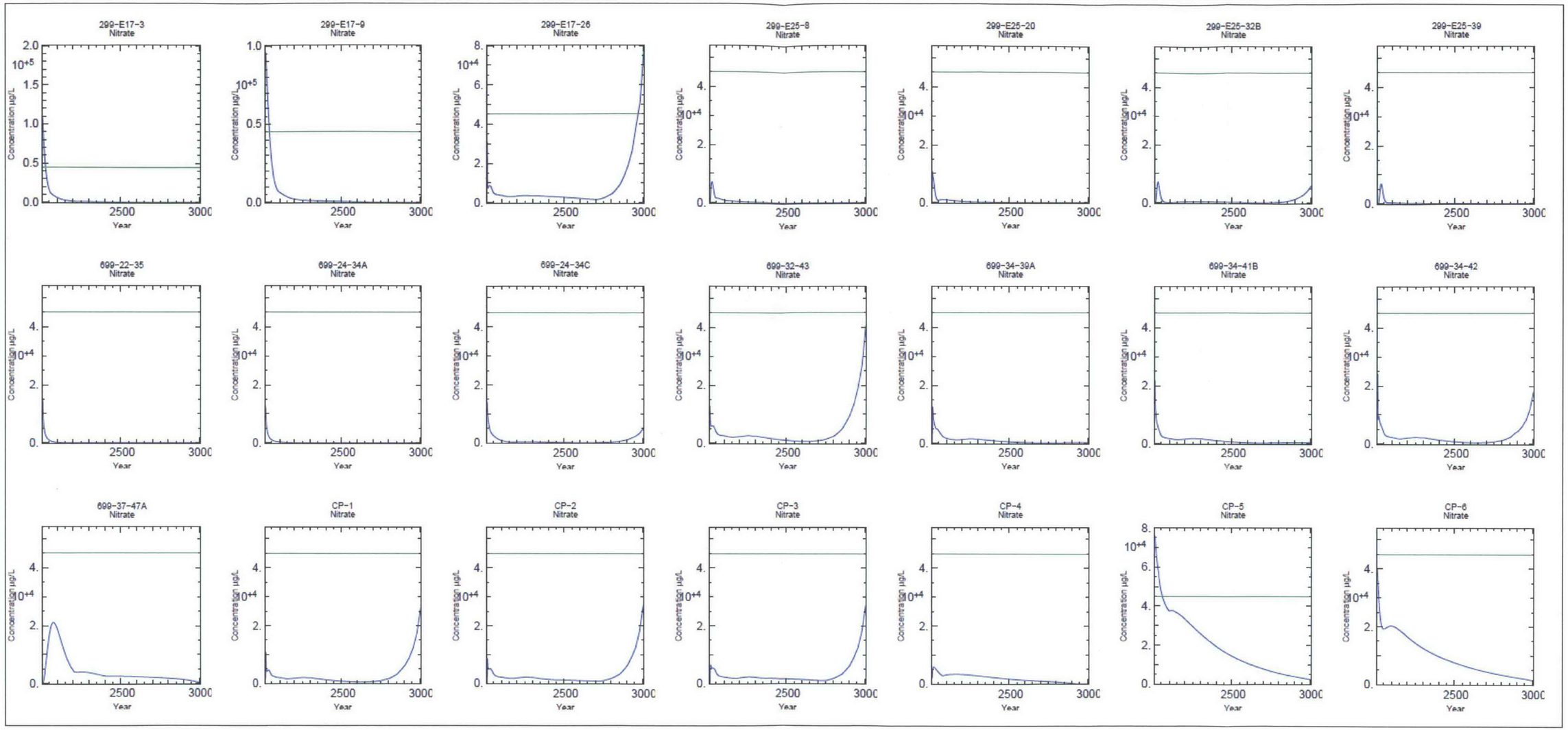


**Figure 5-16. Largest Nitrate Concentrations at Monitor Locations**

## Table 5-2. Maximum Concentration of Nitrate (µg/L) for Monitoring Locations at Selected Time Steps

| Time (Years) | 299-E17-26 | 299-E17-3 | 299-E17-9 | 299-E25-20 | 299-E25-32B | 299-E25-39 | 299-E25-8 | 699-22-35 | 699-23-34A | 699-24-34A | 699-24-34C | 699-32-43 | 699-34-39A | 699-34-41B | 699-34-42 | 699-37-47A | 699-42-39B | CP-1 | CP-2 | CP-3 | CP-4 | CP-5 | CP-6 |
|---|---|---|---|---|---|---|---|---|---|---|---|---|---|---|---|---|---|---|---|---|---|---|---|
| 1 | 3.08E+04 | 1.08E+05 | 9.60E+04 | 5.13E+03 | 2.15E-01 | 3.98E-03 | 9.33E+01 | 1.53E+04 | 7.81E+01 | 1.26E+04 | 1.40E+04 | 4.56E+03 | 4.35E+02 | 1.50E+04 | 1.44E+04 | 1.88E+01 | 6.57E-11 | 1.69E+03 | 1.03E+02 | 3.32E-01 | 2.13E+03 | 7.60E+04 | 4.01E+04 |
| 5 | 7.63E+03 | 9.17E+04 | 8.95E+04 | 9.27E+03 | 2.89E+02 | 1.00E+02 | 2.21E+03 | 9.02E+03 | 2.87E+02 | 7.97E+03 | 1.04E+04 | 8.80E+03 | 1.24E+04 | 1.22E+04 | 1.08E+04 | 4.68E+02 | 3.84E-06 | 6.54E+03 | 7.94E+03 | 3.71E+03 | 4.71E+03 | 7.38E+04 | 3.69E+04 |
| 10 | 8.09E+03 | 7.31E+04 | 7.80E+04 | 8.16E+03 | 2.86E+03 | 1.90E+03 | 6.58E+03 | 5.41E+03 | 4.23E+02 | 5.00E+03 | 7.45E+03 | 6.01E+03 | 8.33E+03 | 9.37E+03 | 9.52E+03 | 1.82E+03 | 8.10E-04 | 4.21E+03 | 4.94E+03 | 6.39E+03 | 5.88E+03 | 6.94E+04 | 3.15E+04 |
| 50 | 4.38E+03 | 1.21E+04 | 1.99E+04 | 9.02E+02 | 6.65E+02 | 8.48E+02 | 1.56E+03 | 6.87E+02 | 4.07E+02 | 8.63E+02 | 2.17E+03 | 3.31E+03 | 3.73E+03 | 2.44E+03 | 3.11E+03 | 1.90E+04 | 2.13E+01 | 2.61E+03 | 2.90E+03 | 3.30E+03 | 3.70E+03 | 4.54E+04 | 1.94E+04 |
| 100 | 3.54E+03 | 5.33E+03 | 5.88E+03 | 9.13E+02 | 9.23E+01 | 3.35E+02 | 7.76E+02 | 1.20E+02 | 1.73E+02 | 2.60E+02 | 8.15E+02 | 2.45E+03 | 1.62E+03 | 1.70E+03 | 2.18E+03 | 1.78E+04 | 2.08E+02 | 1.92E+03 | 2.12E+03 | 2.29E+03 | 3.23E+03 | 3.76E+04 | 2.02E+04 |
| 200 | 3.46E+03 | 1.23E+03 | 1.90E+03 | 4.21E+02 | 3.94E+02 | 1.86E+02 | 4.15E+02 | 2.39E+01 | 2.75E+01 | 4.22E+01 | 3.90E+02 | 2.30E+03 | 1.36E+03 | 1.62E+03 | 2.10E+03 | 3.97E+03 | 4.23E+02 | 1.82E+03 | 1.94E+03 | 2.04E+03 | 3.31E+03 | 3.30E+04 | 1.63E+04 |
| 300 | 3.52E+03 | 8.50E+02 | 1.13E+03 | 2.08E+02 | 4.34E+02 | 1.29E+02 | 2.15E+02 | 1.63E+01 | 1.42E+01 | 2.96E+01 | 4.17E+02 | 2.43E+03 | 1.44E+03 | 1.71E+03 | 2.20E+03 | 3.71E+03 | 1.91E+02 | 1.94E+03 | 2.08E+03 | 2.16E+03 | 2.83E+03 | 2.55E+04 | 1.24E+04 |
| 400 | 3.14E+03 | 4.90E+02 | 7.74E+02 | 1.13E+02 | 3.56E+02 | 1.01E+02 | 1.15E+02 | 1.13E+01 | 1.15E+01 | 2.22E+01 | 2.73E+02 | 1.55E+03 | 8.94E+02 | 1.03E+03 | 1.35E+03 | 2.54E+03 | 8.14E+01 | 1.24E+03 | 1.47E+03 | 1.84E+03 | 2.26E+03 | 1.91E+04 | 9.66E+03 |
| 500 | 2.80E+03 | 2.63E+02 | 5.41E+02 | 5.31E+01 | 2.59E+02 | 8.67E+01 | 5.37E+01 | 7.96E+00 | 9.18E+00 | 1.68E+01 | 1.73E+02 | 9.93E+02 | 5.39E+02 | 6.31E+02 | 8.26E+02 | 2.50E+03 | 3.97E+01 | 7.78E+02 | 1.25E+03 | 1.61E+03 | 1.74E+03 | 1.43E+04 | 7.56E+03 |
| 600 | 2.19E+03 | 6.31E+00 | 3.06E+02 | 0.00E+00 | 1.91E+02 | 7.05E+01 | 0.00E+00 | 5.69E+00 | 7.29E+00 | 1.29E+01 | 1.19E+02 | 6.96E+02 | 2.93E+02 | 3.57E+02 | 5.29E+02 | 2.32E+03 | 1.89E+01 | 5.34E+02 | 1.05E+03 | 1.38E+03 | 1.31E+03 | 1.06E+04 | 5.89E+03 |
| 700 | 1.68E+03 | 0.00E+00 | 0.00E+00 | 0.00E+00 | 1.95E+02 | 2.93E+01 | 0.00E+00 | 4.11E+00 | 5.76E+00 | 9.97E+00 | 1.46E+02 | 9.36E+02 | 2.03E+02 | 2.67E+02 | 5.81E+02 | 2.08E+03 | 1.42E+01 | 6.81E+02 | 8.68E+02 | 1.10E+03 | 9.64E+02 | 7.76E+03 | 4.52E+03 |
| 800 | 4.76E+03 | 0.00E+00 | 0.00E+00 | 0.00E+00 | 4.16E+02 | 0.00E+00 | 0.00E+00 | 3.00E+00 | 4.57E+00 | 1.33E+01 | 3.63E+02 | 2.62E+03 | 2.14E+02 | 3.66E+02 | 1.39E+03 | 1.78E+03 | 7.72E+00 | 1.78E+03 | 1.88E+03 | 1.91E+03 | 6.48E+02 | 5.63E+03 | 3.42E+03 |
| 900 | 1.92E+04 | 0.00E+00 | 0.00E+00 | 0.00E+00 | 1.52E+03 | 0.00E+00 | 0.00E+00 | 2.20E+00 | 1.25E+01 | 3.90E+01 | 1.24E+03 | 9.91E+03 | 2.25E+02 | 4.36E+02 | 4.55E+03 | 1.32E+03 | 0.00E+00 | 6.41E+03 | 6.58E+03 | 6.38E+03 | 1.86E+02 | 3.98E+03 | 2.50E+03 |
| 1000 | 8.00E+04 | 0.00E+00 | 0.00E+00 | 0.00E+00 | 6.25E+03 | 0.00E+00 | 0.00E+00 | 1.63E+00 | 4.57E+01 | 1.48E+02 | 5.15E+03 | 4.10E+04 | 2.43E+02 | 5.07E+02 | 1.86E+04 | 1.38E+02 | 0.00E+00 | 2.65E+04 | 2.76E+04 | 2.75E+04 | 0.00E+00 | 2.43E+03 | 1.56E+03 |

### 5.2.3 Iodine-129

Iodine-129 is present in within 200-PO-1 Groundwater OU portion of the model domain as a continuous plume extending from the vicinity of the PUREX plant in the southeast corner of 200-East Area to the southeast corner of the Central Plateau Groundwater Model domain. This plume exhibits a linear aspect and generally follows the direction of groundwater flow along the paleochannel. Most of the initial condition plume exhibits groundwater concentrations of iodine-129 less than 10 pCi/L.

Initial iodine concentrations for the simulation are displayed in Figure 5-17. Iodine in the model domain of the 200-PO-1 OU exists above MCL in the 200-East area, between 200-East and B-Pond, and in the channel region. As with nitrate transport a significant amount of iodine is simulated to move southeast from the 200-BP-5 OU into 200-PO-1 within the first year of the simulation (Figure 5-18). The majority of the iodine in 200-East is distributed north and northeast of the deepest part of the Hanford channel. The simulated flow velocities north of the deep channel are less than in the channel. Movement in this region is barely evident in Figure 5-18.

After 25 years (Figure 5-19), a hole appears in the plots of peak concentration in the channel southeast of 200-East. In the channel the concentrations in the Hanford unit, mostly layer 1, and in the Cold Creek unit have dropped below ½ MCL. However in the Ringold E unit concentrations remain above MCL. These differences are a reflection of the differing groundwater velocity. The hole appears in the plot because the model does not have Ringold E in that region. As indicated earlier, contamination of the Ringold E unit is uncertain. The Cold Creek unit directly overlays the lower Ringold mud unit and is represented in both layers 2 and 3 in this region (Figure 3-3 and Figure 3-4).

A small lobe of iodine that started between 200-East Area and B-Pond has moved slowly to the southeast (Figure 5-20 and Figure 5-21). This movement is consistent with the existence of the lobe in the initial distribution. It is an example of local complexity that is supported by measurements and by the simulated results. The simulation also indicates some movement of the plume to the east from the channel region at concentrations below MCL. This occurs in a region that has not been sampled for iodine contamination. This region is composed of the Cold Creek unit with hydraulic conductivity intermediate between the Hanford formation and the Ringold units. There is a relatively slow flow eastward into this unit from the paleochannel. Note that the Iodine-129 plume does not enter the Ringold units that host the relatively stagnant nitrate plume east of the 200-East Area.

Table 5-3 presents the time varying concentration results for the monitoring locations. Temporal plots of concentration at monitor locations are presented in Figure 5.3.6. Only locations that have concentrations above 0.1×MCL at some time are displayed.

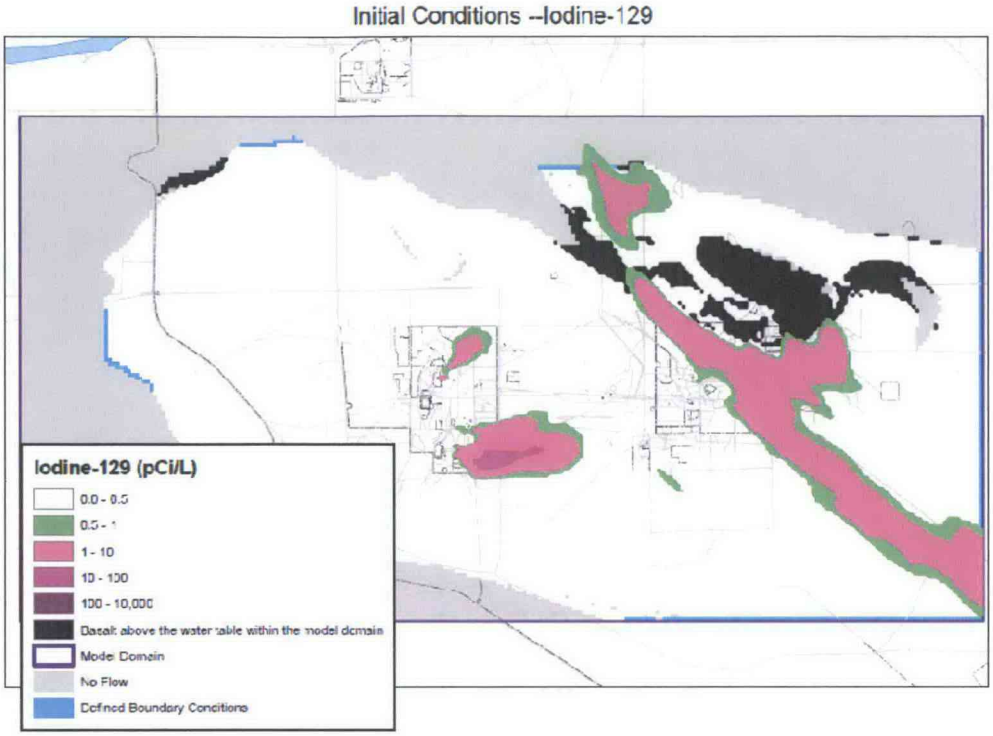


**Figure 5-17. Initial Iodine-129 Concentrations (2008)**

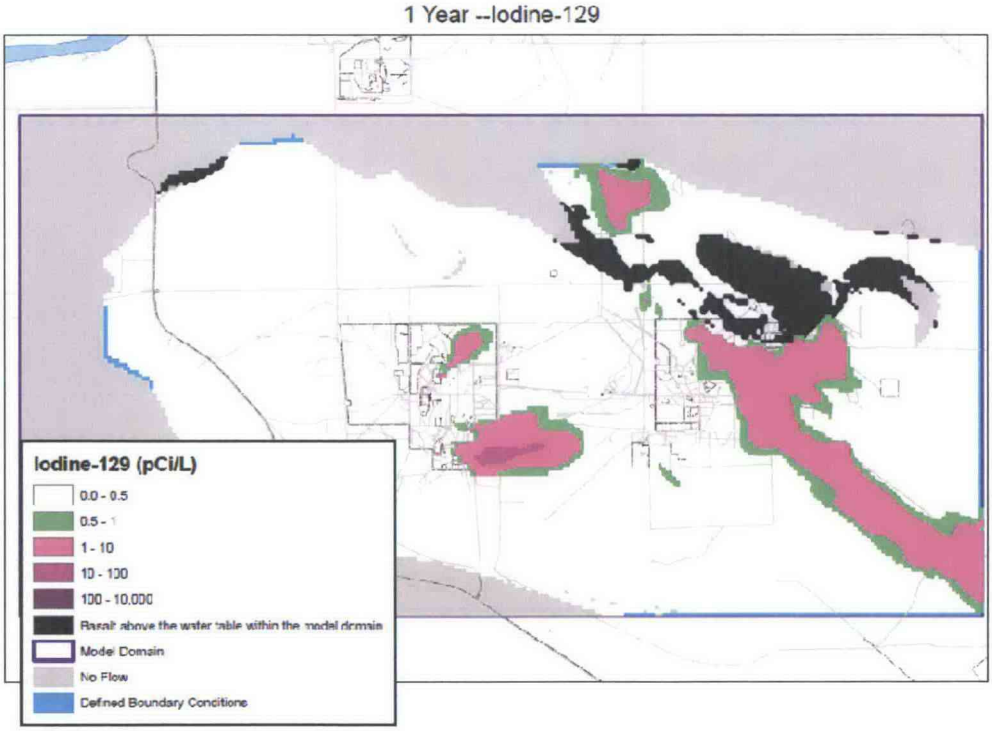


**Figure 5-18. Iodine-129 Concentrations after One Year of Transport (2009)**

Time 25 Years --Iodine-129

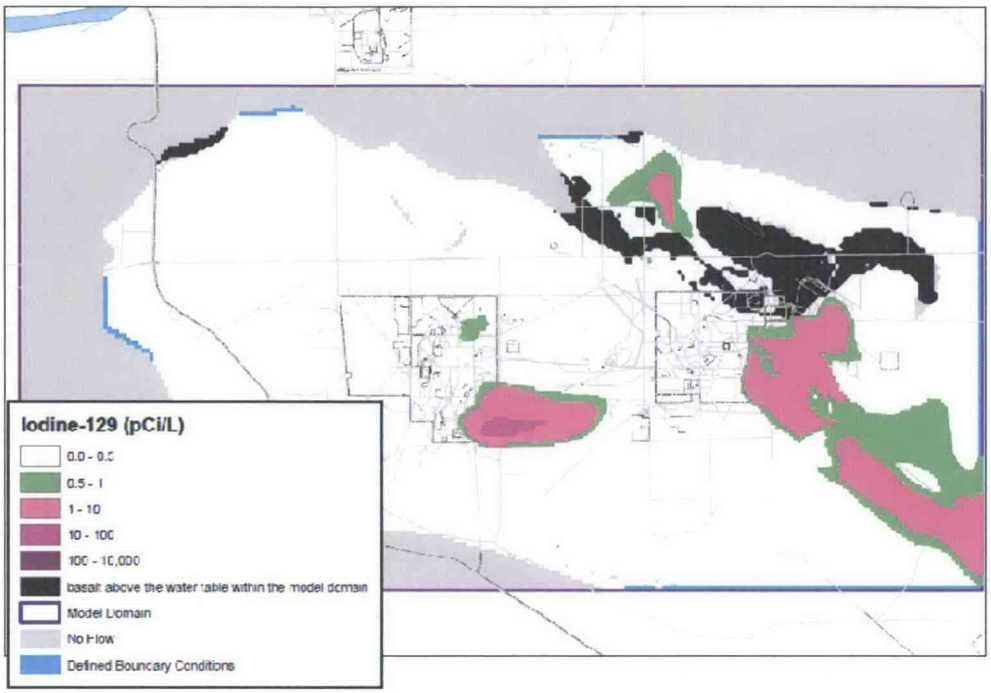


**Figure 5-19. Iodine-129 Concentrations after 25 Years of Transport (2034)**

Time 75 Years --Iodine-129

**Figure 5-20. Iodine-129 Concentrations after 75 Years of Transport (2084)**

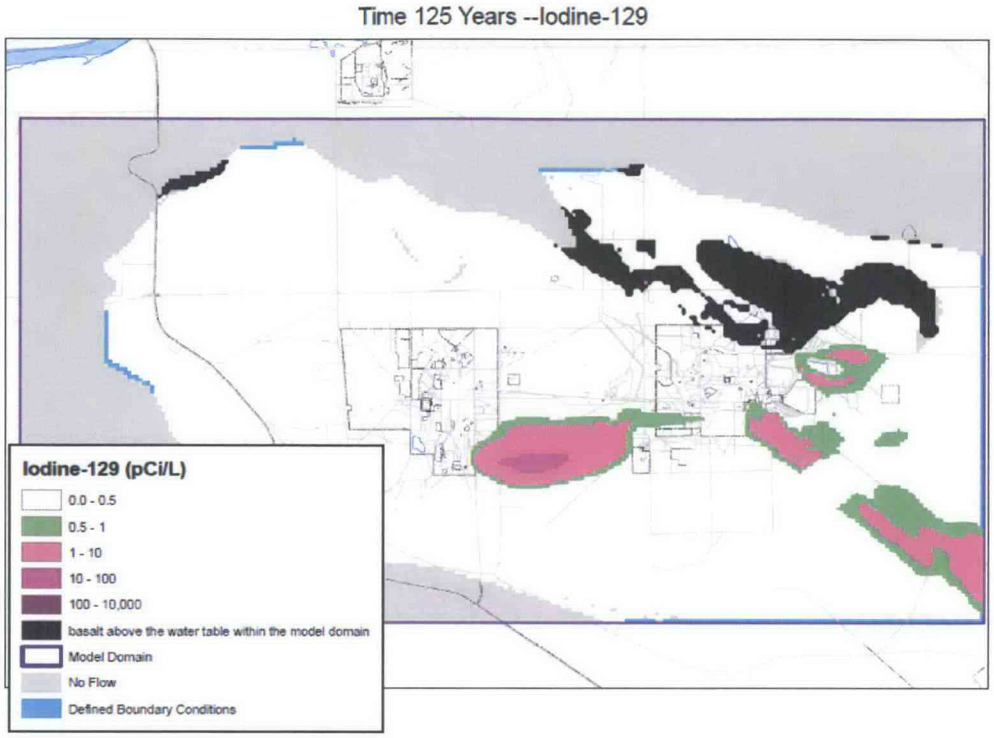


**Figure 5-21. Iodine-129 Concentrations after 125 Years of Transport (2134)**

## Table 5-3 Maximum Concentration of Iodine-129 (pCi/L) for Monitoring Locations at Selected Time Steps

| Time (Years) | 299-E17-26 | 299-E17-3 | 299-E17-9 | 299-E25-20 | 299-E25-32B | 299-E25-39 | 299-E25-8 | 699-22-35 | 699-23-34A | 699-24-34A | 699-24-34C | 699-32-43 | 699-34-39A | 699-34-41B | 699-34-42 | 699-37-47A | 699-42-39B | CP-1 | CP-2 | CP-3 | CP-4 | CP-5 | CP-6 |
|---|---|---|---|---|---|---|---|---|---|---|---|---|---|---|---|---|---|---|---|---|---|---|---|
| 1 | 2.94E-01 | 7.42E+00 | 3.90E+00 | 2.90E+00 | 2.04E+00 | 1.90E+00 | 4.92E+00 | 3.41E-19 | 7.32E-13 | 8.84E-14 | 4.36E-03 | 7.62E-01 | 6.71E-01 | 2.57E+00 | 2.48E+00 | 2.97E+00 | 7.04E-01 | 1.22E+00 | 1.84E+00 | 6.92E-01 | 1.65E-10 | 4.39E-17 | 0.00E+00 |
| 5 | 1.41E-01 | 6.79E+00 | 3.92E+00 | 3.54E+00 | 2.47E+00 | 2.06E+00 | 5.54E+00 | 2.63E-13 | 1.58E-11 | 7.84E-07 | 7.40E-02 | 5.93E-01 | 1.06E+00 | 2.30E+00 | 2.13E+00 | 2.96E+00 | 6.88E-01 | 1.26E+00 | 1.83E+00 | 9.60E-01 | 3.00E-05 | 9.68E-11 | 1.85E-13 |
| 10 | 3.66E-02 | 6.07E+00 | 3.90E+00 | 3.14E+00 | 2.93E+00 | 2.49E+00 | 4.74E+00 | 1.90E-12 | 6.73E-09 | 1.00E-05 | 9.54E-02 | 4.28E-01 | 1.05E+00 | 1.68E+00 | 1.75E+00 | 2.94E+00 | 6.71E-01 | 1.24E+00 | 1.80E+00 | 9.84E-01 | 2.52E-06 | 8.69E-08 | 2.10E-09 |
| 50 | 1.24E-01 | 2.21E+00 | 2.47E+00 | 4.09E-01 | 8.77E-01 | 1.10E+00 | 6.06E-01 | 9.93E-08 | 8.00E-05 | 4.70E-04 | 5.96E-02 | 1.34E-01 | 6.92E-01 | 4.25E-01 | 2.91E-01 | 2.77E+00 | 7.65E-01 | 1.19E+00 | 1.49E+00 | 8.02E-01 | 4.50E-04 | 6.20E-04 | 3.10E-04 |
| 100 | 1.16E-01 | 8.71E-01 | 1.08E+00 | 1.70E-01 | 1.69E-01 | 2.30E-01 | 4.14E-01 | 4.74E-07 | 3.20E-04 | 1.51E-03 | 4.86E-02 | 8.52E-02 | 3.79E-01 | 1.53E-01 | 1.33E-01 | 2.42E+00 | 8.23E-01 | 1.09E+00 | 1.18E+00 | 9.45E-01 | 9.01E-03 | 4.43E-03 | 2.91E-03 |
| 200 | 2.23E-01 | 4.35E-01 | 3.98E-01 | 1.96E-01 | 2.17E-02 | 1.13E-01 | 1.98E-01 | 1.90E-06 | 9.60E-04 | 2.83E-03 | 6.87E-02 | 1.44E-01 | 1.32E-01 | 1.17E-01 | 1.33E-01 | 1.38E+00 | 7.73E-01 | 8.65E-01 | 7.47E-01 | 9.79E-01 | 7.54E-02 | 5.18E-02 | 5.22E-03 |
| 300 | 3.10E-01 | 2.10E-01 | 2.33E-01 | 1.49E-01 | 7.37E-02 | 8.40E-02 | 1.23E-01 | 4.17E-06 | 1.43E-03 | 3.86E-03 | 5.64E-02 | 2.13E-01 | 1.30E-01 | 1.46E-01 | 1.84E-01 | 6.65E-01 | 6.58E-01 | 6.72E-01 | 5.51E-01 | 7.89E-01 | 1.50E-01 | 1.53E-01 | 2.17E-02 |
| 400 | 3.07E-01 | 1.09E-01 | 1.42E-01 | 1.02E-01 | 1.04E-01 | 6.56E-02 | 8.32E-02 | 1.00E-05 | 1.50E-03 | 3.55E-03 | 4.13E-02 | 2.13E-01 | 1.16E-01 | 1.36E-01 | 1.79E-01 | 3.10E-01 | 4.94E-01 | 5.12E-01 | 4.64E-01 | 6.05E-01 | 1.82E-01 | 2.02E-01 | 4.72E-02 |
| 500 | 2.55E-01 | 6.18E-02 | 9.69E-02 | 6.89E-02 | 1.15E-01 | 5.33E-02 | 5.54E-02 | 1.00E-05 | 1.28E-03 | 2.85E-03 | 3.35E-02 | 1.77E-01 | 9.11E-02 | 1.05E-01 | 1.40E-01 | 2.69E-01 | 3.34E-01 | 3.82E-01 | 4.51E-01 | 5.30E-01 | 1.76E-01 | 1.90E-01 | 5.94E-02 |
| 600 | 2.41E-01 | 3.89E-02 | 7.13E-02 | 4.67E-02 | 1.13E-01 | 4.46E-02 | 3.74E-02 | 1.00E-05 | 1.02E-03 | 2.38E-03 | 2.69E-02 | 1.44E-01 | 6.88E-02 | 7.78E-02 | 1.05E-01 | 2.70E-01 | 2.12E-01 | 2.80E-01 | 4.25E-01 | 4.91E-01 | 1.52E-01 | 1.53E-01 | 5.59E-02 |
| 700 | 2.16E-01 | 2.67E-02 | 5.46E-02 | 3.20E-02 | 1.04E-01 | 3.86E-02 | 2.56E-02 | 1.00E-05 | 8.30E-04 | 1.91E-03 | 2.17E-02 | 1.20E-01 | 5.27E-02 | 6.07E-02 | 8.43E-02 | 2.43E-01 | 1.30E-01 | 2.30E-01 | 3.88E-01 | 4.41E-01 | 1.24E-01 | 1.14E-01 | 4.56E-02 |
| 800 | 1.98E-01 | 1.93E-02 | 4.27E-02 | 2.22E-02 | 9.07E-02 | 3.50E-02 | 1.77E-02 | 1.00E-05 | 6.60E-04 | 1.52E-03 | 1.75E-02 | 9.61E-02 | 4.14E-02 | 4.85E-02 | 6.75E-02 | 2.05E-01 | 7.90E-02 | 2.11E-01 | 3.47E-01 | 3.86E-01 | 9.80E-02 | 8.25E-02 | 3.38E-02 |
| 900 | 1.88E-01 | 1.46E-02 | 3.39E-02 | 1.58E-02 | 7.69E-02 | 3.23E-02 | 1.24E-02 | 4.82E-06 | 5.20E-04 | 1.20E-03 | 1.35E-02 | 7.29E-02 | 3.27E-02 | 3.75E-02 | 5.16E-02 | 1.92E-01 | 4.83E-02 | 1.89E-01 | 3.05E-01 | 3.32E-01 | 7.64E-02 | 5.89E-02 | 2.58E-02 |
| 1000 | 1.71E-01 | 1.14E-02 | 2.71E-02 | 1.13E-02 | 6.39E-02 | 3.01E-02 | 8.73E-03 | 3.77E-06 | 4.00E-04 | 9.20E-04 | 1.02E-02 | 5.56E-02 | 2.53E-02 | 3.32E-02 | 3.95E-02 | 1.88E-01 | 2.98E-02 | 1.68E-01 | 2.64E-01 | 2.93E-01 | 6.67E-02 | 4.22E-02 | 2.18E-02 |

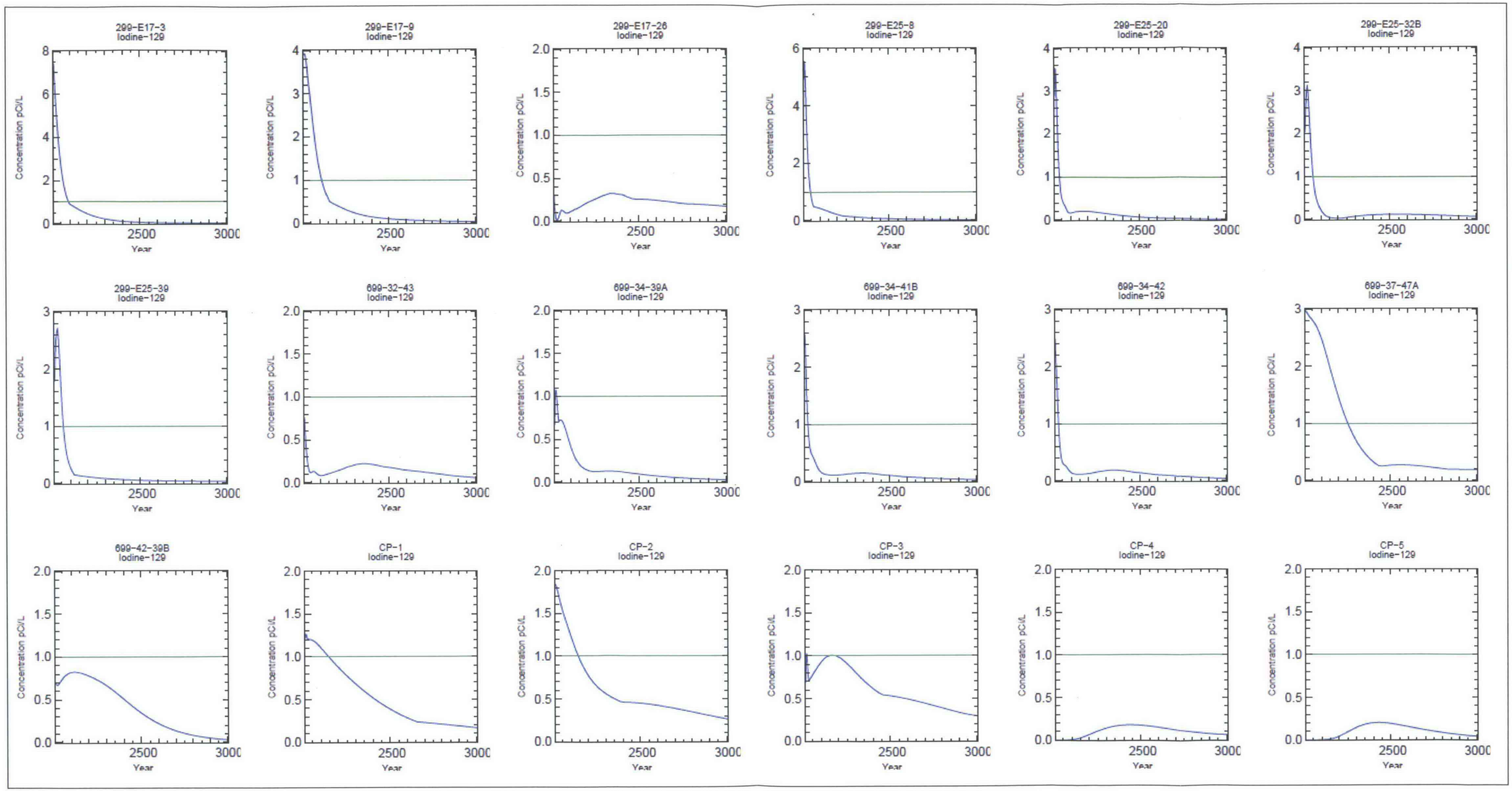


**Figure 5-22. Largest Iodine-129 Concentrations at Monitor Locations**

### 5.2.4 Trichloroethene

TCE is present in the model domain in a localized plume extending from the southeast side of the PUREX plant and associated with the PUREX cribs. Another localized TCE plume area is associated with the Non-Radioactive Dangerous Waste Landfill (NRDWL), located outside the 200-East Area and near the southeast corner of the Central Plateau Groundwater Model boundary but this plume is below ½ MCL.

The region contaminated with trichloroethene above ½ MCL is barely visible in Figure 5-23 showing the initial trichloroethene distribution as a small patch in the southeast corner of 200-East Area. The patch in the southeast corner of 200-East is easier to see in Figure 5-24 (one year of transport). The contamination visible in Figure 5-24 is in the Ringold E unit (Layer 3). After 25 simulated years of transport (Figure 5-25) no concentrations greater than ½ MCL are evident in the 200-PO-1 OU.

Table 5-4 presents the time varying concentration results for the monitoring locations.

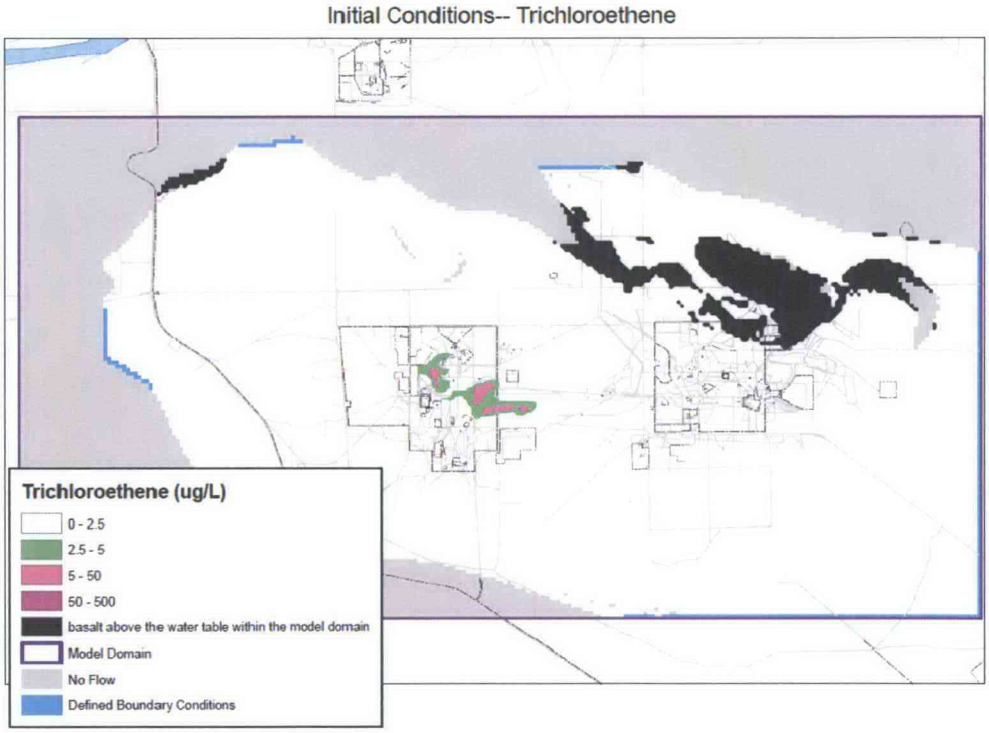


**Figure 5-23. Initial Trichloroethene Distribution (2008)**

1 Year-- Trichloroethene

**Figure 5-24. Trichloroethene after One Year of Transport (2009)**

Time 25 Years -- Trichloroethene

**Figure 5-25. Trichloroethene after 25 Year of Transport (2034)**

**Table 5-4. Maximum Concentration of Trichloroethene (µg/L) for Monitoring Locations at Selected Time Steps**

| Time (Years) | 299-E17-26 | 299-E17-3 | 299-E17-9 | 299-E25-20 | 299-E25-32B | 299-E25-39 | 299-E25-8 | 699-22-35 | 699-23-34A | 699-24-34A | 699-24-34C | 699-32-43 | 699-34-39A | 699-34-41B | 699-34-42 | 699-37-47A | 699-42-39B | CP-1 | CP-2 | CP-3 | CP-4 | CP-5 | CP-6 |
|---|---|---|---|---|---|---|---|---|---|---|---|---|---|---|---|---|---|---|---|---|---|---|---|
| 1 | 6.00E-05 | 1.33E-01 | 1.19E-02 | 6.30E-04 | 2.82E-13 | 6.91E-13 | 8.95E-10 | 4.06E-01 | 4.20E-01 | 4.47E-01 | 4.76E-01 | 8.93E-02 | 2.61E-07 | 5.00E-05 | 3.00E-05 | 1.77E-09 | 2.72E-47 | 2.17E-03 | 3.00E-04 | 2.55E-07 | 1.76E-18 | 9.80E-27 | 1.95E-31 |
| 5 | 2.00E-05 | 2.91E-01 | 8.61E-03 | 1.16E-02 | 2.09E-08 | 1.77E-07 | 1.00E-05 | 2.68E-01 | 2.92E-01 | 3.18E-01 | 3.77E-01 | 9.21E-03 | 5.55E-03 | 8.60E-03 | 4.08E-03 | 1.00E-05 | 0.00E+00 | 2.41E-02 | 1.04E-03 | 1.60E-04 | 2.10E-07 | 1.44E-12 | 5.73E-15 |
| 10 | 4.61E-06 | 1.86E-01 | 2.17E-02 | 6.53E-03 | 2.00E-05 | 1.00E-05 | 5.00E-05 | 1.74E-01 | 1.99E-01 | 2.20E-01 | 2.87E-01 | 2.26E-03 | 1.13E-02 | 9.33E-03 | 2.97E-03 | 3.00E-04 | 1.52E-28 | 1.57E-02 | 1.47E-03 | 1.04E-03 | 4.98E-08 | 7.44E-09 | 4.42E-10 |
| 50 | 6.71E-03 | 7.43E-02 | 1.82E-02 | 3.80E-04 | 1.00E-05 | 1.00E-05 | 1.00E-05 | 2.85E-02 | 4.01E-02 | 4.87E-02 | 8.44E-02 | 4.56E-03 | 3.85E-03 | 3.81E-03 | 4.49E-03 | 1.65E-02 | 1.73E-11 | 1.89E-02 | 3.51E-03 | 2.88E-03 | 1.27E-06 | 1.00E-05 | 1.00E-05 |
| 100 | 1.59E-02 | 3.79E-02 | 1.10E-02 | 2.90E-04 | 1.00E-05 | 1.00E-05 | 1.00E-05 | 6.71E-03 | 1.33E-02 | 1.68E-02 | 3.40E-02 | 1.09E-02 | 6.25E-03 | 7.40E-03 | 9.62E-03 | 3.75E-02 | 3.04E-08 | 2.33E-02 | 8.96E-03 | 8.51E-03 | 2.63E-06 | 2.00E-05 | 1.00E-05 |
| 200 | 3.67E-02 | 8.65E-03 | 9.63E-03 | 4.90E-04 | 1.00E-05 | 1.00E-05 | 1.00E-05 | 7.30E-04 | 2.32E-03 | 2.94E-03 | 7.24E-03 | 2.13E-02 | 1.22E-02 | 1.41E-02 | 1.90E-02 | 2.42E-02 | 6.58E-07 | 1.67E-02 | 1.85E-02 | 2.10E-02 | 1.00E-05 | 4.00E-05 | 2.00E-05 |
| 300 | 4.29E-02 | 9.38E-03 | 1.27E-02 | 4.40E-04 | 1.00E-05 | 1.00E-05 | 2.00E-05 | 5.50E-04 | 1.10E-03 | 1.32E-03 | 4.75E-03 | 2.88E-02 | 1.59E-02 | 1.98E-02 | 2.62E-02 | 2.26E-02 | 1.06E-06 | 2.25E-02 | 2.34E-02 | 2.38E-02 | 1.00E-05 | 8.00E-05 | 4.00E-05 |
| 400 | 3.80E-02 | 8.43E-03 | 1.17E-02 | 3.40E-04 | 2.00E-05 | 1.00E-05 | 3.00E-05 | 4.10E-04 | 8.50E-04 | 1.04E-03 | 4.54E-03 | 2.54E-02 | 1.50E-02 | 1.75E-02 | 2.29E-02 | 1.91E-02 | 1.44E-06 | 2.02E-02 | 2.21E-02 | 2.43E-02 | 2.00E-05 | 1.00E-04 | 4.00E-05 |
| 500 | 3.25E-02 | 5.26E-03 | 7.18E-03 | 2.60E-04 | 1.00E-05 | 1.00E-05 | 2.00E-05 | 3.10E-04 | 6.60E-04 | 8.20E-04 | 3.22E-03 | 1.65E-02 | 9.98E-03 | 1.10E-02 | 1.44E-02 | 1.35E-02 | 2.02E-06 | 1.30E-02 | 1.58E-02 | 1.94E-02 | 3.00E-05 | 1.10E-04 | 4.00E-05 |
| 600 | 2.92E-02 | 2.49E-03 | 5.52E-03 | 1.90E-04 | 2.00E-05 | 1.00E-05 | 1.00E-05 | 2.40E-04 | 5.80E-04 | 8.00E-04 | 2.08E-03 | 9.45E-03 | 5.41E-03 | 5.69E-03 | 7.55E-03 | 9.43E-03 | 2.36E-06 | 7.04E-03 | 1.19E-02 | 1.63E-02 | 4.00E-05 | 1.00E-04 | 3.00E-05 |
| 700 | 2.44E-02 | 1.34E-03 | 3.79E-03 | 1.30E-04 | 2.00E-05 | 1.00E-05 | 1.00E-05 | 1.90E-04 | 6.30E-04 | 8.30E-04 | 1.28E-03 | 4.99E-03 | 2.78E-03 | 2.88E-03 | 3.78E-03 | 7.71E-03 | 2.09E-06 | 3.70E-03 | 1.05E-02 | 1.40E-02 | 4.00E-05 | 7.00E-05 | 2.00E-05 |
| 800 | 1.85E-02 | 8.80E-04 | 2.41E-03 | 9.00E-05 | 2.00E-05 | 1.00E-05 | 1.00E-05 | 1.50E-04 | 4.70E-04 | 6.10E-04 | 9.60E-04 | 2.99E-03 | 1.57E-03 | 1.62E-03 | 2.22E-03 | 7.39E-03 | 1.50E-06 | 2.86E-03 | 8.69E-03 | 1.19E-02 | 3.00E-05 | 5.00E-05 | 2.00E-05 |
| 900 | 1.34E-02 | 5.60E-04 | 1.51E-03 | 6.00E-05 | 2.00E-05 | 1.00E-05 | 3.90E-06 | 1.20E-04 | 2.90E-04 | 3.70E-04 | 6.10E-04 | 1.94E-03 | 1.07E-03 | 1.51E-03 | 1.44E-03 | 6.94E-03 | 9.10E-07 | 2.44E-03 | 6.94E-03 | 9.42E-03 | 3.00E-05 | 3.00E-05 | 1.00E-05 |
| 1000 | 9.43E-03 | 3.60E-04 | 9.70E-04 | 4.00E-05 | 2.00E-05 | 1.00E-05 | 1.03E-06 | 1.00E-04 | 2.50E-04 | 3.20E-04 | 4.40E-04 | 1.32E-03 | 1.13E-03 | 1.73E-03 | 1.61E-03 | 6.41E-03 | 3.54E-07 | 2.17E-03 | 5.43E-03 | 7.52E-03 | 2.00E-05 | 2.00E-05 | 1.00E-05 |

This page intentionally left blank.

### 5.2.5 Technetium-99

Technetium-99 is the model domain as a relatively small plume associated with WMA A-AX tank farm to the northeast of the PUREX plant area and in larger quantities in 200-BP-5 (Figure 5-26). There are also many small plumes distributed throughout the 200-West area. Most of the initial condition plume exhibits groundwater concentrations less than 900 pCi/L (MCL).

The simulation indicates rapid dispersal of the plumes in 200-BP-5 after only one year of transport (Figure 5-27). The part that remains above MCL is located in a patch of Cold Creek unit. In 200-PO-1 there is some indication of movement to the southwest, but because the technetium-99 above ½ MCL initially resides in the Cold Creek unit the movement is small compared to the movement in the Hanford formation.

After twenty-five simulated years no technetium-99 remains above ½ MCL in the 200-PO-1 OU (Figure 5-28). The ZP-1 pump and treat system has brought levels in the 200-ZP-1 OU below ½ MCL. The plumes in the vicinity of 216-S-8 and 216-S-18 have merged and been pulled slightly north. Near 216-S-8 technetium-99 is still above MCL. After 75 years (Figure 5-29) this plume is all below MCL but still has some levels about ½ MCL. The ½ MCL region of the plume has moved somewhat less than a kilometer to the east. No simulated technetium-99 concentrations above ½ MCL remain after 125 years.

Table 5-5 presents the time varying concentration results for the monitoring locations. Temporal plots of concentration at monitor locations are presented in Figure 5-30. Only locations that have concentrations above 0.1×MCL at some time are displayed.

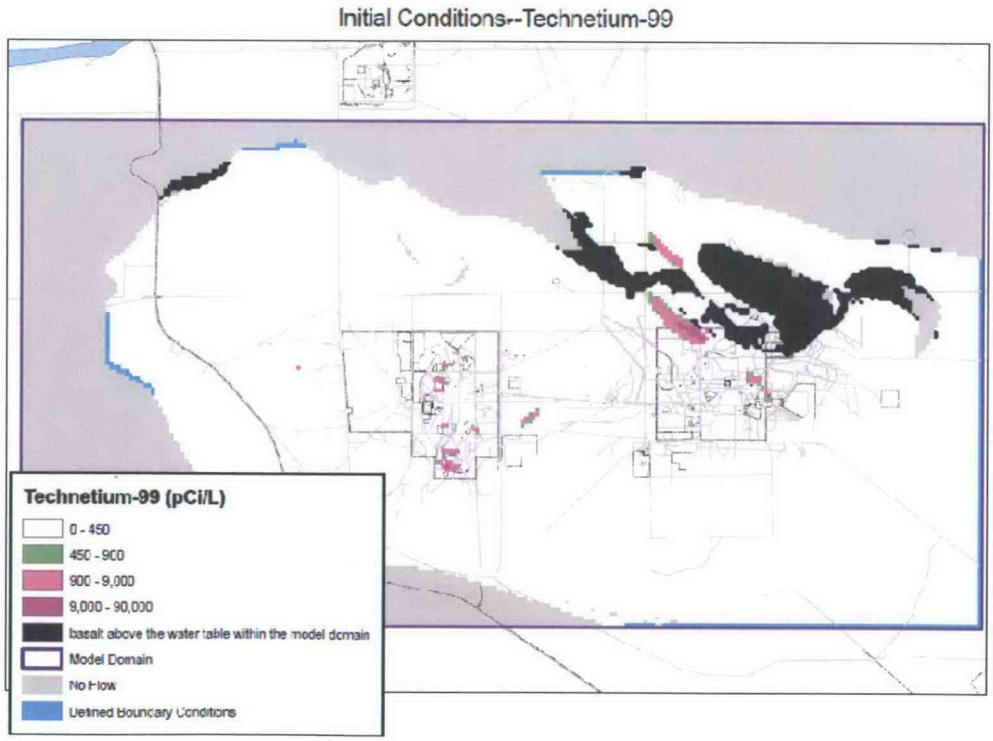


**Figure 5-26. Initial Technetium 99 Distribution (2008)**

1 Year--Technetium-99

**Figure 5-27. Technetium 99 Distribution after One Year of Transport (2009)**

Time 25 Years--Technetium-99

**Figure 5-28. Technetium 99 Distribution after 25 Years of Transport (2034)**

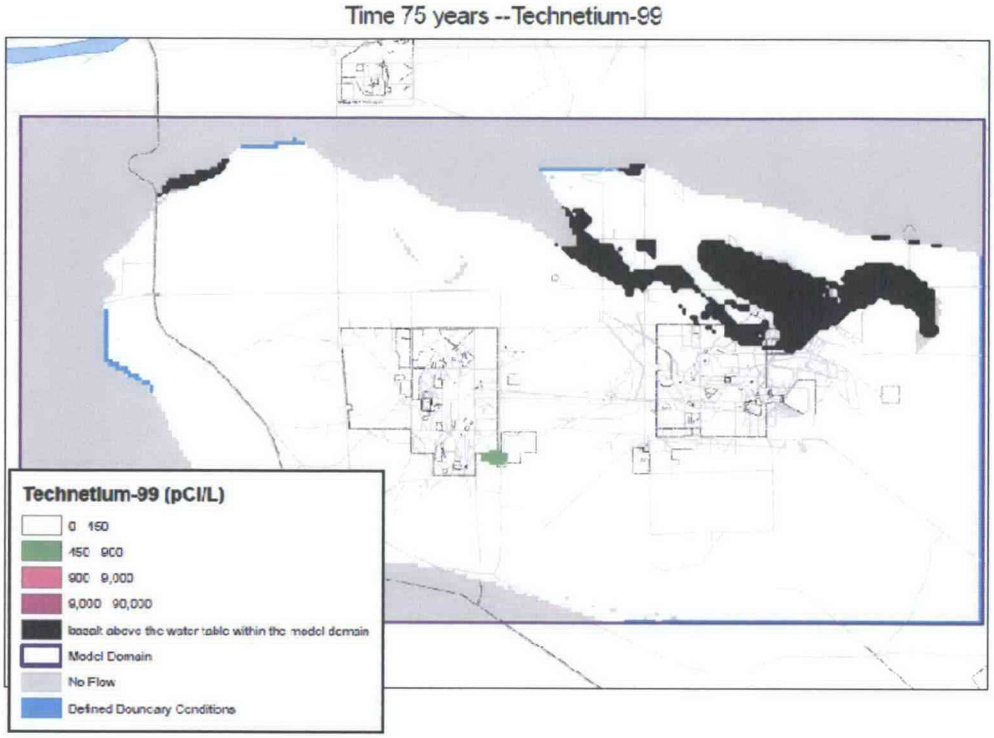


**Figure 5-29. Technetium 99 Distribution after 75 Years of Transport (2084)**

This page intentionally left blank.

**Table 5-5. Maximum Concentration of Technetium-99 (pCi/L) for Monitoring Locations at Selected Time Steps**

| Time (Years) | 299-E17-26 | 299-E17-3 | 299-E17-9 | 299-E25-20 | 299-E25-32B | 299-E25-39 | 299-E25-8 | 699-22-35 | 699-23-34A | 699-24-34A | 699-24-34C | 699-32-43 | 699-34-39A | 699-34-41B | 699-34-42 | 699-37-47A | 699-42-39B | CP-1 | CP-2 | CP-3 | CP-4 | CP-5 | CP-6 |
|---|---|---|---|---|---|---|---|---|---|---|---|---|---|---|---|---|---|---|---|---|---|---|---|
| 1 | 9.63E-02 | 2.88E+00 | 1.01E+01 | 5.30E+01 | 1.97E-02 | 3.50E-04 | 7.17E+00 | 1.67E-29 | 2.54E-22 | 2.43E-23 | 1.35E-17 | 5.08E-03 | 1.20E-04 | 3.97E-02 | 2.65E-02 | 9.74E-07 | 8.14E-22 | 1.00E-05 | 1.76E-06 | 1.10E-11 | 1.77E-14 | 3.00E-23 | 3.46E-28 |
| 5 | 1.52E+01 | 5.36E+01 | 4.77E+01 | 2.18E+02 | 1.37E+01 | 4.36E+00 | 1.24E+02 | 3.79E-13 | 4.55E-11 | 2.73E-06 | 3.90E-01 | 1.15E+01 | 1.44E+01 | 3.17E+01 | 2.74E+01 | 2.02E-02 | 1.37E-12 | 1.16E+01 | 6.62E+00 | 4.55E-01 | 8.70E-04 | 2.06E-08 | 2.00E-10 |
| 10 | 2.54E+00 | 4.79E+01 | 1.48E+01 | 1.32E+02 | 5.81E+01 | 3.37E+01 | 1.68E+02 | 5.92E-11 | 9.80E-07 | 5.80E-04 | 1.60E+00 | 8.60E+00 | 2.89E+01 | 2.79E+01 | 1.41E+01 | 2.61E-01 | 1.17E-10 | 6.57E+00 | 9.07E+00 | 8.61E+00 | 2.20E-04 | 7.00E-05 | 1.00E-05 |
| 50 | 2.01E+00 | 6.27E+00 | 5.62E+00 | 1.41E+01 | 7.95E+00 | 9.81E+00 | 3.07E+01 | 1.00E-05 | 2.70E-03 | 9.11E-03 | 2.85E-01 | 1.59E+00 | 9.12E+00 | 3.62E+00 | 2.48E+00 | 3.97E+00 | 1.08E-03 | 1.34E+00 | 1.63E+00 | 1.89E+00 | 1.24E-01 | 1.06E-01 | 6.59E-02 |
| 100 | 1.56E+00 | 3.44E+00 | 2.80E+00 | 1.34E+01 | 1.15E+00 | 4.24E+00 | 1.51E+01 | 2.00E-05 | 4.46E-03 | 1.29E-02 | 2.02E-01 | 1.15E+00 | 1.96E+00 | 9.13E-01 | 1.05E+00 | 2.87E+00 | 6.63E-01 | 8.88E-01 | 1.08E+00 | 1.21E+00 | 2.14E+00 | 1.35E+00 | 1.59E-01 |
| 200 | 1.04E+01 | 1.69E+00 | 2.31E+00 | 5.50E+00 | 7.38E+00 | 2.27E+00 | 7.21E+00 | 3.00E-05 | 7.69E-03 | 2.63E-02 | 9.83E-01 | 6.70E+00 | 3.35E+00 | 4.18E+00 | 5.80E+00 | 1.54E+00 | 2.95E+00 | 5.07E+00 | 5.28E+00 | 5.36E+00 | 5.28E+00 | 5.91E+00 | 1.43E+00 |
| 300 | 9.43E+00 | 1.52E+00 | 2.04E+00 | 2.27E+00 | 7.78E+00 | 1.52E+00 | 3.01E+00 | 9.00E-05 | 2.40E-02 | 6.61E-02 | 1.17E+00 | 7.00E+00 | 3.37E+00 | 3.98E+00 | 5.57E+00 | 1.86E+00 | 1.30E+00 | 5.39E+00 | 5.83E+00 | 6.23E+00 | 3.93E+00 | 3.74E+00 | 1.39E+00 |
| 400 | 8.91E+00 | 1.09E+00 | 1.48E+00 | 1.01E+00 | 5.89E+00 | 1.27E+00 | 1.32E+00 | 1.40E-04 | 2.47E-02 | 6.25E-02 | 9.20E-01 | 5.53E+00 | 2.41E+00 | 2.90E+00 | 4.12E+00 | 1.41E+00 | 4.47E-01 | 4.26E+00 | 4.58E+00 | 4.84E+00 | 2.31E+00 | 1.75E+00 | 7.32E-01 |
| 500 | 7.55E+00 | 6.48E-01 | 1.19E+00 | 5.02E-01 | 3.88E+00 | 1.15E+00 | 6.13E-01 | 1.30E-04 | 1.83E-02 | 4.43E-02 | 5.66E-01 | 3.16E+00 | 1.42E+00 | 1.63E+00 | 2.29E+00 | 1.07E+00 | 1.72E-01 | 2.49E+00 | 3.17E+00 | 4.23E+00 | 1.68E+00 | 8.47E-01 | 4.84E-01 |
| 600 | 6.20E+00 | 5.86E-01 | 8.91E-01 | 4.90E-01 | 2.40E+00 | 1.10E+00 | 4.43E-01 | 9.00E-05 | 1.13E-02 | 2.65E-02 | 3.04E-01 | 1.67E+00 | 1.17E+00 | 1.26E+00 | 1.17E+00 | 8.87E-01 | 8.88E-02 | 1.32E+00 | 2.78E+00 | 3.60E+00 | 1.32E+00 | 7.03E-01 | 3.11E-01 |
| 700 | 4.36E+00 | 1.97E+00 | 1.41E+00 | 2.05E+00 | 1.53E+00 | 1.22E+00 | 1.89E+00 | 6.00E-05 | 5.97E-03 | 1.34E-02 | 1.10E-01 | 4.97E-01 | 1.53E+00 | 1.38E+00 | 6.40E-01 | 8.59E-01 | 9.52E-02 | 6.83E-01 | 2.22E+00 | 2.95E+00 | 1.02E+00 | 5.86E-01 | 2.15E-01 |
| 800 | 2.30E+00 | 8.37E+00 | 5.22E+00 | 8.87E+00 | 5.88E+00 | 5.05E+00 | 8.17E+00 | 3.00E-05 | 1.67E-03 | 2.84E-03 | 1.32E-02 | 3.58E-01 | 1.66E+00 | 1.59E+00 | 7.59E-01 | 3.07E+00 | 2.61E-01 | 4.58E-01 | 1.51E+00 | 2.19E+00 | 8.52E-01 | 5.09E-01 | 1.76E-01 |
| 900 | 0.00E+00 | 3.83E+01 | 2.24E+01 | 4.06E+01 | 2.54E+01 | 2.16E+01 | 3.70E+01 | 1.00E-05 | 1.23E-03 | 2.11E-03 | 1.32E-02 | 3.36E-01 | 5.63E+00 | 6.42E+00 | 8.35E-01 | 1.30E+01 | 1.04E+00 | 3.31E-01 | 7.31E-01 | 1.42E+00 | 1.59E+00 | 1.42E+00 | 2.58E-01 |
| 1000 | 0.00E+00 | 1.60E+02 | 9.60E+01 | 1.71E+02 | 1.11E+02 | 9.51E+01 | 1.57E+02 | 1.00E-05 | 1.40E-04 | 1.50E-04 | 9.68E-03 | 3.65E-01 | 2.26E+01 | 2.60E+01 | 8.71E-01 | 5.51E+01 | 4.54E+00 | 3.76E-02 | 0.00E+00 | 0.00E+00 | 6.16E+00 | 5.84E+00 | 1.04E+00 |

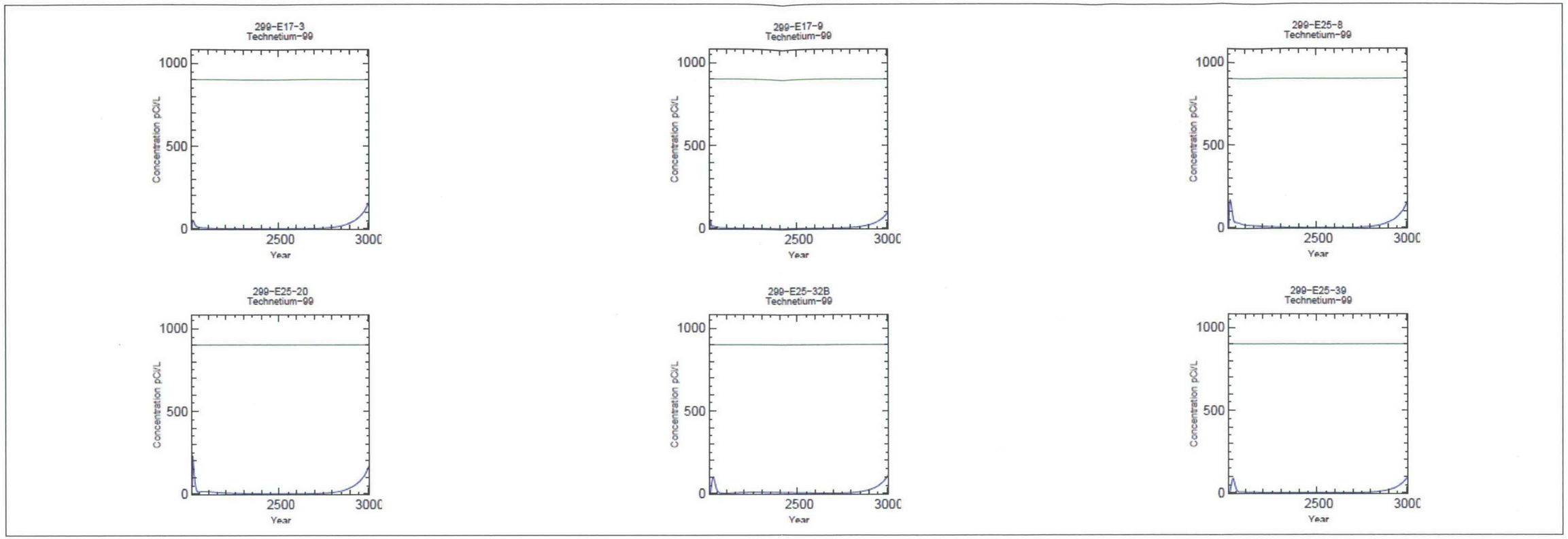


**Figure 5-30. Technetium-99 Concentrations at Monitor Locations**

### 5.2.6 Uranium

Uranium is present in the model domain in a localized plume near the south side of the PUREX plant and associated with the PUREX cribs (Figure 5-31). The uranium plume is collocated with tritium and iodine-129, nitrate, and TCE in that area. The initial condition plume exhibits groundwater concentration less than 300 μg/L total uranium.

The initial distribution includes the relatively low permeability Ringold E unit. There are two plumes in the initial distribution within the 200-East area of 200-BP-5 OU. The southern most of these plumes was placed partially in the Ringold A unit which directly underlies the Hanford formation in some places. The southeastern tip of the northern plume is located in model cells composed of the Cold Creek HSU. The southwestern tip is the apparent source area for this plume. That is prior to the starting time of the simulation this plume has been moving northwest toward the Gable gap. There is a small uranium plume in the 200-ZP-1 OU and a large plume above MCL east of 216-U-15 and a couple of plume above ½ MCL in the vicinity of U-Pond in 200-UP-1.

After one year of transport simulation (Figure 5-32), the northwest tip of the northern plume has dispersed. The southeastern source area of this plume has not moved appreciably. The southern 200-BP-5 plume has migrated southwestward and the size of the plume above MCL has diminished significantly. Only sight evidence of movement to the east/southeast is evident in the other OUs. Twenty-five years into the simulation (Figure 5-33) the plumes in 200-BP-5 have diminished significantly with no residuals above MCL. The uranium plume in 200-PO-1 indicates a few hundred meters of movement to the southeast The large plume in 200-UP-1 has broadened to the north and the western edge has move east a hundred meters or so. The plumes near U-Pond have diminished in size.

Seventy-five years into the simulation (Figure 5-34) results in a plume about half the original size in 200-PO-1, but still above MCL. In 200-UP-1 the large plume is little changed, but the U-Pond area has only a small visage of the original plume above ½ MCL. After one-hundred and twenty-five years (Figure 5-35), the picture is little changed. Movement over the last 50 years of simulation, in the 200-UP-1, is on the order of 100 meters. The plume in 200-PO-1 is smaller, but still above MCL.

Table 5-6 presents the time varying concentration results for the monitoring locations. Temporal plots of concentration at monitor locations are presented in Figure 5-36. Only locations that have concentrations above 0.1×MCL at some time are displayed.

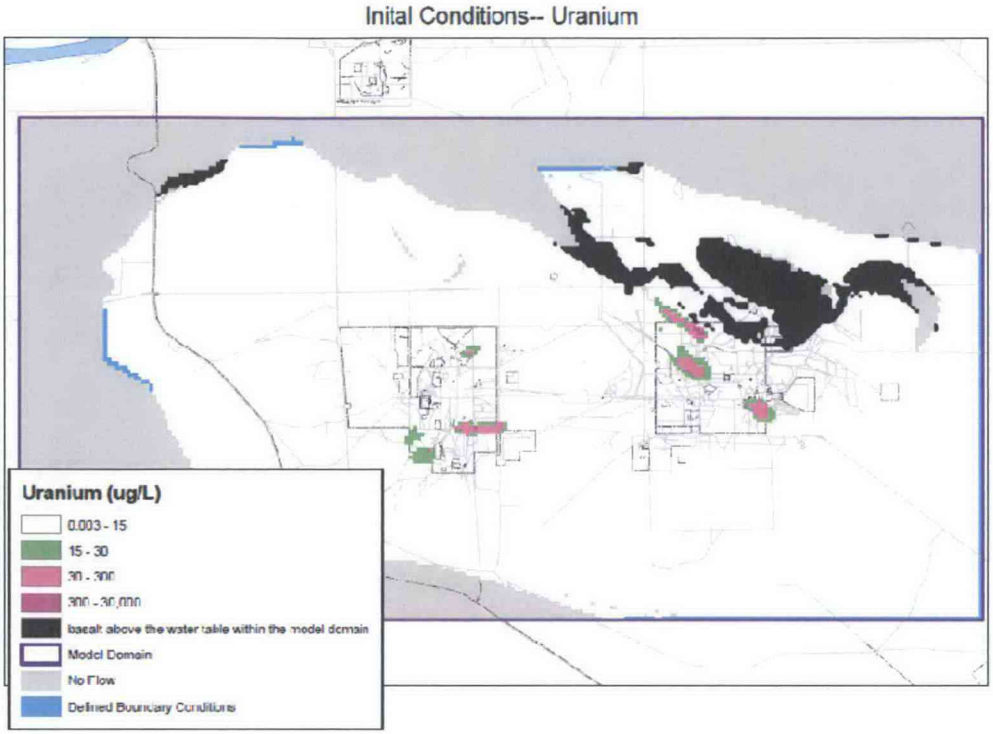


**Figure 5-31. Initial Uranium Distribution (2008)**

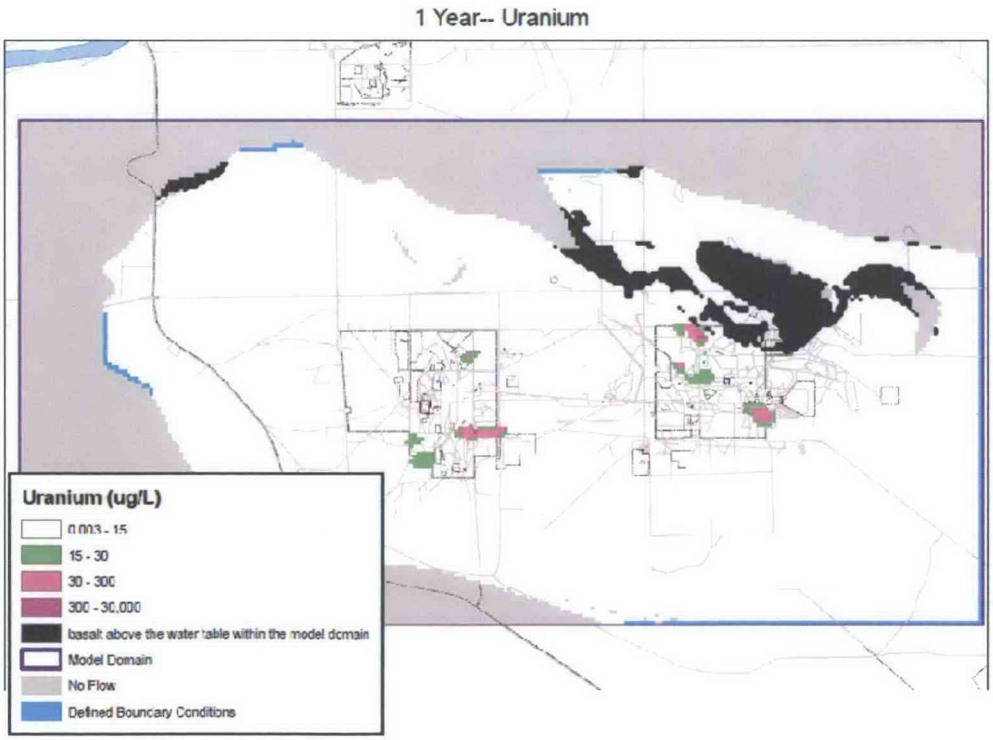


**Figure 5-32. Uranium Distribution after One Year of Transport (2009)**

**Figure 5-33. Uranium Distribution after 25 Years of Transport (2034)**

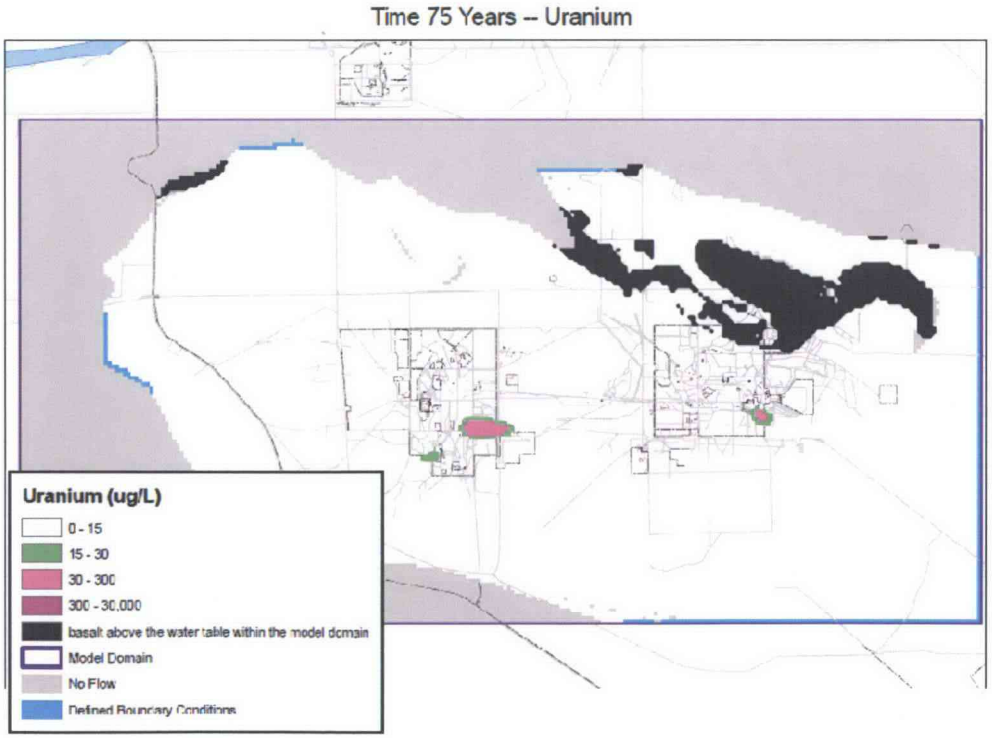


**Figure 5-34. Uranium Distribution after 75 Years of Transport (2084)**

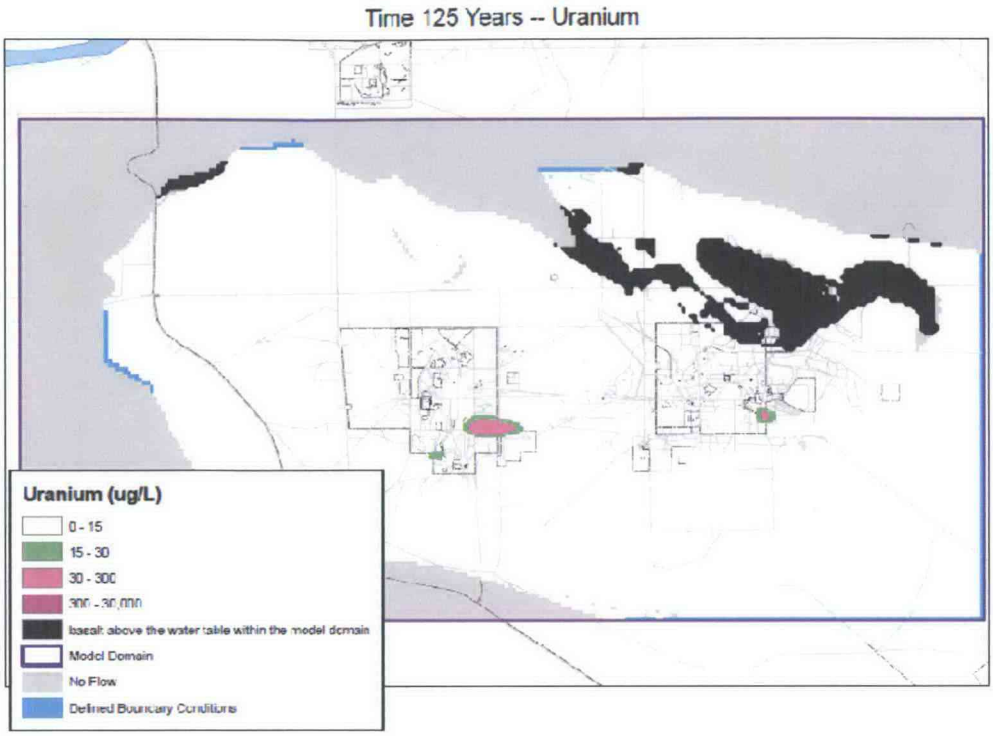


**Figure 5-35. Uranium Distribution after 125 Years of Transport (2134)**

## Table 5-6. Maximum Concentration of Uranium (µg/L) for Monitoring Locations at Selected Time Steps

| Time (Years) | 299-E17-26 | 299-E17-3 | 299-E17-9 | 299-E25-20 | 299-E25-32B | 299-E25-39 | 299-E25-8 | 699-22-35 | 699-23-34A | 699-24-34A | 699-24-34C | 699-32-43 | 699-34-39A | 699-34-41B | 699-34-42 | 699-37-47A | 699-42-39B | CP-1 | CP-2 | CP-3 | CP-4 | CP-5 | CP-6 |
|---|---|---|---|---|---|---|---|---|---|---|---|---|---|---|---|---|---|---|---|---|---|---|---|
| 1 | 1.91E-02 | 3.43E+01 | 6.97E+00 | 0.00E+00 | 2.28E-14 | 1.35E-14 | 9.03E-15 | 2.31E-69 | 0.00E+00 | 1.20E-49 | 7.09E-41 | 1.57E-12 | 1.91E-17 | 1.15E-10 | 2.73E-11 | 5.72E-07 | 1.75E-60 | 1.21E-34 | 0.00E+00 | 1.79E-47 | 1.93E-33 | 9.49E-46 | 1.24E-53 |
| 5 | 9.45E-02 | 3.72E+01 | 2.06E+00 | 4.37E-01 | 2.15E-09 | 0.00E+00 | 6.50E-07 | 0.00E+00 | 2.84E-19 | 9.63E-23 | 4.15E-10 | 5.87E-02 | 6.10E-04 | 2.83E-01 | 2.33E-01 | 8.00E-05 | 1.06E-43 | 2.30E-04 | 1.00E-05 | 6.40E-11 | 3.69E-13 | 1.62E-22 | 1.01E-27 |
| 10 | 1.28E+00 | 3.77E+01 | 2.72E+00 | 1.29E+00 | 2.98E-07 | 0.00E+00 | 1.00E-04 | 1.79E-20 | 1.18E-11 | 1.74E-15 | 5.60E-04 | 1.71E-01 | 1.12E-01 | 8.32E-01 | 5.96E-01 | 7.60E-04 | 8.43E-37 | 2.00E-01 | 3.78E-02 | 3.00E-05 | 1.35E-10 | 4.07E-15 | 8.11E-19 |
| 50 | 2.72E-02 | 2.88E+01 | 8.75E+00 | 1.22E+00 | 3.87E-02 | 9.61E-03 | 4.03E-01 | 1.41E-10 | 0.00E+00 | 6.00E-05 | 6.48E-02 | 3.33E-01 | 1.53E+00 | 1.55E+00 | 7.76E-01 | 1.57E-01 | 1.76E-19 | 2.00E-01 | 3.26E-01 | 4.18E-01 | 1.66E-06 | 1.00E-05 | 5.01E-07 |
| 100 | 1.98E-02 | 1.77E+01 | 9.01E+00 | 3.98E-01 | 3.12E-01 | 2.11E-01 | 3.08E-01 | 4.10E-09 | 2.00E-05 | 2.90E-04 | 2.36E-02 | 1.08E-01 | 6.90E-01 | 5.88E-01 | 4.33E-01 | 1.08E+00 | 5.30E-12 | 8.95E-02 | 1.12E-01 | 2.14E-01 | 1.00E-05 | 1.80E-04 | 7.00E-05 |
| 200 | 1.85E-02 | 7.04E+00 | 4.81E+00 | 8.24E-02 | 1.84E-01 | 2.41E-01 | 1.02E-01 | 6.72E-08 | 8.00E-05 | 3.70E-04 | 9.10E-03 | 2.81E-02 | 4.33E-01 | 1.45E-01 | 8.80E-02 | 3.34E+00 | 7.94E-07 | 4.49E-02 | 4.84E-02 | 5.77E-02 | 6.00E-05 | 8.80E-04 | 7.00E-04 |
| 300 | 1.39E-02 | 5.50E+00 | 2.87E+00 | 8.48E-02 | 3.38E-02 | 4.41E-02 | 7.53E-02 | 1.98E-07 | 1.60E-04 | 5.10E-04 | 7.52E-03 | 1.61E-02 | 2.08E-01 | 8.08E-02 | 4.51E-02 | 5.15E+00 | 1.00E-04 | 1.85E-02 | 3.93E-02 | 2.51E-02 | 6.60E-04 | 1.57E-03 | 1.13E-03 |
| 400 | 1.84E-02 | 4.04E+00 | 2.54E+00 | 9.89E-02 | 9.46E-03 | 2.58E-02 | 6.36E-02 | 3.58E-07 | 2.00E-04 | 5.30E-04 | 5.08E-03 | 1.57E-02 | 1.14E-01 | 6.25E-02 | 3.45E-02 | 5.70E+00 | 1.18E-03 | 1.53E-02 | 3.09E-02 | 3.23E-02 | 2.76E-03 | 2.18E-03 | 1.35E-03 |
| 500 | 7.61E-02 | 2.94E+00 | 2.09E+00 | 1.04E-01 | 4.59E-03 | 2.25E-02 | 4.95E-02 | 5.40E-07 | 1.90E-04 | 4.70E-04 | 6.29E-03 | 4.66E-02 | 7.90E-02 | 6.66E-02 | 5.54E-02 | 5.44E+00 | 4.94E-03 | 3.65E-02 | 3.42E-02 | 3.57E-02 | 6.51E-03 | 3.58E-03 | 1.36E-03 |
| 600 | 2.05E-01 | 2.14E+00 | 1.66E+00 | 1.04E-01 | 3.40E-03 | 1.97E-02 | 3.69E-02 | 7.05E-07 | 1.70E-04 | 4.40E-04 | 1.51E-02 | 1.19E-01 | 9.26E-02 | 1.03E-01 | 1.17E-01 | 4.75E+00 | 1.15E-02 | 8.81E-02 | 8.56E-02 | 7.43E-02 | 1.13E-02 | 8.54E-03 | 1.24E-03 |
| 700 | 3.57E-01 | 1.58E+00 | 1.31E+00 | 1.01E-01 | 4.94E-03 | 1.74E-02 | 3.33E-02 | 8.22E-07 | 1.70E-04 | 5.40E-04 | 2.97E-02 | 2.24E-01 | 1.39E-01 | 1.63E-01 | 2.06E-01 | 3.91E+00 | 1.90E-02 | 1.66E-01 | 1.66E-01 | 1.53E-01 | 1.62E-02 | 1.50E-02 | 1.18E-03 |
| 800 | 5.26E-01 | 1.17E+00 | 1.03E+00 | 9.49E-02 | 8.65E-03 | 1.55E-02 | 3.05E-02 | 9.02E-07 | 2.20E-04 | 8.10E-04 | 4.61E-02 | 3.30E-01 | 1.89E-01 | 2.27E-01 | 2.99E-01 | 3.10E+00 | 2.51E-02 | 2.46E-01 | 2.52E-01 | 2.46E-01 | 2.05E-02 | 2.14E-02 | 2.41E-03 |
| 900 | 6.20E-01 | 8.83E-01 | 8.13E-01 | 8.80E-02 | 1.18E-02 | 1.40E-02 | 2.75E-02 | 1.00E-06 | 3.30E-04 | 1.27E-03 | 5.90E-02 | 3.94E-01 | 2.26E-01 | 2.65E-01 | 3.48E-01 | 2.39E+00 | 2.87E-02 | 3.00E-01 | 3.20E-01 | 3.23E-01 | 2.38E-02 | 2.66E-02 | 3.97E-03 |
| 1000 | 6.44E-01 | 6.73E-01 | 6.48E-01 | 8.05E-02 | 1.44E-02 | 1.27E-02 | 2.46E-02 | 1.19E-06 | 5.10E-04 | 1.84E-03 | 6.60E-02 | 4.33E-01 | 2.38E-01 | 2.87E-01 | 3.83E-01 | 1.82E+00 | 2.98E-02 | 3.32E-01 | 3.50E-01 | 3.66E-01 | 2.60E-02 | 3.02E-02 | 5.67E-03 |

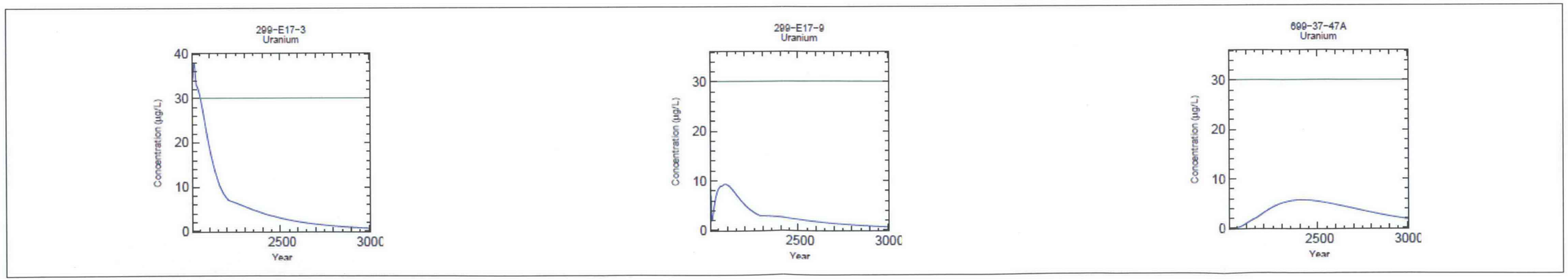


Figure 5-36. Uranium Concentrations at Monitor Locations

This page intentionally left blank.

### 5.2.7 Strontium-90

Strontium-90 is present in the model domain in a small, localized plume near the south side of the PUREX plant and associated with the PUREX cribs (Figure 5.7.1). The strontium-90 plume is collocated with tritium and iodine-129 in that area. The initial plume condition based on the average FY 2008 groundwater monitoring data is shown in Figure 5-10. The initial condition plume exhibits groundwater concentration less than 80 pCi/L strontium-90.

These plumes do not move in the simulation due to a large distribution coefficient, but do diminish in concentration. Therefore, Figure 5.7.1 is the only figure presented for strontium-90. After one year the plume under 21-6-B-9 indicates spreading to neighboring cells. After 25 years, the simulated concentrations are below MCL and after 75 years have dropped below the ½ MCL criteria for plotting.

Table 5.7.1 presents the time varying concentration results for the monitoring locations.

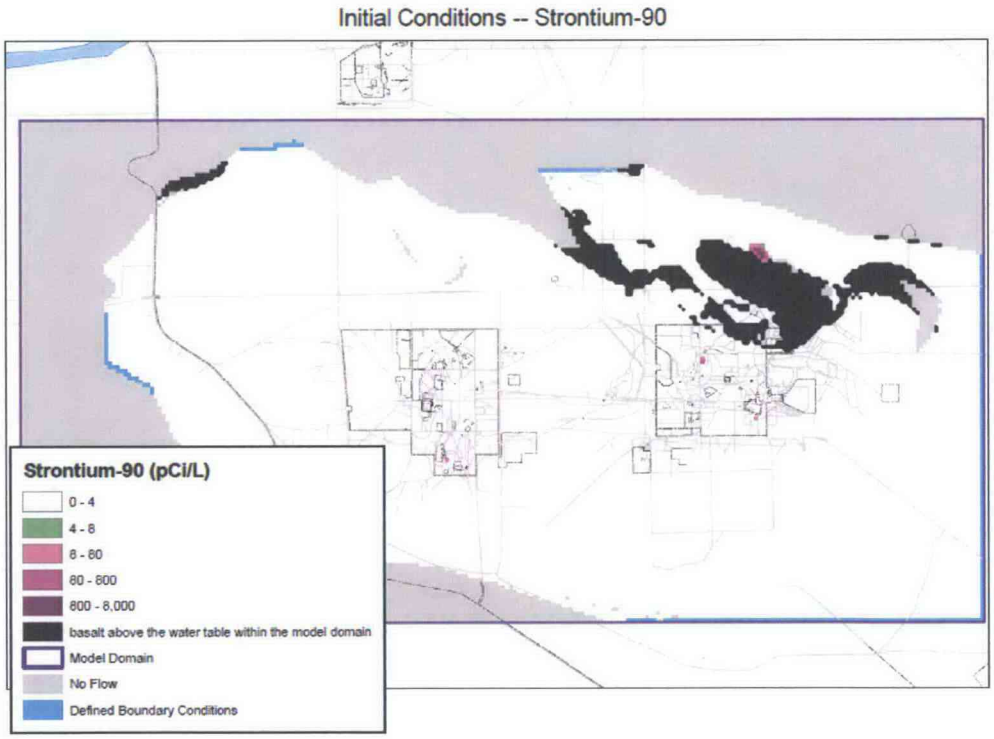


**Figure 5-37. Initial Strontium-90 Distribution (2008)**

This page intentionally left blank.

## Table 5-7. Maximum Concentration of Strontium-90 (pCi/L) for Monitoring Locations at Selected Time Steps

| Time (Years) | 299-E17-26 | 299-E17-3 | 299-E17-9 | 299-E25-20 | 299-E25-32B | 299-E25-39 | 299-E25-8 | 699-22-35 | 699-23-34A | 699-24-34A | 699-24-34C | 699-32-43 | 699-34-39A | 699-34-41B | 699-34-42 | 699-37-47A | 699-42-39B | CP-1 | CP-2 | CP-3 | CP-4 | CP-5 | CP-6 |
|---|---|---|---|---|---|---|---|---|---|---|---|---|---|---|---|---|---|---|---|---|---|---|---|
| 1 | 5.10E-25 | 1.81E-03 | 4.64E-02 | 5.06E-20 | 2.58E-41 | 2.88E-42 | 2.56E-33 | 0.00E+00 | 0.00E+00 | 0.00E+00 | 0.00E+00 | 1.45E-53 | 0.00E+00 | 9.76E-51 | 5.35E-53 | 2.84E-20 | 0.00E+00 | 0.00E+00 | 0.00E+00 | 0.00E+00 | 1.70E-86 | 0.00E+00 | 0.00E+00 |
| 5 | 5.18E-11 | 1.01E-02 | 1.43E-01 | 1.80E-15 | 3.26E-32 | 4.97E-32 | 9.60E-27 | 0.00E+00 | 0.00E+00 | 2.26E-100 | 7.39E-87 | 1.76E-34 | 0.00E+00 | 2.10E-31 | 4.60E-34 | 9.80E-16 | 4.99E-86 | 1.33E-78 | 0.00E+00 | 1.16E-89 | 5.71E-62 | 3.83E-75 | 1.27E-84 |
| 10 | 4.60E-10 | 2.05E-02 | 1.66E-01 | 0.00E+00 | 2.07E-28 | 0.00E+00 | 1.55E-23 | 1.23E-96 | 2.18E-79 | 5.40E-83 | 5.57E-67 | 4.89E-26 | 0.00E+00 | 4.34E-23 | 7.62E-26 | 8.01E-14 | 0.00E+00 | 1.85E-59 | 0.00E+00 | 1.96E-71 | 8.47E-56 | 4.81E-63 | 3.83E-71 |
| 50 | 1.90E-04 | 3.39E-02 | 4.67E-02 | 5.33E-11 | 1.85E-19 | 0.00E+00 | 2.79E-20 | 2.61E-49 | 3.84E-46 | 2.73E-34 | 5.40E-27 | 1.92E-07 | 3.27E-12 | 6.49E-08 | 3.68E-07 | 6.56E-13 | 3.07E-56 | 3.40E-21 | 0.00E+00 | 0.00E+00 | 0.00E+00 | 3.90E-38 | 0.00E+00 |
| 100 | 1.20E-04 | 1.82E-02 | 7.15E-03 | 8.56E-09 | 2.30E-17 | 8.10E-18 | 1.39E-11 | 1.38E-34 | 1.61E-22 | 1.49E-31 | 2.70E-13 | 1.40E-04 | 2.53E-08 | 6.00E-05 | 2.90E-04 | 1.77E-08 | 1.92E-51 | 1.18E-07 | 3.37E-10 | 2.85E-16 | 0.00E+00 | 1.93E-26 | 3.46E-32 |
| 200 | 6.10E-04 | 3.04E-03 | 1.01E-03 | 1.94E-08 | 2.64E-14 | 1.22E-18 | 1.86E-08 | 0.00E+00 | 0.00E+00 | 3.34E-14 | 1.10E-07 | 7.00E-05 | 1.83E-06 | 9.00E-05 | 1.40E-04 | 3.38E-08 | 9.67E-46 | 5.00E-05 | 1.94E-06 | 1.71E-10 | 0.00E+00 | 5.11E-20 | 4.55E-24 |
| 300 | 9.00E-05 | 3.60E-04 | 1.70E-04 | 1.47E-07 | 2.65E-12 | 4.86E-15 | 1.15E-07 | 0.00E+00 | 0.00E+00 | 8.30E-13 | 1.72E-07 | 2.00E-05 | 1.29E-06 | 2.00E-05 | 3.00E-05 | 1.18E-08 | 3.44E-39 | 1.00E-05 | 1.54E-06 | 3.58E-09 | 3.00E-17 | 9.55E-18 | 4.76E-21 |
| 400 | 1.00E-05 | 4.00E-05 | 1.00E-05 | 1.59E-07 | 1.74E-11 | 1.25E-13 | 1.10E-07 | 0.00E+00 | 0.00E+00 | 8.48E-13 | 4.19E-08 | 4.16E-06 | 3.46E-07 | 4.08E-06 | 1.00E-05 | 3.06E-09 | 1.20E-36 | 2.21E-06 | 3.73E-07 | 4.69E-09 | 8.92E-17 | 7.00E-17 | 1.22E-19 |
| 500 | 2.33E-07 | 3.78E-06 | 1.06E-06 | 6.28E-08 | 2.78E-11 | 4.26E-13 | 4.25E-08 | 0.00E+00 | 0.00E+00 | 3.44E-13 | 1.14E-08 | 4.45E-07 | 8.12E-08 | 5.59E-07 | 7.17E-07 | 6.29E-10 | 1.14E-34 | 3.62E-07 | 9.86E-08 | 2.11E-09 | 6.89E-17 | 1.16E-16 | 5.13E-19 |
| 600 | 1.07E-08 | 3.65E-07 | 7.10E-08 | 1.43E-08 | 1.94E-11 | 5.39E-13 | 9.83E-09 | 0.00E+00 | 0.00E+00 | 1.05E-13 | 2.07E-09 | 3.34E-08 | 1.48E-08 | 5.35E-08 | 5.32E-08 | 1.05E-10 | 2.48E-33 | 3.20E-08 | 1.64E-08 | 6.57E-10 | 2.91E-17 | 8.41E-17 | 7.81E-19 |
| 700 | 5.08E-10 | 3.45E-08 | 4.61E-09 | 2.34E-09 | 7.98E-12 | 3.59E-13 | 1.66E-09 | 0.00E+00 | 0.00E+00 | 2.53E-14 | 2.54E-10 | 2.74E-09 | 2.06E-09 | 4.31E-09 | 3.56E-09 | 1.50E-11 | 2.00E-32 | 3.57E-09 | 1.90E-09 | 1.63E-10 | 8.77E-18 | 3.75E-17 | 6.24E-19 |
| 800 | 5.78E-11 | 3.20E-09 | 5.66E-10 | 3.06E-10 | 2.30E-12 | 1.53E-13 | 2.28E-10 | 0.00E+00 | 0.00E+00 | 4.88E-15 | 2.71E-11 | 2.19E-10 | 2.37E-10 | 3.37E-10 | 2.30E-10 | 1.95E-12 | 7.71E-32 | 1.66E-10 | 1.90E-10 | 3.17E-11 | 2.19E-18 | 1.27E-17 | 3.20E-19 |
| 900 | 1.69E-11 | 2.92E-10 | 8.76E-11 | 3.59E-11 | 5.13E-13 | 4.74E-14 | 2.78E-11 | 0.00E+00 | 0.00E+00 | 7.90E-16 | 2.45E-12 | 1.66E-11 | 2.36E-11 | 2.79E-11 | 1.89E-11 | 2.36E-13 | 1.69E-31 | 1.11E-11 | 1.63E-11 | 4.96E-12 | 4.61E-19 | 3.45E-18 | 1.20E-19 |
| 1000 | 1.16E-12 | 2.65E-11 | 5.65E-12 | 4.02E-12 | 9.55E-14 | 1.16E-14 | 3.18E-12 | 0.00E+00 | 0.00E+00 | 1.12E-16 | 2.09E-13 | 1.69E-12 | 2.15E-12 | 2.58E-12 | 3.00E-12 | 2.73E-14 | 2.48E-31 | 1.17E-12 | 1.32E-12 | 6.53E-13 | 8.23E-20 | 7.80E-19 | 3.70E-20 |

This page intentionally left blank.

### 5.2.8 Tetrachloroethene

The largest initial concentrations of tetrachloroethene were less than 2.5 μg/L which is less than ½ MCL. Hence, no plume maps or tabular results for tetrachloroethene are displayed.

### 5.2.9 Carbon Tetrachloride

Carbon tetrachloride was the only contaminant where an estimate of distribution by layer was considered successful. Carbon tetrachloride only exists above MCL in the 200-ZP-1 and 200-UP-1 OUs (Figure 5-38). Figure 5-39shows the effect of the ZP-1 pump-and-treat system on the carbon tetrachloride plume. The plume size has been significantly reduced in the 200-ZP-1 OU and less do in the 200-UP-1 OU. The seventy-five years simulation results (Figure 5-40) indicate that degradation of carbon tetrachloride along with the change of flow directions reduces the peak concentrations significantly. After 125 years (Figure 5-41) the plume has moved eastward over a kilometer in the last 50 years and shows reduced concentration from degradation. The 50 year period from 125 to 175 years (Figure 5-42) reveals no concentrations above MCL and a stagnated front edge of the ½ MCL concentration level because the eastward movement is balanced by degradation of carbon tetrachloride. By 200 years degradation has reduce the simulated concentrations below ½ MCL. Tabular results for carbon tetrachloride are not displayed.

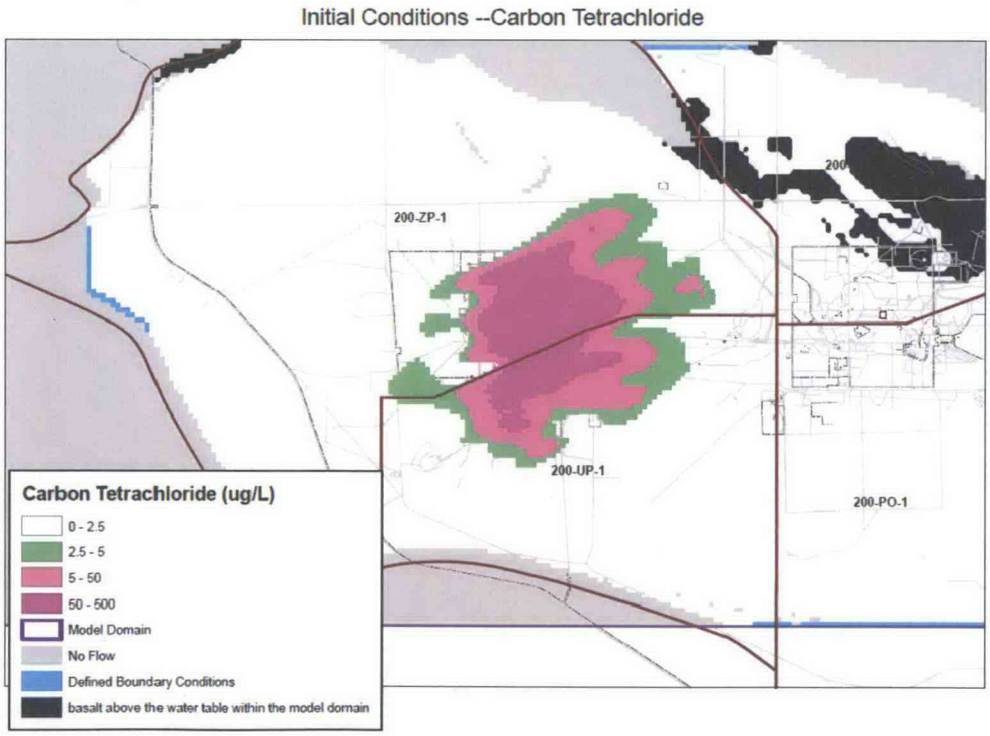


**Figure 5-38. Initial Carbon Tetrachloride Distribution (2008)**

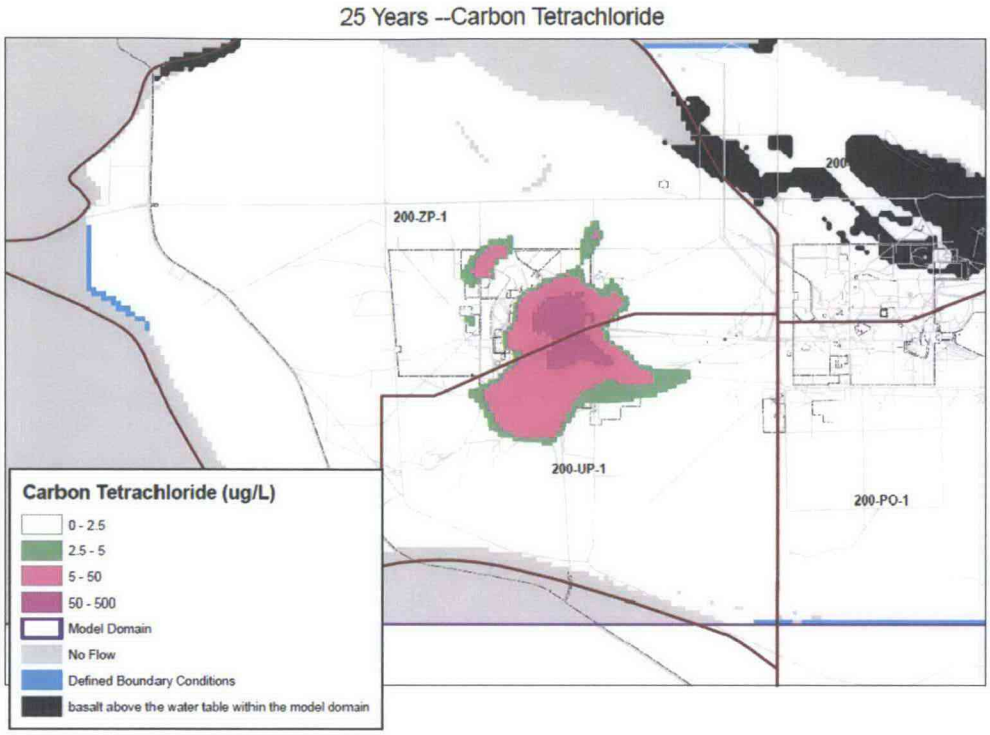


**Figure 5-39. Carbon Tetrachloride Distribution after 25 Years of Transport (2034)**

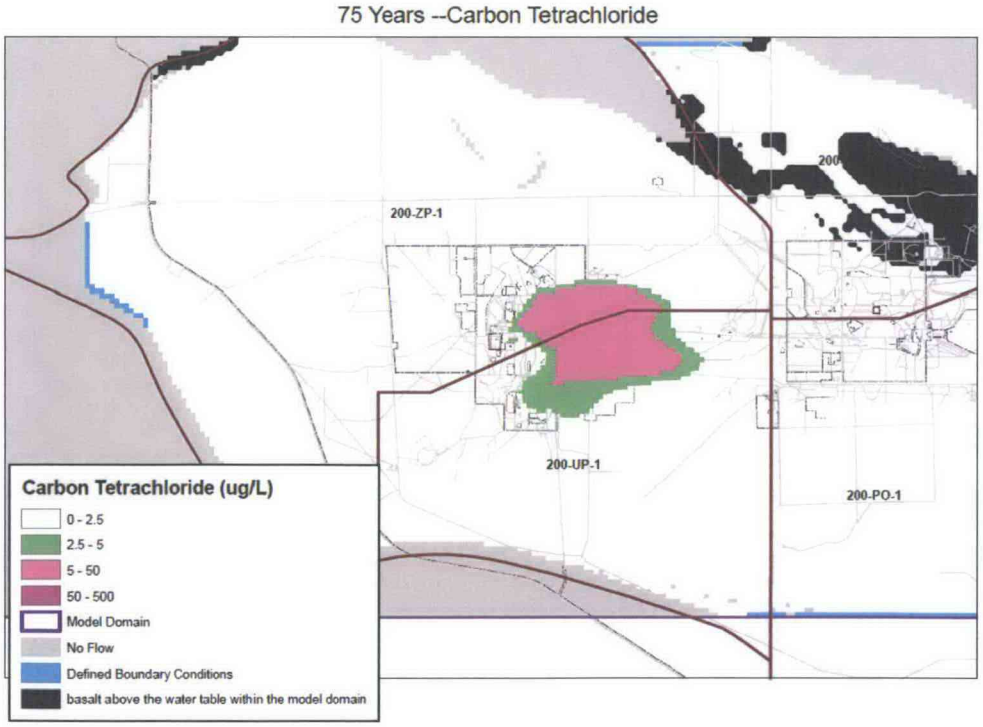


**Figure 5-40. Carbon Tetrachloride Distribution after 75 Years of Transport (2084)**

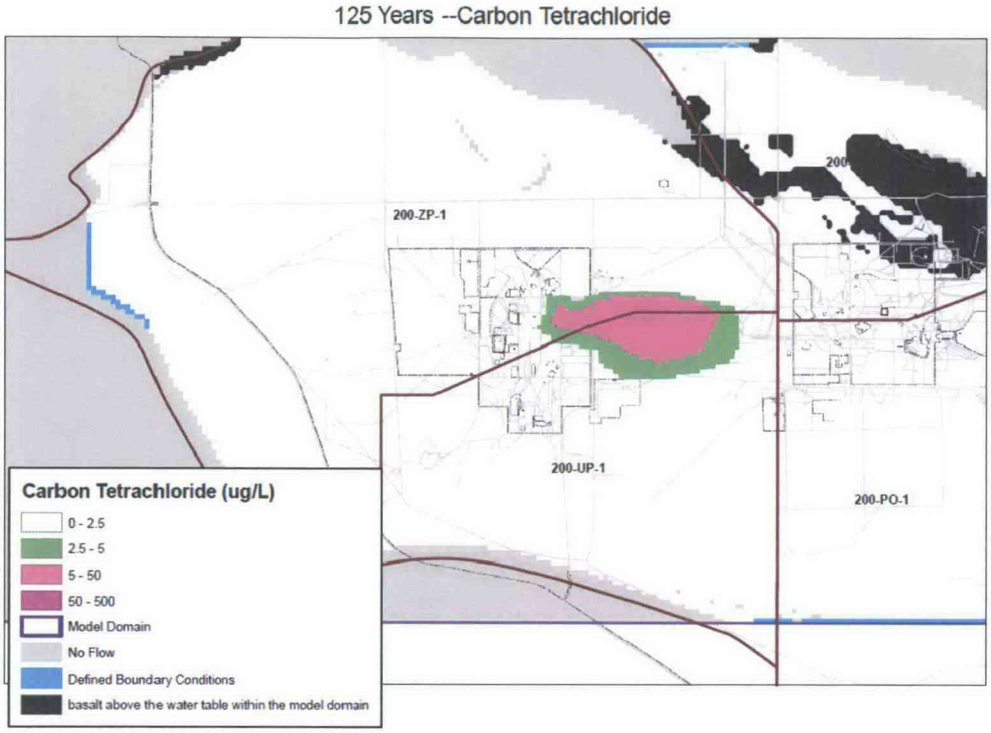


**Figure 5-41. Carbon Tetrachloride Distribution after 125 Years of Transport (2134)**

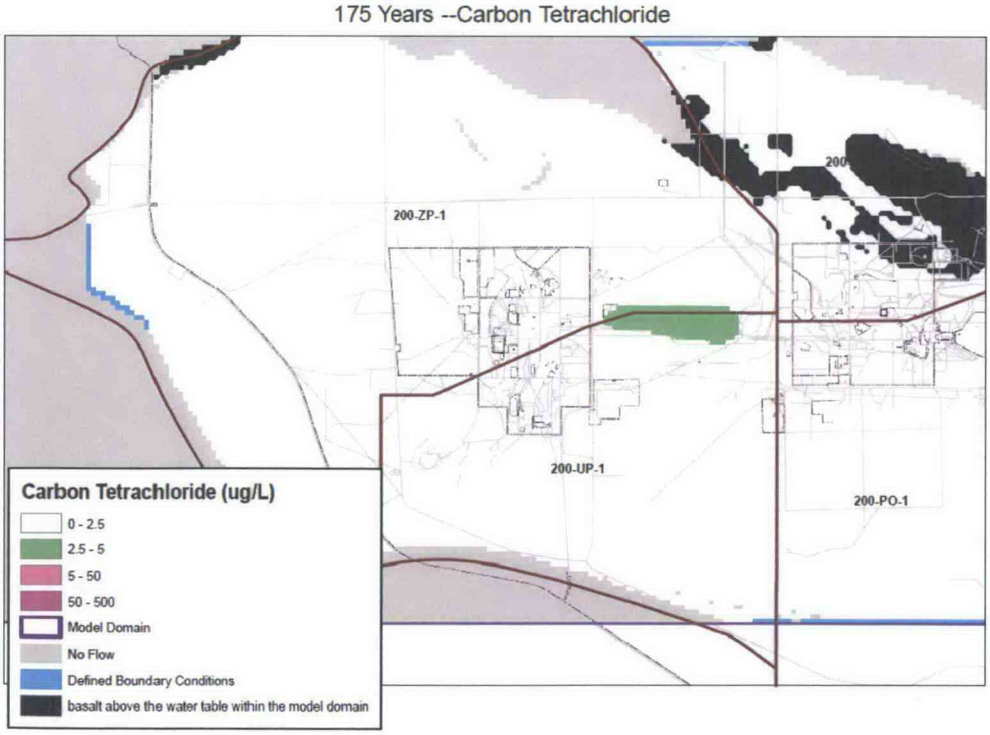


**Figure 5-42. Carbon Tetrachloride Distribution after 175 Years of Transport (2184)**

# 6 Results/Conclusions

Modeling results are shown in Section 5. A discussion of uncertainty in the simulation is provided in this section to place the calculation results in context.

## 6.1 Uncertainty in Simulated Future Conditions

We have not attempted to quantify uncertainty in the fate and transport simulations. What follows is a qualitative discussion of sources of uncertainty in the simulations and how those uncertainties might influence the predictions of future contaminant distributions. Five sources of uncertainty are identified that can affect the fate and transport calculation results: (1) uncertainty in representing initial contaminant concentration distribution; (2) uncertainty caused by neglecting future contaminant sources; (3) conceptual model uncertainty in flow and transport modeling; (4) parameter uncertainty; and (5) uncertainty introduced by computational problems. The uncertainty discussion is based on the current modeling objectives—using the model to evaluate future conditions under no-action scenario and to demonstrate whether a need for action exists. As the model is used in feasibility studies to compare remedial alternatives, a more thorough calibration will be undertaken to support these evaluations. Further refinements of the model are also expected as the model is used for design of remedial alternatives. At that stage, a formal quantitative evaluation of model uncertainties will be presented.

### 6.1.1 Uncertainty in Initial Contaminant Distribution

The representation of initial distribution of contaminant concentrations is affected by the following uncertainties:

- Uncertainties in reported concentration measurements
- Errors in reported concentration measurements
- Variability in estimates of measurement detection limits
- Method used to assimilate non-detect measurements into the measurement data set
- Representativeness of individual samples with respect to the region surrounding the sample
- Biases and variability introduced by the kriging algorithm
- Choice and influence of control points
- Truncation of the kriging estimates below ½ MCL
- Lack of three-dimensional contaminant concentration measurements and modeling assumptions made to define the initial plumes in 3 dimensions

For most contaminants, uncertainty in contaminant measurements is probably a negligible factor when interpreting the results of fate and transport calculation. The exception may be iodine-129 for which large uncertainties exist even with some measurements above MCL. The probability of large measurement errors is typically very low due to stringent quality controls applied by various analytical laboratories. However, sometimes measurement errors do occur. For example, one 2009 measurement of technetium that has a very large value in the data we obtained from the HEIS database has been identified as in error. The same sample is now reported to be below detection limit in the HEIS database.

The method used to accommodate samples below detection limits is also a source of uncertainty. The reader should keep in mind that non-detect measurements are identified as such in the data received from

HEIS. If the non-detect flag is set then the measurement value in the data are set to the non-detect value for non-radioactive constituents. Concentrations that are not measured by radioactive decay products are treated as if the contaminant level were one-half of the measurement detection limit, except for nitrate which is treated as if the contaminant level were at the detection limit. Measurements using decay products are treated as if the reported measurement is correct unless the reported value is negative. These rules create an intentional bias toward larger estimates in the vicinity of regions where contamination is detected compared to treating non-detects as zero concentration. It also introduces a similar bias in measurements far away from known regions of contamination. The distal bias contributes an unacceptable overestimation of contaminant concentration beyond the region. Therefore, the estimated contaminant concentrations are truncated at levels below ½ MCL to eliminate this unacceptable overestimation.

Truncation greatly reduces uncertainty introduced by measurement detection limits and the treatment of samples below the detection limits. For contaminants with typical non-detect values larger than MCL the intentional bias towards larger estimates of contaminated regions is retained. If the detection limits are below ½ MCL then uncertainty due to the treatment of non-detect measurements is probably overwhelmed by the bias introduced by truncation of the contamination estimates at ½ MCL.

Representativeness of fluid samples acquired from a wellbore with respect to defining contamination in the region of the wellbore is far too complex an issue to discuss in detail here. Contaminant concentrations may be effected by disturbances in the aquifer due to well emplacement. The actual placement of a monitoring well within the aquifer may induce local changes to the flow regime and migration of contaminants. Also, a larger proportion of the sample may come from high conductivity layers in the formation. This condition could introduce a bias in concentration if there are local variations in concentration due to contaminant migration pathways. Suffice it to say that representativeness of samples could be a source of large uncertainties in individual measurements and could even introduce consistent biases in a region.

Another component of the representativeness and comparability of samples is related to collection of samples at varying times. For establishing initial plume concentrations, a simple selection criterion was introduced. The selection criterion was to apply the 2008 sample data preferentially rather than averaging all the data acquired at a location. For locations that do not have 2008 sample data, the most recent measurement was used if it was after 2005. In all cases, multiple samples acquired during a given year were averaged. Note that the strategy of reducing temporal uncertainty is consistent with the assumption that individual measurement uncertainties are small. Given the scale and dynamics of contaminant migration the time based sampling strategy has probably reduced uncertainty due to when samples were acquired to negligible levels.

Developing initial plume configuration from limited spatial dataset also leads to uncertainty in initial concentration. The kriging based interpolation routine was introduced to reduce this uncertainty. The issue is how far a sample result can be extrapolated away from the wellbore or model cell containing the wellbore. Kriging uses a diminishing influence with distance as defined by the exponential variogram structure. Kriging reduces but cannot eliminate uncertainty due to sparse sampling as it does not represent the physics of the processes that caused contaminants to migrate in the subsurface. It is instead an interpolation algorithm. To reflect the influence of fluid flow direction on contaminant distribution shape, a bias in the kriging algorithm was introduced by making the variogram longer in the average direction of flow than in other directions and shortest perpendicular to this direction. The average ground water flow direction was determined to be consistent with contaminant contours within about 30 degrees of azimuth. It was kept constant within each of the eastern and western portions of the Central Plateau model domain. Thus it only approximates flow direction at the scale of individual contaminant plume, sometimes quite poorly. A particular problem with using kriging to define contaminant distributions is that while flow is in

a particular direction, kriging is symmetric with respect to the measurement point (i.e., the influence is the same in the direction of flow as it is in the opposite direction). One of the reasons for using control points was to reduce the influence of this limitation.

Control points allow the imposition of the analyst's subjective bias into the interpolation. Control points were used to accomplish the following four goals:

- Overcome the directionality problem described above.
- Connect regions of large concentration that were shown connected in the plume maps presented in the 2008 Hanford site groundwater annual report.
- Force very small regions of contamination above MCL (often few single cell blocks in the finite difference grid) to be represented as above MCL.
- Define contaminant plumes that have been inferred by limited measurements and knowledge of distributions or process knowledge as represented in the 2008 ground water report contaminant contours.

Control points introduce bias and uncertainty because their placement and interpretation of their influence is subjective. They are mainly used to apply professional judgment where insufficient data exist to fully describe site conditions. The net effect of control points is to reduce bias and uncertainty while defining plume configurations that are consistent with the 2008 groundwater annual report.

As with the introduction of control points, truncation of the plume estimates at ½ MCL reduces the overall bias and uncertainty in the contaminant distribution but also introduces its own bias; where measurements do not exist, concentrations are set to zero. Truncation does not affect regions of large contaminant concentrations, but does result in a probable underestimate of total contaminant mass to avoid a much larger overestimate than would occur if truncation were not used.

There are far more contaminant measurements that are representative of near water table contaminant concentration than there are measurements representative of deep conditions. Only carbon tetrachloride was deemed to have enough measurements at depth to provide a basis for determining separate concentrations for each model layer and only in the western part of the model domain. For other contaminants, measurements representative of the upper three layers were used to define a single contaminant distribution that was then applied equally to the top three layers of the model. This introduces bias in that the larger number of measurements near the surface dominates the estimates so that estimated contamination near the water table is propagated to greater depth. It is expected that this results in an overestimate of total contaminant mass. By assuming no contamination exists in layers four and five obviously biases the contaminant estimates in these layers in a non-conservative fashion, but this is supported by the absence of observed concentrations in the deeper parts of the groundwater aquifers. Layers four and five also tend to be less permeable than the overlying layers and thus not applying the contaminant concentrations that is observed near the water-table is deemed reasonable.

The review of transport results presented in Section 5 indicates that the bias toward deep contamination caused by applying the kriged concentrations to the top three layers has introduced contaminants into low permeability HSUs. Contaminants move in these units more slowly than in the higher, more permeable, units. There is a large uncertainty with regard to contamination of deeper HSUs, and hence the representativeness of the slow movement of many plumes.

### 6.1.2 Uncertainty from Neglecting Future Contribution from Vadose Contaminant Sources to Groundwater

The current analysis is limited to the estimation of the effects of current ground water contamination on future ground water contamination and the resultant risk to human health and the environment due to that contribution. The influence of future movement of contaminant presently in the vadose zone down to the saturated aquifer is outside the scope of this analysis and, therefore, the magnitude and timing of any future, or continuing contaminant contributions from this source are not accounted for. Not all of the observed groundwater contaminant plumes in 200-UP-1 Groundwater OU are associated with continuing vadose source contributions. Some plumes do underlie locations of historical releases to ground that may exhibit continuing vadose contribution to groundwater contamination.

The evaluation and remediation of secondary contaminant sources within the vadose zone falls under the responsibility of the specific source OU(s). Since the direct contribution of residual vadose sources to future contaminant concentrations is outside the scope of this analysis, the major source of uncertainty within the scope of the analysis is due to possible non-linear influences on fate and transport. The conceptual model for transport of current contamination assumes that the important processes are linear; that is, changes in magnitude of contamination propagate as changes in magnitude only; not as changes in how the processes work. For small concentrations this is a good assumption, it is doubtful that additional discharge from the vadose zone to the aquifer would impact the validity of the linearity assumption. Continuing contributions from vadose zone sources, however, could affect the overall magnitude of contaminant mass (as resulting concentration) in groundwater as well as the longevity of the high concentration portions of groundwater plumes.

### 6.1.3 Conceptual Model Uncertainty

It is often argued that conceptual model uncertainty is usually the dominant form of uncertainty in a modeling exercise. That is probably true for this model as well. One important source of uncertainty is the assumption that planned use of the Central Plateau will be accurate for the next one thousand years, roughly twenty times the time period that the Hanford facility has been maintained by the federal government to date. Changes in use of the plateau could alter the current artificial and natural recharge estimates in the model and thus impact the ground water flow velocities. The few after-the-fact audits of long term predictions that have been conducted have indicated that assumptions of future use are typically (if not invariably) the major cause of prediction error. Such uncertainty can lead in either conservative or non-conservative directions with equal likelihood. The impact of conceptual model related uncertainties can be investigated through sensitivity analyses.

Another important source of uncertainty is the assumption of spatially invariant hydraulic properties of the HSUs. The fluvial environments that lead to deposition of most of the aquifer are associated with heterogeneous structures, especially for the Hanford and Cold Creek units. Local variations in properties can cause local regions of relatively large flow rates and hence faster transport of contaminants. These can be significant as evidenced by the experience obtained from calibrating the model. During the calibration, the Cold Creek unit near the 200-East Area was found to be more permeable than a representative value would allow. The hydrologic unit definition of this portion of the Cold Creek unit was changed to Hanford formation to provide a more accurate reflection of the very permeable coarse grain nature of this portion of the Cold Creek unit. This region was identified because it was very important to the flow calibration. There are probably other smaller regions that had less impact on the hydraulic calibration but still could have a strong but more localized influence on flows.

A source of uncertainty in the transport predictions derives from the assumption of constant effective porosity value for a given HSU. The effective porosity is used in converting water mass flux calculated

by MODFLOW to groundwater velocity used in MT3DMS for fate and transport calculations. Heterogeneity in the form of lenses, bar structures, and over bank deposits are common at a scale below the 100 m by 100 m grid size of the Central Plateau model and could lead to varying effective porosity values and groundwater velocities. Furthermore, some of these features can create preferential pathways and lead to faster contaminant movement locally than predicted by the current model.

The conceptual model and parameterization of boundary conditions has a major influence on ground water flow and hence transport of contaminants. Representing the two gaps along the northern border of the model with specified heads is uncertain because the values have to be predicted from past trends. There are two major sources of uncertainty that influence the importance of the gap. The first is the uncertainty of how much flow is entering the model domain from the western streams, from surface infiltration, and through leakage upward from the basalt. Of these, flux from the western streams dominates. The values obtained from calibration of the 200-ZP-1 groundwater flow model were used for these terms. The second source of uncertainty is non-equilibrium storage in the aquifer. The Central Plateau is not in equilibrium with respect to inflow and outflow. The Central Plateau unconfined aquifer still exhibits more outflow than inflow because of the remaining fraction of the tremendous buildup of stored water in the aquifer during the operational period of the Hanford site. The aquifer is still attenuating this build up that ended with termination of production activities at the Hanford site in 1989.

Fluid flow and hence transport is extremely sensitive to the interpretation of geology in the entire portion of the model east and southeast of the 200-East Area. This region is complex geologically and there is not a one to one correspondence between geologic formation and proper hydraulic representation as previously described in this section. Strict reliance on geologic characterization was found to be incorrect. There may be almost as much variation of hydraulic conductivity within the Hanford formation and within the Cold Creek unit as there is between representative values for these hydro-stratigraphic units. To create a model that matched historic head data, interpretation of some drilling logs had to be re-examined, and many of the logs that were re-examined could be, and needed to be, interpreted differently than had been done previously. The conceptual model of hydrostratigraphy was influenced by historic contaminant plume interpretations that indicate the presence of a large conductive channel from just south of the 200-East Area to the southeast corner of the Central Plateau groundwater model domain. The hydraulic head data strongly correlates with this interpretation. There is, however, little geologic data from well log interpretation to corroborate this interpretation. While there is enough evidence to support a highly conductive channel, there is insufficient evidence to accurately define its shape and size. The uncertainty implies that there is insufficient evidence to provide good constraint of the velocity of groundwater flow in the channel. Potentially, examination of historic plume movement could help constrain flow velocities in the channel, but this has not been done.

### 6.1.4 Hydraulic Parameter Value Uncertainty

We have discussed aspects of conceptualization of HSUs as homogeneous features with effective single valued properties. The present discussion focuses on the selection of the effective values. Hydraulic parameters are; hydraulic conductivity, specific storage, and specific yield. Hydraulic conductivity values were established through calibration. The match to hydraulic head difference between Well 299-E23-1 near the 200-East Area and Well 699-24-33 was very sensitive to the hydraulic conductivity of the Hanford unit. This well pair was selected because of the perceived importance of the Hanford unit in defining the conductive channel. The sensitivity ensured that only a narrow range of effective hydraulic conductivity of the Hanford formation would result in a good match. However because the fluid flux going through the channel is uncertain and the size of the channel is uncertain, the representativeness of the effective parameter for the hydraulic conductivity of the Hanford formation is also uncertain. In terms of transport velocity uncertainty, the uncertainty in a value of the hydraulic conductivity for the Hanford

unit is relatively unimportant compared to the fluid mass flux uncertainty and uncertainty in the size of the channel.

The existence of a channel, as indicated by maps of historic contaminant distributions, indicates that there is a significant difference between the Hanford formation hydraulic conductivity and the effective hydraulic conductivity of the Cold Creek unit. The calibration resulted in an effective hydraulic conductivity of 100 m/day for the Cold Creek unit and 8500 m/day for the Hanford formation. The hydraulic head difference between well 299-E23-1 and well 699-24-33 was not sensitive to changes in hydraulic conductivity of the Cold Creek unit as long as it was significantly less than the Hanford formation. It is expected that, in terms of the most important aspects, contaminant transport is not sensitive to Cold Creek hydraulic conductivity.

The effective values for hydraulic conductivity of the Ringold A and Ringold E units were selected in the calibration by matching the hydrograph of well 299-W12-1 during 1976. This was done after selection of values for the Hanford unit and the Cold Creek unit. It is expected that the effective values are less well constrained than for the Hanford formation in the channel but much better than for the Cold Creek unit. The relative hydraulic conductivity between the Ringold A and Ringold E units are probably not well constrained and are important to transport uncertainty. However, the resultant uncertainty is probably much smaller than the uncertainty due to effective porosity.

The calibration was insensitive to changes in the conductivity of the Ringold Mud unit. The Ringold Mud may act as a much greater barrier to flow into the Ringold A unit than is currently simulated. It is unlikely that would have much influence on transport in the 200-PO-1 Groundwater OU, but might have a nonconservative impact on transport from the 200-UP-1 Groundwater OU to the 200-PO-1 Groundwater OU.

### 6.1.5 Uncertainty in Transport Parameters

As advection is the primary transport mechanism in the current modeling study, the transport parameters of interest are primarily effective porosity, bulk density, and $K_d$. These parameters are used in to determine the retardation factor that is applied to various COPCs. Because of lack of available information on spatial variability of these parameters, only best estimate values are considered in the modeling study.

The effective porosity and bulk density values applied in the transport model is representative of the sandy gravel sediment type of the Hanford Formation and the Ringold Formation (PNNL-18564). Although HSUs are composed of sediment layers of varying grain sizes (from gravel to mud size), but since the transport of contaminants is expected to preferentially occur along the coarser grained, higher hydraulic conductivity portion of the aquifer, applying the sandy gravel sediment property to the HSUs is deemed adequate. Furthermore, because of the long transport distances modeled, averaging of the properties over large rock volumes is reasonable as it leads to reduced uncertainty range.

The $K_d$ of the contaminants is generally highly variable and depends primarily on the available sorption sites on the sorbent (function of surface area), dissolved concentration of contaminant, and chemical parameters such as pH, partial pressure of $CO_2$, etc. Each of these parameters can vary over time and space and effect the $K_d$ of the contaminant and thereby the uncertainty in its estimate. Because of the large transport distances considered and the coarse discretization of the model grid, the best-estimate approach for $K_d$ is considered. The $K_d$ values for COPCs reported for the uncontaminated sandy gravel sediment type is used in the model to be consistent with the effective porosity and bulk density estimates. For carbon tetrachloride, the $K_d$ values is calculated based on the batch sorption experiments on uncontaminated sediments (rather than desorption experiments on the contaminated sediments), while for

other chlorinated hydrocarbons, $K_d$ is based on empirical calculation assuming low organic carbon fraction. In almost all cases, the $K_d$ value estimation is based on the assumption of dilute concentrations in groundwater that interacts with the sandy gravel sediments are largely uncontaminated.

The degradation of chlorinated hydrocarbons is also uncertain and dependent on the biogeochemical conditions in the aquifer. A conservative assumption of no degradation of chlorinated hydrocarbons (except for carbon tetrachloride) is considered, which is reasonable for the current modeling objective.

### 6.1.6 Summary of Uncertainty in Fate and Transport Simulations

While the computed fate and transport of contaminants in the 200-UP-1 Groundwater OU suffer from some computational uncertainty issues, the results in this section are not expected to change once the numerical implementation is in place for future plumes. Neglecting computational issues the major source of uncertainty is probably the vertical distribution of the initial contamination distributions. Other important sources of uncertainty are flow into the model from the western subsurface streams, the size of the southeast channel, the choice of appropriate values for the distribution constants, effective porosity, and hydraulic conductivity of various HSUs, and the future use of the Central Plateau.

# 7 References


CHPRC-00257 Rev 0, *MODFLOW and Related Codes Functional Requirements Document,* 2009, CH2M HILL Plateau Remediation Company, Richland, Washington.

CHPRC-00258 Rev 0, *MODFLOW and Related Codes Software Management Plan, 2009,* CH2M HILL Plateau Remediation Company, Richland, Washington.

CHPRC-00259 Rev 0, *MODFLOW and Related Codes Software Test Plan,* 2009, CH2M HILL Plateau Remediation Company, Richland, Washington.

CHPRC-00260 Rev 0, *MODFLOW and Related Codes Acceptance Test Report,* 2009, CH2M HILL Plateau Remediation Company, Richland, Washington.

CHPRC-00261 Rev 0, *MODFLOW and Related Codes Requirements Traceability Matrix,* 2009, CH2M HILL Plateau Remediation Company, Richland, Washington.

BHI-01496, *Groundwater/Vadose Zone Integration Project Hanford Soil Inventory Model*, Bechtel Hanford, Inc., Richland, Washington.

Deutsch, Clayton V. and Andre G. Journel, 1992, *GSLIB Geostatistical Software Library and User's Guide*, Oxford University Press, New York.

DOE/RL-2007-28, *Feasibility Study for the 200-ZP-1 Operable Unit*, Rev. 0, U.S. Department of Energy, Richland Operations Office, Richland, Washington. Available at: http://www5.hanford.gov/arpir/?content=findpage&AKey=0808050315, http://www5.hanford.gov/arpir/?content=findpage&AKey=00098828.

DOE/RL-2008-01, 2008, *Hanford Site Groundwater Monitoring for Fiscal Year 2007*, Rev. 0, U.S. Department of Energy, Richland Operations Office, Richland, Washington. Available at: http://www5.hanford.gov/arpir/?content=findpage&AKey=00098824.

DOE/RL-2008-56, *200-West Area Pre-Conceptual Design for Final Extraction/Injection Well Network: Modeling Analyses*, U.S. Department of Energy, Richland Operations Office, Richland, Washington.

DOE/RL-2008-78, *200 West Area 200-ZP-1 Pump-and-Treat Remedial Design/Remedial Action Work Plan*, Draft A, U.S. Department of Energy, Richland Operations Office, Richland, Washington. Available at: http://www5.hanford.gov/arpir/?content=findpage&AKey=0904130567.

DOE/RL-2009-38, *Description of Modeling Analysis in Support of the 200-ZP-1 Remedial Design Redial Action Work Plan*, Rev. 0, U.S. Department of Energy, Richland Operations Office, Richland, Washington. Available at: http://www5.hanford.gov/arpir/?content=findpage&AKey=0095363.

DOE/RL-2009-85, *Remedial Investigation Report for the 200-PO-1 Groundwater Operable Unit*, U.S. Department of Energy, Richland Operations Office, Richland, Washington.

Doherty, John, 2007, *User's Manual for PEST Version 11*, Watermark Numerical Computing, Brisbane, Australia.

ECF-200PO1-10-0259, *Central Plateau MODFLOW Model - Version 2*, Rev. 0, CH2M Hill Plateau Remediation Company, Richland, Washington.

ECF-200PO1-09-2007, *200-PO-1 Operable Unit Remedial Investigation Report -- Contaminant Fate and Transport Modeling in the Distal Portion of OU*, Rev.2, CH2M HILL Plateau Remedaiton Company, Richland, Washington.

USGS Open File Report 00-92, 2000, *MODFLOW-2000, the U.S. Geological Survey Modular Ground-water Model -- User Guide to Modularization Concepts and the Ground-Water Flow Process*, U. S. Geological Survey, Denver, Colorado. Available at: http://water.usgs.gov/nrp/gwsoftware/modflow2000/ofr00-92.pdf.

USGS Open File Report 94-464, 1994, *User's Guide for MODPATH/MODPATH-PLOT, Version 3: A Particle Tracking Post-processing Package for MODFLOW, the U. S. Geological Survey Finite-difference Ground-water Flow Model*, U. S. Geological Survey, Denver, Colorado. Available at: http://water.usgs.gov/nrp/gwsoftware/modpath5/ofr94464.pdf.

PNNL-14753, Rev. 1, 2006, *Groundwater Data Package for Hanford Assessments*, Pacific Northwest National Laboratory, Richland, Washington. Available at: http://www.pnl.gov/main/publications/external/technical_reports/PNNL-14753Rev1.pdf.

PNNL-18100, 2008, *Spatial Analysis of Contaminants in 200 West Area Groundwater in Support of the 200-ZP-1 Operable Unit Pre-Conceptual Remedy Design*, Pacific Northwest National Laboratory, Richland, Washington. Available at: http://www.pnl.gov/main/publications/external/technical_reports/PNNL-18100.pdf.

PNNL-18564, 2009, Selection and Traceability of Parameters to Support Hanford-Specific RESRAD Analysis Fiscal Year 2008 Status Report, Pacific Northwest National Laboratory, Richland, Washington. Available at: http://www.pnl.gov/main/publications/external/technical_reports/PNNL-18564.pdf.

PRC-PRO-IRM-309, *Controled Software Management*, Rev. 0, CH2M HILL Plateau Remedaiton Company, Richland, Washington.

Rumbaugh, James O. and Douglas B. Rumbaugh, 2007, *Guide to Using Groundwater Vistas*, Version 5, Environmental Simulations, Inc., Reinholds, Pennsylvannia. Available at: http://www.groundwatermodels.com/Groundwater_Vistas.php.

SERDP-99-1, 1999, *MT3DMS: A modular three-dimensional multispecies transport model for simulation of advection, dispersion, and chemical reactions of contaminants in groundwater systems; Documentation and user's guide*, U.S. Army Engineer Research and Development Center, Vicksburg, Mississippi. Available at: http://hydro.geo.ua.edu/mt3d/mt3dmanual.pdf.

# Appendix A

# Software Checkout and Installation Forms

# CHPRC SOFTWARE INSTALLATION AND CHECKOUT FORM

**Software Owner Instructions:**
Complete Fields 1-13, then run test cases in Field 14. Compare test case results listed in Field 15 to corresponding Test Report outputs. If results are the same, sign and date Field 19. If not, resolve differences and repeat above steps.

**Software Subject Matter Expert Instructions:**
Assign test personnel. Approve the installation of the code by signing and dating Field 21, then maintain form as part of the software support documentation.

**GENERAL INFORMATION:**

1. Software Name: MODFLOW 2000 & MT3DMS (CHPRC Build 0001) Software Version No.: 0001

**EXECUTABLE INFORMATION:**

2. Executable Name (include path):

   mf2k-0001.exe & mt3d-0001.exe

3. Executable Size (bytes): mf2k-0001.exe 2,995 Kb; mt3d-0001.exe 1,011 Kb

**COMPILATION INFORMATION:**

4. Hardware System (i.e., property number or ID):

   WC95463

5. Operating System (include version number):

   Windows XP Professional Version 2002 Service Pack 3

**INSTALLATION AND CHECKOUT INFORMATION:**

6. Hardware System (i.e., property number or ID):

   INTERA CONFIGCONTROL (USER: AMENA MAYENNA)

7. Operating System (include version number):

   MICROSOFT WINDOWS XP PROFESSIONAL VERSION 2002 SERVICE PACK 3

8. Open Problem Report? ◉ No ○ Yes PR/CR No.

**TEST CASE INFORMATION:**

9. Directory/Path:

   Tests invoked by batch files \test\mf-itc-1\mf-itc-1.bat and \test\mt-itc-1\mt-itc-1.bat

10. Procedure(s):

    CHPRC-00259 Rev 0, MODFLOW and Related Codes Software Test Plan

11. Libraries:

    Statically Linked

12. Input Files:

    Found in \test

13. Output Files:

    Found in \test

14. Test Cases:

    MF-ITC-1 and MT-ITC-1

15. Test Case Results:

    AS EXPECTED

16. Test Performed By:

17. Test Results: ● Satisfactory, Accepted for Use ○ Unsatisfactory

18. Disposition (include HISI update):

## CHPRC SOFTWARE INSTALLATION AND CHECKOUT FORM (continued)

1. Software Name: MODFLOW 2000 & MT3DMS (CHPRC Build 0001) Software Version No.: 0001

Prepared By:

| | | |
|---|---|---|
| 19. Software Owner (Signature) | William E. Nichols<br>Print | 9/24/2009<br>Date |
| 20. Test Personnel: | | |
| x Amena Moth Mayenna<br>Sign | Amena Moth Mayenna<br>Print | 09/24/2009<br>Date |
| Sign | Print | Date |
| Sign | Print | Date |
| Approved By: | | |
| 21. CW Connell<br>Software SME (Signature) | Carl W. Connell<br>Print | 10/14/09<br>Date |



A-6005-149 (REV 0)

# CHPRC SOFTWARE INSTALLATION AND CHECKOUT FORM

**Software Owner Instructions:**

Complete Fields 1-13, then run test cases in Field 14. Compare test case results listed in Field 15 to corresponding Test Report outputs. If results are the same, sign and date Field 19. If not, resolve differences and repeat above steps.

**Software Subject Matter Expert Instructions:**

Assign test personnel. Approve the installation of the code by signing and dating Field 21, then maintain form as part of the software support documentation.

**GENERAL INFORMATION:**

1. Software Name: MODFLOW 2000 & MT3DMS (CHPRC Build 0001) Software Version No.: 0001

**EXECUTABLE INFORMATION:**

2. Executable Name (include path):

   mf2k-0001.exe & mt3d-0001.exe

3. Executable Size (bytes): mf2k-0001.exe 2,995 Kb; mt3d-0001.exe 1,011 Kb

**COMPILATION INFORMATION:**

4. Hardware System (i.e., property number or ID):

   WC95463

5. Operating System (include version number):

   Windows XP Professional Version 2002 Service Pack 3

**INSTALLATION AND CHECKOUT INFORMATION:**

6. Hardware System (i.e., property number or ID):

   INTERA PROPERTY TAG 00379, HP G70-460US NOTEBOOK PC

7. Operating System (include version number):

   WINDOWS VISTA™ HOME PREMIUM, SERVICE PACK 1

8. Open Problem Report? ◉ No ○ Yes PR/CR No.

**TEST CASE INFORMATION:**

9. Directory/Path:

   Tests invoked by batch files \test\mf-itc-1\mf-itc-1.bat and \test\mt-itc-1\mt-itc-1.bat

10. Procedure(s):

    CHPRC-00259 Rev 0, MODFLOW and Related Codes Software Test Plan

11. Libraries:

    Statically Linked

12. Input Files:

    Found in \test

13. Output Files:

    Found in \test

14. Test Cases:

    MF-ITC-1 and MT-ITC-1

15. Test Case Results:

    RESULTS MATCHED BASELINE CASE RESULTS

16. Test Performed By:

17. Test Results: ● Satisfactory, Accepted for Use ○ Unsatisfactory

18. Disposition (include HISI update):

    COMPUTER ADDED TO HISI

## CHPRC SOFTWARE INSTALLATION AND CHECKOUT FORM (continued)

1. Software Name: MODFLOW 2000 & MT3DMS (CHPRC Build 0001) Software Version No.: 0001

Prepared By:

| | | |
|---|---|---|
| 19. | William E. Nichols | 11 NOV 2009 |
| Software Owner (Signature) | Print | Date |

20. Test Personnel:

| | | |
|---|---|---|
| | WILLIAM E. NICHOLS | 11 NOV 2009 |
| Sign | Print | Date |
| | Amena Moth Mayenna | 11 Nov 2009 |
| Sign | Print | Date |
| | | |
| Sign | Print | Date |

Approved By:

| | | |
|---|---|---|
| 21. | Carl W. Connell | |
| Software SME (Signature) | Print | Date |



A-6005-149 (REV 0)

## CHPRC SOFTWARE INSTALLATION AND CHECKOUT FORM

**Software Owner Instructions:**

Complete Fields 1-13, then run test cases in Field 14. Compare test case results listed in Field 15 to corresponding Test Report outputs. If results are the same, sign and date Field 19. If not, resolve differences and repeat above steps.

**Software Subject Matter Expert Instructions:**

Assign test personnel. Approve the installation of the code by signing and dating Field 21, then maintain form as part of the software support documentation.

**GENERAL INFORMATION:**

1. Software Name: MODFLOW 2000 & MT3DMS (CHPRC Build 0001) Software Version No.: 0001

**EXECUTABLE INFORMATION:**

2. Executable Name (include path):

   mf2k-0001.exe & mt3d-0001.exe

3. Executable Size (bytes): mf2k-0001.exe 2,995 Kb; mt3d-0001.exe 1,011 Kb

**COMPILATION INFORMATION:**

4. Hardware System (i.e., property number or ID):

   WC95463

5. Operating System (include version number):

   Windows XP Professional Version 2002 Service Pack 3

**INSTALLATION AND CHECKOUT INFORMATION:**

6. Hardware System (i.e., property number or ID):

   INTERA PROPERTY TAG 00351, HP PAVILION dv7 LAPTOP COMPUTER

7. Operating System (include version number):

   WINDOWS VISTA™ HOME PREMIUM SERVICE PACK 1

8. Open Problem Report? ◉ No ○ Yes PR/CR No.

**TEST CASE INFORMATION:**

9. Directory/Path:

   Tests invoked by batch files \test\mf-itc-1\mf-itc-1.bat and \test\mt-itc-1\mt-itc-1.bat

10. Procedure(s):

    CHPRC-00259 Rev 0, MODFLOW and Related Codes Software Test Plan

11. Libraries:

    Statically Linked

12. Input Files:

    Found in \test

13. Output Files:

    Found in \test

14. Test Cases:

    MF-ITC-1 and MT-ITC-1

15. Test Case Results:

    BOTH TESTS PASSED – RESULTS IDENTICAL TO BASELINE TEST RESULTS

16. Test Performed By:

17. Test Results: ● Satisfactory, Accepted for Use ○ Unsatisfactory

18. Disposition (include HISI update):

    PLATFORM + USER ADDED TO HISI

## CHPRC SOFTWARE INSTALLATION AND CHECKOUT FORM (continued)

1. **Software Name:** MODFLOW 2000 & MT3DMS (CHPRC Build 0001) **Software Version No.:** 0001

**Prepared By:**

| | | |
|---|---|---|
| 19. | William E. Nichols | 11 NOV 2009 |
| Software Owner (Signature) | Print | Date |

20. **Test Personnel:**

| | | |
|---|---|---|
| | WILLIAM E. NICHOLS | 11 NOV 2009 |
| Sign | Print | Date |
| | Amena Motu Mayenna | 11 Nov 2009 |
| Sign | Print | Date |
| | | |
| Sign | Print | Date |

**Approved By:**

| | | |
|---|---|---|
| 21. | Carl W. Connell | |
| Software SME (Signature) | Print | Date |



A-6005-149 (REV 0)